Evaluation of power control with different electrical and control concept of wind farm

Part 1 – small island grid

Margaris, Ioannis; Hansen, Anca Daniela

Publication date:
2009

Document Version
Publisher's PDF, also known as Version of record

Project funded by the European Commission under the 6th (EC) RTD Framework Programme (2002- 2006) within the framework of the specific research and technological development programme "Integrating and strengthening the European Research Area"

Project UpWind

Contract No.:
019945 (SES6)

"Integrated Wind Turbine Design"

Work Package 9: Electrical grid

Deliverable D 9.4.3

Evaluation of power control with different electrical and control concept of wind farm

Part 1 – small island grid

AUTHORS:	Ioannis Margaris
AFFILIATION:	National Technical University of Athens
ADDRESS:	9 Iroon Politechneiou Str., 15773, Zografou, Athens (GR)
TEL.:	+30 210 7722874
EMAIL:	imarg@power.ece.ntua.gr
FURTHER AUTHORS:	Anca D. Hansen
REVIEWER:	Poul Sørensen, Nikolaos Hatziargyriou
APPROVER:	Poul Sørensen, Nikolaos Hatziargyriou

Document Information

DOCUMENT TYPE	Report
DOCUMENT NAME:	Evaluation of power control with different electrical and control concept of wind farm
DOCUMENT NUMBER:	
REVISION:	**FINAL**
REV.DATE:	June 2010
CLASSIFICATION:	Final: R0 (General Public)
STATUS:	**FINAL**

Abstract:

This report investigates the impact of wind power in non interconnected power systems with increasing wind power penetration. Issues such as power fluctuations, short circuits and FRT capability of wind turbines and frequency control support are under focus. The study case of Rhodes power system is used to simulate the response of the system in various scenarios.

Contents

STATUS, CONFIDENTIALITY AND ACCESSIBILITY									
Status				**Confidentiality**				**Accessibility**	
S0	Approved/Released			**R0**	General public	**(X)**		Private web site	
S1	Reviewed			**R1**	Restricted to project members			Public web site	**(X)**
S2	Pending for review			**R2**	Restricted to European. Commission			Paper copy	
S3	Draft for comments	**X**		**R3**	Restricted to WP members + PL				
S4	Under preparation			**R4**	Restricted to Task members +WPL+PL				

PL: *Project leader* **WPL:** *Work package leader* **TL:** *Task leader*

1. Introduction

Autonomous power systems are characterized by the absence of interconnections with neighbouring systems due to geographical, economic and political reasons. These systems face particular problems associated with safety and reliability during the design and operation procedure associated with safety and reliability. Typical problems include large variations in frequency because of the low inertia and the large fluctuations voltage due to the low short circuit ratio. The quality of the provided electricity to consumers is threatened. At the same time, special features of non interconnected systems, such as concentration of production in a limited number of power stations, the large size of the units in relation to the load, the need for larger spinning reserve due to the absence of interconnections, and the small stability margins raise the impact on safety and cost of operation.

Under these conditions, the effective handling of transient phenomena arising due to serious disorders is particularly critical. The systems should respond adequately to dynamic events and ensure static and dynamic safety. The most common faults that may cause undesired events are the loss of transmission lines, the sudden loss of load, and short circuits – especially three phase errors – and loss of production units. Based on collected operational data, incidents of loss of unit during operation are quite common and cause serious problems, therefore require special treatment. In several cases, such events have led in the past in smaller or even general black-outs.

These problems are becoming more intense due to the increasing penetration of wind power in the last decade. Since renewable energy sources and particularly wind energy have stochastic behaviour, the power output is not guaranteed. This is the main factor that imposes restrictions on the expansion because in general, distributed energy sources do not contribute to the control and regulation of the system in the same way as conventional units. Another important point, which differentiates the turbines compared with conventional synchronous generators used in electric systems, is associated with the technology of converting mechanical energy into electrical. The wind turbines are in large proportion equipped with asynchronous generators (possibly in

conjunction with electronic power converters) and therefore have substantial differences in the dynamic response over conventional units. For these reasons, limits are always imposed in the instantaneous penetration of wind power. These limits vary across the power systems, depending on the specific circumstances prevailing in each autonomous system, both in terms of conventional units (e.g. production technology, control capabilities, etc.) and wind farms (size and technology of the wind turbines, dispersion of wind turbines on the island, etc.). It is often the case that the limit set by the system operator for the instantaneous penetration of wind power is around 30% -40% of the load. In order to allow both the evaluation of the dynamic behaviour of autonomous systems after severe disturbances (e.g. ability of the system to restore frequency back to the desired limits after a major disturbance, such as loss of production and / or lines) as well as the definition of safe penetration limits, it is essential to conduct numerous studies. These include transient stability, load - frequency regulation, etc. The development of appropriate models for dynamic simulations in non interconnected systems is critical.

2. Power system model

2.1 Thermal power plant models

The conventional generating capacity comprises usually diesel, gas and steam plants with different ratings and control attributes. Each thermal plant contains several control blocks, which are essential for power system of dynamic simulations. In Fig. 1, the basic configuration for a thermal power plant, [1], is illustrated, including voltage controller, primary controller (governor), primary mover unit and the synchronous generator. In many cases, due to lack of accurate data, simplified models for the conventional units are used in simulations. In this study, the exact models for each unit were used to ensure optimal representation of the interaction between wind farms and the power system.

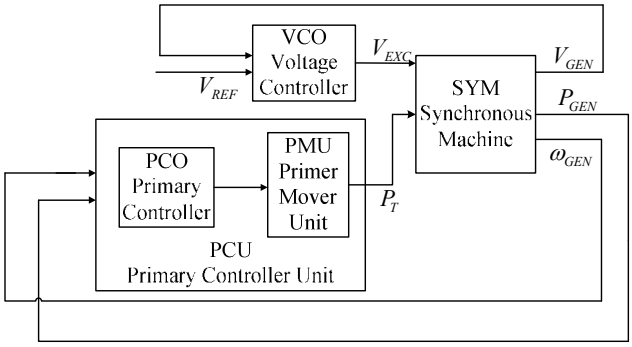

Fig. 1. Conventional thermal power plant model.

The following three different models, already existing as built-in standard models in PowerFactory [2], are used for the governors: GAST2A model for the gas turbines, DEGOV1 model for the diesel generators and IEEEG1 general model for the steam plants.

A detailed description of the GAST2A built-in model in PSS/E for the governor used in the gas plant is described in [3], while details on the corresponding standard IEEEG1 model for the governor in the steam plant can be found in [2]. The following figures sketch the diagrams of governor models, i.e. DEGOV1, IEEEG1 and GAST2A model.

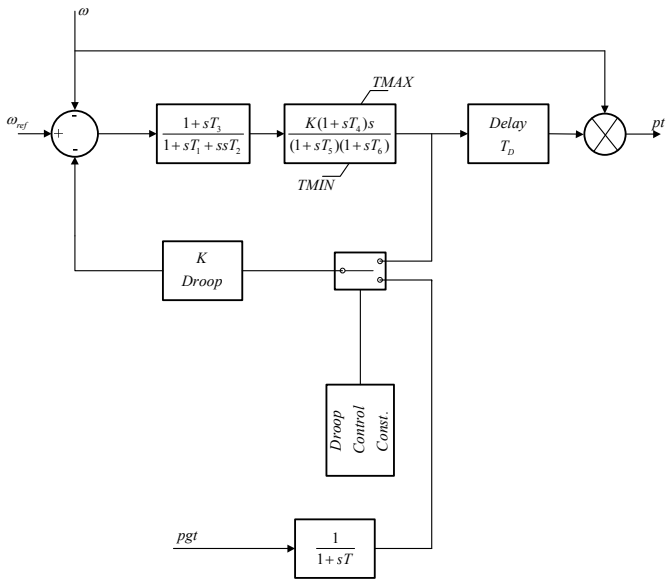

Fig. 2. Governor model DEGOV1 used in diesel generators.

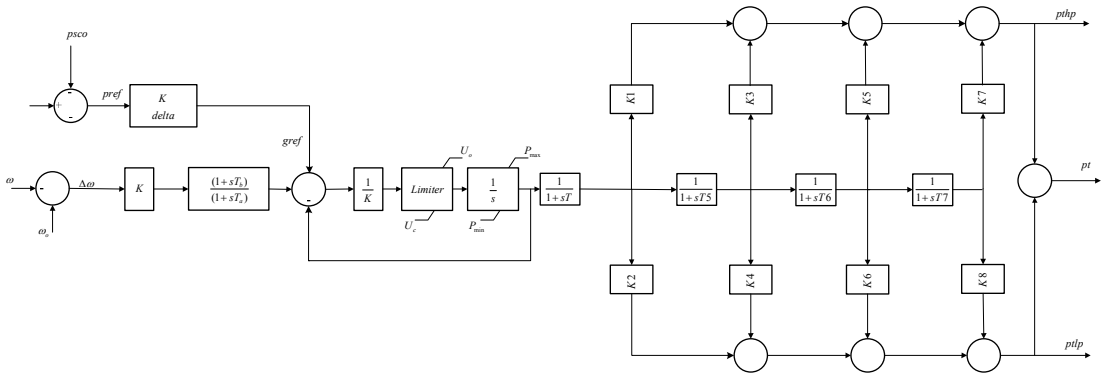

Fig. 3. Governor model IEEEG1 used in steam units.

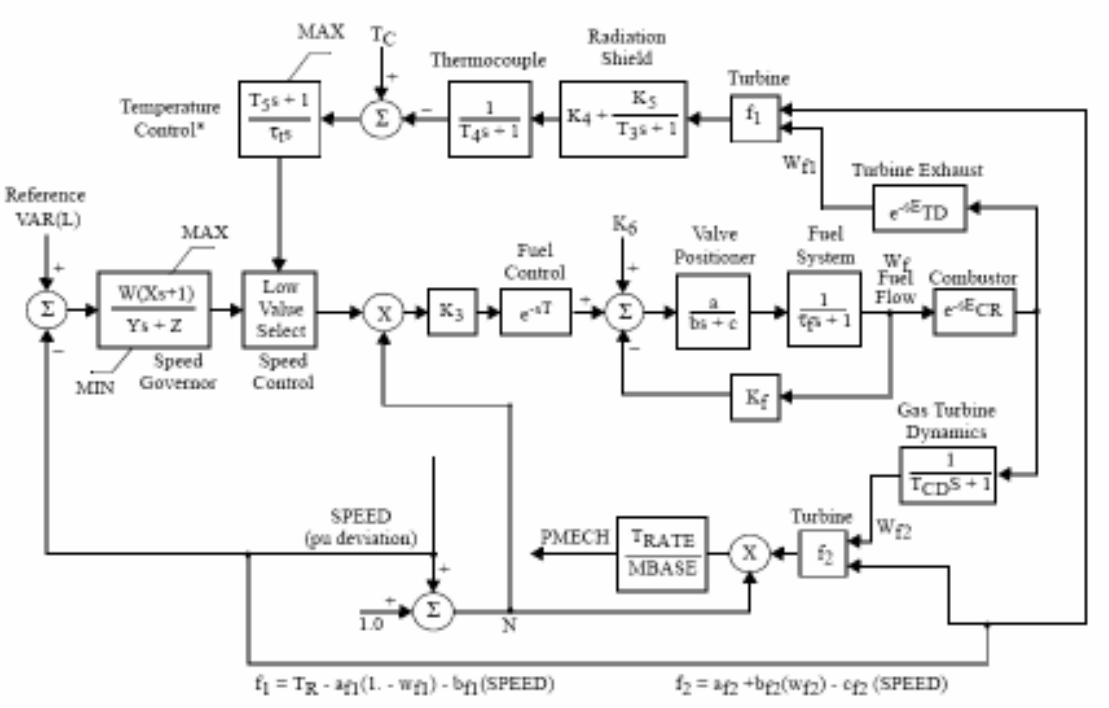

Fig. 4. Governor model GAST2A used in gas units.

The parameters of these models, validated both in Matlab and PSS/E software packages, are presented in [3].

For the Automatic Voltage Regulators (AVR), the built-in SEXS model of PowerFactory is used with adjusted parameters for each unit. A diagram for the standard AVR model is illustrated in Fig. 5:

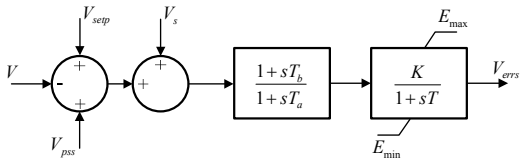

Fig. 5. Schematic of AVR model (SEXS model) used in conventional units.'

2.2 Dynamic load models

The electrical loads of the systems include typically various kinds of electrical devices. An appropriate approach for the dynamic modeling of the loads connected to Medium Voltage (MV) feeders is to assume constant impedance of the loads during dynamic simulations, [4]:

$$P = P_0 (V / V_0)^2 \qquad (2.1)$$

$$Q = Q_0 (V / V_0)^2 \qquad (2.2)$$

where P, P_0 and Q, Q_0 are the active and reactive power consumed by the load for voltage equal to reference voltage V, V_0 respectively.

2.3 Protection system

The protection system was also modeled in the simulation platform. The settings for both under/over voltage and under/over frequency protection system are crucial for the operation and dynamic response of the system during transient instances. As mentioned in the Introduction, non interconnected system, like the one used in this report as a study case, face the problem of significant variations in voltage and frequency. The relays, which act on either the production (protection of the conventional units or protection of the wind turbines), or the demand side (relays attached on the Medium Voltage feeders) decide the disconnection of equipment or loads, when the limits set by the system operator (or the production unit user) are violated. Regarding the loads, this leads to the so called load shedding, which often determines also the dynamic security margins for the system. It is often the case, in isolated systems, with low inertia, that during frequency variations, large proportion of the load is disconnected to avoid further frequency drop and possible frequency instability, i.e. due to sudden loss of a production unit.

The voltage and frequency protection system was modeled specifying the lower (or upper) limit of the value and the time duration, during which the variable measured, is out of the accepted range.

One kind of under/over frequency protection operating in modern power systems is the so called ROCOF protection (Rate of Change of Frequency). The relays controlled by this system, open when the frequency changes at a rate faster than the specified one for a specific time. Thus, a part of the substation loads is disconnected. However, in many non-interconnected systems, especially those designed many decades ago, the under/over frequency protection system controlling the relays at substation loads measures the actual frequency and not the rate of change. Thus, if the frequency drops lower than a specified limit for specific time duration, the relay is ordered to open.

These two different protection schemes are illustrated as frequency-time zones in Fig. 6 and are the ones under focus in this article.

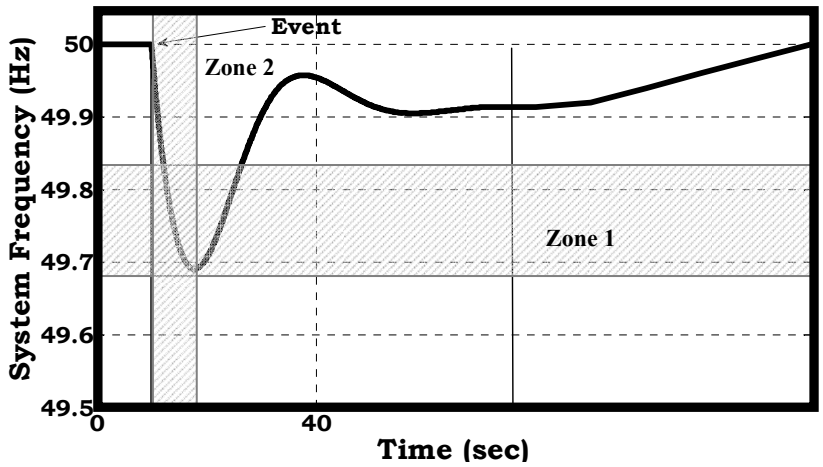

Fig. 6. Frequency protection system zones

As a case study the small size island system of Rhodes is used. Rhodes power system for the reference year 2012 includes a 150 kV transmission system, two power plants, distributed in the north and in the south, as shown in Fig. 7, and five wind farms. A significant proportion of the generation comes from wind turbines and diesel units. In 2012, the total installed wind power capacity and the maximum annual power demand are assumed to be about 48 MW and 233 MW, respectively (see TABLE I).

Fig. 7. Rhodes power system.

The basic characteristics of Rhodes power system in 2012 are summarized in TABLE I:

TABLE I
BASIC CHARACTERISTICS OF RHODES AUTONOMOUS SYSTEM IN 2012

Rhodes power system	
Max Power Demand (MW)	233.1
Rated Thermal Power (MW)	322.9
Rated Wind Power Generation (MW)	48.8

The present Rhodes power system model is based on dynamic models of conventional generating units, loads and wind turbines. In order to be able to perform power system simulation studies for 2012, the present system model has to be modified with additional generating units and wind farms, which are expected to be online by the year of study, 2012, [5]. The protection system, mainly under/over frequency and voltage protection relay is also included in the dynamic power system model. In the reference year study 2012, five wind farms with different technologies will be connected online in Rhodes power system. TABLE II depicts the wind turbine technology and the size of each wind farm.

TABLE II
WIND FARMS IN RHODES POWER SYSTEM IN 2012

	Wind Turbine Technology	**Installed Capacity (MW)**
Wind Farm A1	DFIG	11.05
Wind Farm A2	DFIG	5.95
Wind Farm B1	PMSG	18
Wind Farm B2	PMSG	3
Wind Farm C	ASIG	11.7

2.4 Load scenarios

Regarding the first step of the approach, the operating scenarios have to be carefully defined. These scenarios are based on collected operational data of the power system and correspond to the possible severe condition of operation. In this way, it is ensured that their analysis covers the intermediate modes of operation in terms of security. Three reference scenarios were defined as follows:

- The Peak Load Demand scenario – (SCENA).
- The Maximum Wind Power Production scenario (in absolute values of power) – (SCENB).
- The Maximum Wind Power Penetration scenario (in percentage of the load demand) – (SCENC).

The first scenario is the base case scenario and is used to evaluate the operational mode of the system in terms of security without significant wind power production, because annual peak load occurs in a hot summer day with typically very low wind. The second scenario is used to investigate security with large wind power production levels. In this case the levels of wind penetration are quite high going beyond 20% of the total load demand. The third scenario examines a penetration level above the 30% margin, which has been used until now for wind energy as a rule of thumb in autonomous island systems.

2.5 Static security analysis

Under the different scenarios, the secure operation of the system for steady operation has to be ensured, based on the N and N-1 criteria. Among the security requirements which have to be fulfilled by the power system are the following:

- The loading of the transmission lines should be within the accepted limits.
- Bus voltages should be in the range of ±5% around the nominal voltage for normal operation (N)
- Bus voltages should be in the range of ±10% around the nominal voltage for emergency operation (N-1).

3. Wind farm models

This chapter summarizes the work done on modeling and development of the dynamic control of the wind farms. Models and control strategies for three different types of wind farms have been developed, with the aim to optimize the operation of the wind farms considering their participation in the grid support (fault ride-through, active and reactive power control, frequency control and voltage control). Models and control for three different types of wind turbines have been developed:

- Fixed speed active stall wind turbine concept
- Variable speed doubly-fed induction generator wind turbine concept
- Variable speed multi-pole permanent magnet synchronous generator wind turbine concept

These wind turbine concept models can be used and even extended for the study of different aspects, e.g. the assessment of power quality, control strategies, connection of the wind turbine at different types of grid and storage systems. Different control strategies have been developed and implemented for these wind turbine concepts, their performance in normal or fault operation being assessed and discussed by means of simulations.

A simplified block scheme of the wind turbine models is shown in Fig. 8. The basic block scheme of the wind turbine consists of a wind model, an aerodynamic model, a transmission system, generator model and a control block model.

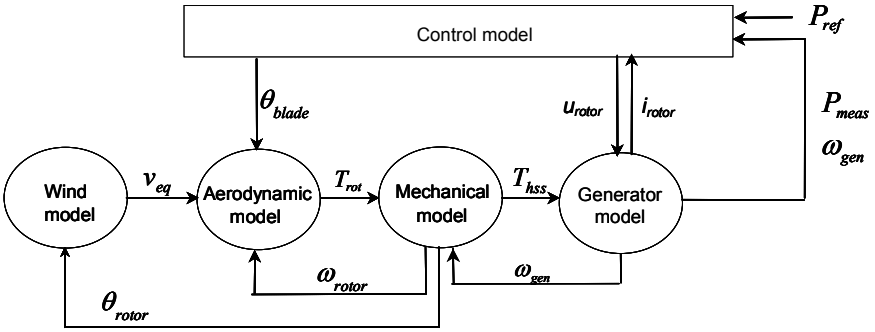

Fig. 8. Scheme of wind turbine models.

I. Wind model

The wind model used is described in detail in [6]. The main advantages of this wind model are the fast computation, reduced memory requirements and the ease of use, either for variable or constant speed models. This wind speed model is very suitable for simultaneous simulation of a large number of wind turbines, making it possible to estimate efficiently the impact of a large wind farm on the power quality.

The structure of the wind model is shown in Fig. 9. It provides an equivalent wind speed v_{eq} to the aerodynamic model. The wind model includes two sub-models: a hub wind model and a rotor wind model.

The hub wind model models the fixed-point wind speed at hub height for each wind turbine. In this hub wind model, the park scale coherence is taken into account in the case when a whole wind farm is modeled. The second is the rotor wind model, which includes the averaging effect of the wind speeds over the whole rotor, the rotational sampling effect, and a tower shadow model. The wind shear is not included in the rotor wind model, as it only has a small influence on the power fluctuations.

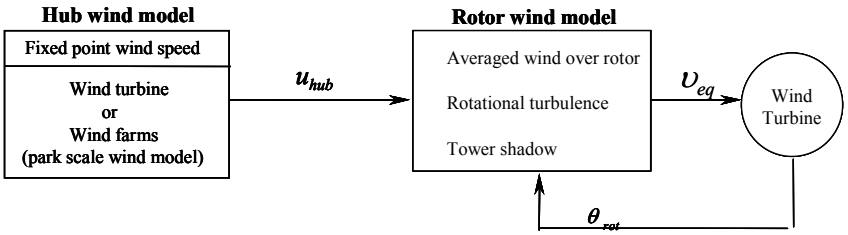

Fig. 9. Structure of the wind model.

Notice that the rotor position ϑ_{rot} is used in the wind model, and therefore this wind model can be used both variable speed and constant speed.

II. Mechanical model

In the mechanical model, the emphasis is put only on those parts of the dynamic structure of the wind turbine that contribute to the interaction with the grid. Therefore only the drive train is considered in the first place, because this part of the wind turbine has the most significant influence on the power fluctuations. The other parts of the wind turbine structure, e.g. tower and the flap bending modes are neglected.

The mechanical model is shown in Fig. 10. It is essentially a two mass model connected by a flexible low-speed shaft characterized by a stiffness k and a damping c. The high-speed shaft is assumed stiff. Moreover, an ideal gear with the exchange ratio $1:n$ gear is included.

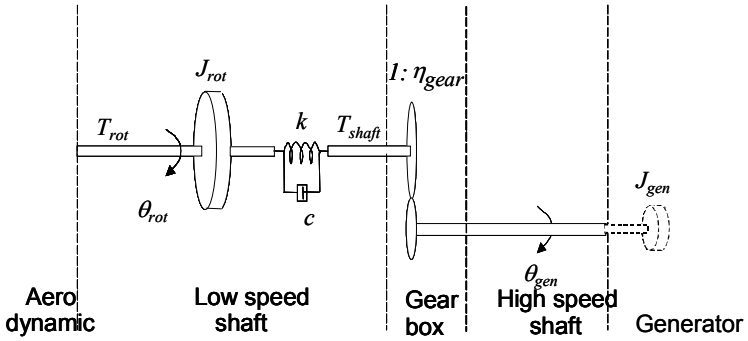

Fig. 10. Mechanical model of wind turbine drive train.

The two masses correspond to the large turbine rotor inertia J_{rot}, representing the blades and hub, and to the small inertia J_{gen} representing the induction generator. The generator inertia is actually included in the generator models in DIgSILENT.

The drive train converts the aerodynamic torque T_{rot} of the rotor into the torque on the low speed shaft T_{shaft}. The dynamical description of the mechanical model consists of three differential equations, namely:

$$\begin{aligned} \dot{\theta}_{rot} &= \omega_{rot} && [rad/s] \\ \dot{\theta}_{k} &= \omega_{rot} - \frac{\omega_{gen}}{n_{gear}} && [rad/s] \\ \dot{\omega}_{rot} &= (T_{rot} - T_{shaft})/J_{rot} && [rad/s^2] \end{aligned} \qquad (1)$$

Where $\vartheta_k = \theta_{rot} - \theta_{gen}/n_{gear}$ is the angular difference between the two ends of the flexible shaft. The mechanical torque on the low speed shaft and the mechanical power of the generator are:

$$\begin{aligned} T_{shaft} &= c\,(\omega_{rot} - \frac{\omega_{gen}}{n_{gear}}) + k\,\theta_k && [Nm] \\ P_t &= \omega_{gen}\,\frac{T_{shaft}}{n_{gear}} && [W] \end{aligned} \qquad (2)$$

The damping coefficient c is given by:

$$c = 2 \xi \sqrt{k J_{rot}} \tag{3}$$

where ξ is the damping ratio and can be expressed using the logarithmic decrement δ_s:

$$\xi = \frac{\delta_s}{\sqrt{\delta_s^2 + 4\pi^2}} \tag{4}$$

The logarithmic decrement is the logarithm of the ratio between the amplitude at the beginning of the period and the amplitude at the end of the next period of the oscillation:

$$\delta_s = \ln\left(\frac{a(t)}{a(t+t_p)}\right) \tag{5}$$

where a denotes the amplitude of the signal.

III. Aerodynamic model

The aerodynamic model is based on tables with the aerodynamic power efficiency $C_p(\theta,\lambda)$ or torque coefficient $C_q(\theta,\lambda)$, which depend on the pitch angle ϑ and on the tip speed ratio λ. This is a quasistatic aerodynamic model which determines the output aerodynamic torque directly from the input wind speed according to:

$$T_{rot} = \frac{P_{rot}}{\omega_{rot}} = \frac{1}{2\ \omega_{rot}}\ \rho\ \pi\ R^2\ \ u^3\ \ C_p(\theta,\ \lambda) \qquad \text{a)}$$

or

$$T_{rot} = \frac{1}{2}\ \rho\ \pi\ R^3\ \ u^2\ \ C_q(\theta,\ \lambda) \qquad \text{b)}$$

The aerodynamic model can also include a model for dynamic stall as described in [7]. The implemented model for dynamic stall is based on Øye's dynamic stall model [8].

IV. Aggregation modeling

Aggregated modeling of large wind farms is commonly used to facilitate the investigation of the impact of a large wind farm on the dynamics of the power system to which it is connected. This type of modeling is often used in system studies where the concern is not on the individual wind turbines but on the impact of the entire farm on the power system. The advantage of an aggregated model is that it eliminates the need to develop a detailed model of the wind farm with tens or hundreds of wind turbines and their interconnections and that it reduces both the complexity of the system and the computation time substantially.

The idea of the aggregation is to represent an entire large wind farm in voltage stability investigations by one equivalent lumped wind turbine with re-scaled power capacity. According to [9], the mutual interaction between converter control systems of the wind turbines equipped with the DFIG can be neglected.

PowerFactory DIgSILENT offers a built-in directly aggregation technique for the electrical system (i.e. generator, power converter, transformer, capacitor, inductance) of the wind turbine [10]: for example, the generator and the transformers, can be modeled directly by a certain number of parallel machines or transformers, respectively, while the other electrical components (power converter, capacitance, inductance) and control can be up scaled accordingly to the increased power flow. The mechanical part of the wind farm aggregated model, namely the shaft model, the aerodynamics and the pitch system, is modeled as for one individual wind turbine. The mechanical power used as input to the aggregated generator is then the mechanical output from one turbine multiplied with the number of turbines in the wind farm.

3.1 Fixed speed SCIG

Two versions of models for the active stall controlled wind turbine have been developed and used at Risø-DTU National Laboratory. The two models reflect the wind turbine development and according to requirements in e.g. the Danish grid codes.

The first version described in [11] was developed to simulate the first generation of active stall / combi stall turbines. Originally, the concept was developed because the blades became too big for tip breakers, and therefore the whole blade had to become

pitchable. This pitch was further used to remove one of the problems with passive stall, namely that the maximum power and maximum shaft torque cannot be controlled actively, since the maximum power of a passive stall controlled wind turbine is influenced e.g. by weather conditions (air density) and grid frequency. This first generation of active stall controlled wind turbines would reduce the pitch activity to a minimum, and thus had a relatively slow power control. Also reactive power control was slow, because the capacitor bank used mechanical contactors.

The second model described in [12] was optimized for grid support, and it is in that respect expected to be quite similar to the Nysted wind turbine. On the active power control side, it responds within a few seconds to changes in the power set point, and on the reactive power side, it assumes dynamic phase compensation using a thyristor switched capacitor bank.

Fig. 11 illustrates a typical example layout of the active stall wind turbine. The induction generator, soft starter, the capacitor bank for reactive power compensation and the step-up transformer are all placed in the nacelle, and thus the transformer is considered part of the wind turbine. The control of active and reactive power is based on measured power at the Main Switch Point MSP.

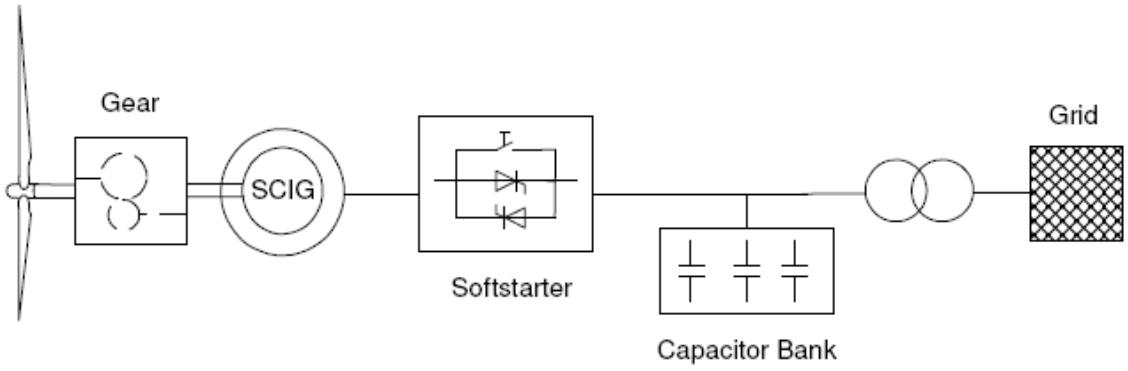

Fig. 11. Active stall wind turbine layout including softstarter and capacitor bank.

3.1.1 Grid support active power controller

Wind turbine active power controller must be able to adjust the wind turbine production to the power reference demanded by the system operator. In case of normal operation conditions, the wind turbine has to produce maximum power. In power

limitation operation mode, the wind turbine has to limit its production to the power reference received from a wind farm controller or directly from the system operator. The power reference required from the wind turbine can be equal to the rated power of the wind turbine or less than that. Fig. 12 illustrates the power curve and C_p curves for a 2 MW active stall wind turbine for different imposed power setpoints.

Notice that by imposing a power set point lower than the designed rated power of the wind turbine, the wind turbine range with high aerodynamic efficiency is, as expected, reduced, while the maximum aerodynamic efficiency is moving toward lower wind speeds.

The model described in [11] is a traditional power controller designed for a typical active stall wind turbine. This traditional controller is very slow because it tries to reduce the pitch activity as much as possible to limit the stress of the pitch system. Such a controller design is not optimal for grid support, since in this case the wind turbine or the wind farm is asked to act as a fast active element in the power system. To speed up the power control, a new active stall power controller is proposed and described in this chapter. To provide the best grid support, the aim is to use a simpler power controller, which enables fast control of the wind turbine power to different power setpoints imposed for example by system operator.

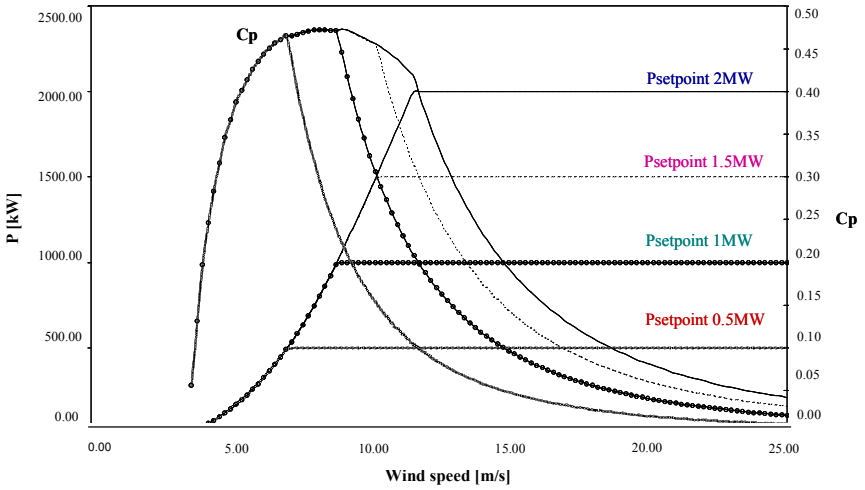

Fig. 12. Power curve and Cp curve for different wind turbine power setpoints.

Fig. 13 illustrates the power control scheme for an active stall wind turbine described in [12]. A PI controller with antiwind-up ensures a correct active power production from

the wind turbine both in power optimization control and power limitation control modes. The input of the controller is the error signal between the measured active power at the Main Switch Point (MSP) and an imposed active power reference. The PI controller produces the pitch angle reference θ_{ref}, which is further compared to the actual pitch angle ϑ and then the error $\Delta\theta$ is corrected by the servomechanism. In order to get a realistic response in the pitch angle control system, the servomechanism model accounts for a servo time constant T_{servo} and the limitation of both the pitch angle and its gradient. The output of the actuator is the actual pitch angle of the blades.

The available power of the wind turbine can be monitored at each instant, based on the wind turbine's power curve and the filtered wind speed u_f, as illustrated in Fig. 13. The wind speed is filtered appropriately to avoid unnecessary fluctuations.

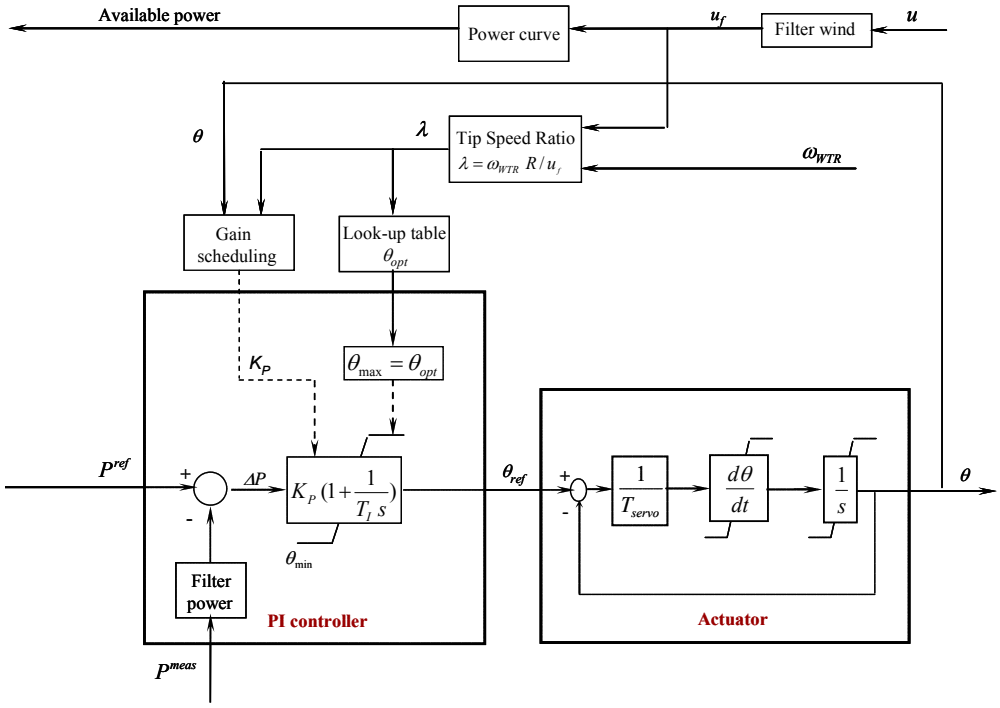

Fig. 13. Grid support active power control scheme.

In the power optimization control mode, the controller has to maximize the power production. In this case the difference between the measured power and its reference value is always positive and is integrated up until the pitch reference angle reaches the upper limit of the controller. The optimal pitch angle is thus given by the upper limitation of the controller. This upper limitation is calculated on-line based on an "optimal pitch"

look-up table as a function of the estimated tip speed ratio $\lambda = \omega_{WTR} R / u_f$, where ω_{WTR} is the wind turbine rotor speed, R is the rotor radius and u_f is the filtered wind speed.

In the power limitation control mode the error signal ΔP of the controller is negative and therefore the pitch angle moves from the upper limitation and starts to actively drive the measured power to the power reference. Notice that the measured power used in the error signal is low pass filtered in order to avoid the 3p fluctuations (three times the rotational frequency) in the power causing the pitch angle to fluctuate with the 3p frequency as well. This is because it is assumed that the pitch system is too slow to remove the 3p from the power, and thus the 3p fluctuations in the power would stress the system unnecessarily.

Compared with the controller presented in [11], the controller presented in [12]. contains an additional gain scheduling control of the pitch angle in order to compensate for the existing non-linear aerodynamic characteristics. The gain scheduling is necessary to ensure that the total gain of the system remains unchanged irrespective of the operational point of the wind turbine. The non-linear aerodynamic characteristics imply that the effect of pitching on the power varies depending on the operational point. The goal of the gain scheduling is therefore to change the proportional gain of the controller K_p in such a way that the total gain of the system remains unchanged irrespective of the operational point of the wind turbine. The pitch sensitivity, namely the effect of pitching, can be expressed mathematically by $\frac{dP}{d\theta}$. The total gain K_{system} of the system can be then expressed as the proportional gain of the PI controller, K_P, times the pitch sensitivity of the system $\frac{dP}{d\theta}$, as follows:

$$K_{system} = K_P \frac{dP}{d\theta} = K_0 \left[\frac{dP}{d\theta}\right]^{-1} \frac{dP}{d\theta} = const. \qquad (6)$$

where K_0 is a dimensionless constant independent of the operation point.

The total gain of the system K_{system} is kept constant by changing K_P in such a way that it counteracts the variation of the pitch sensitivity $\frac{dP}{d\theta}$ by the reciprocal sensitivity function $\left[\frac{dP}{d\theta}\right]^{-1}$, hence:

$$K_P = K_0 \left[\frac{dP}{d\theta}\right]^{-1} \tag{7}$$

The pitch sensitivity $\frac{dP}{d\theta}$ of the system depends on the operational point of the wind turbine. The operation point of the wind turbine is characterized directly by the wind speed and the power set point and indirectly by the pitch angle and tip speed ratio. The implementation of the gain scheduling, namely the expression of the non-linear aerodynamic amplification in the system, is performed on-line based on the simulated pitch angle and tip speed ratio, according to:

$$\frac{dP}{d\theta} = \frac{1}{2} \rho \pi R^2 u_f^3 \frac{dC_p}{d\theta} \tag{8}$$

where u_f is the filtered wind speed and the power coefficient $C_p = C_p(\theta, \lambda)$ depends on the pitch angle θ and the tip speed ratio λ. Fig. 14 illustrates the pitch sensitivity for different wind speeds and power set points.

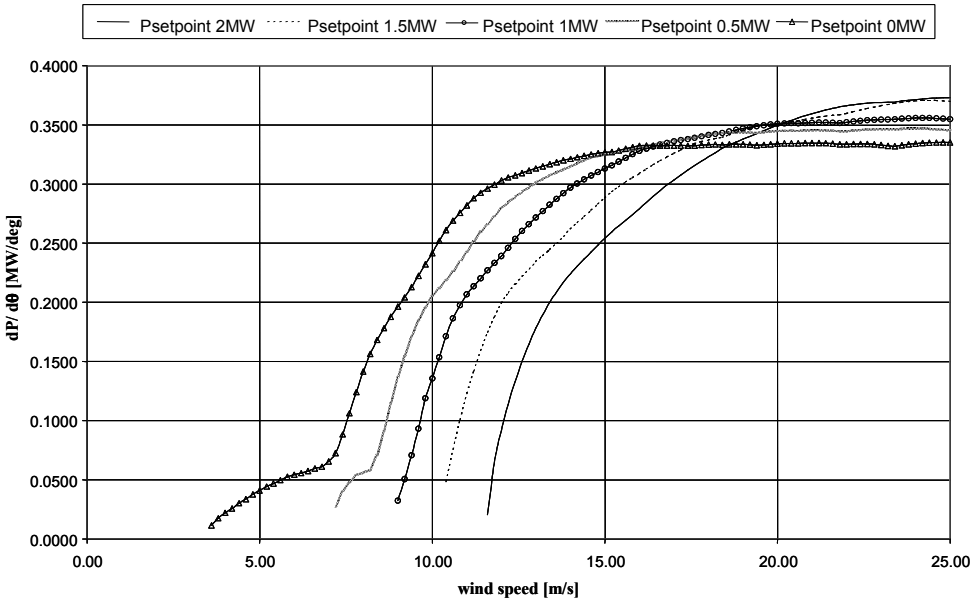

Fig. 14. Pitch sensitivity function versus wind speed for different power set points.

Notice that the pitch sensitivity increases at higher wind speeds. This shows that the more sensitive the system is (larger pitch angles θ / higher wind speeds) the smaller the gain for the controller should be and vice versa. When the active power set point is decreased, the pitch sensitivity becomes significant also for lower wind speeds.

3.1.2 Fault ride –through capability

The fault ride-through capability of an ASIG wind farm, and thus its stabilization at a short circuit fault, can be achieved by reducing the wind turbine power production for duration of few seconds from the moment of fault occurrence.

In this work, the ASIG wind turbine control strategy during grid faults is implemented based on [13]. The idea is that during the fault, the ASIG wind turbine normal controller, illustrated in Fig. 13, is switched off and replaced by a control strategy to reduce directly the mechanical power of the rotor to a predefined level. The ordering of power reduction is given for example when the monitoring of the grid voltage indicates a fault occurrence. When the grid fault is cleared, the wind turbine continues running at reduced power for still few seconds, after which it starts to ramp up the mechanical power of the rotor and re-establish the control for ASIG wind turbine normal operation conditions.

3.1.3 Grid support reactive power controller

Compared with the controller described in [11], the wind turbine controller presented in [12]. contains also an additional controller for the reactive power of the wind turbine. As illustrated in Fig. 11, a capacitor bank is chosen to compensate for the reactive power absorbed by the induction generator or required by the grid operator. The reactive power consumption of an induction generator is a function of its loading and it increases as the active power increases. The power factor of the induction generator at rated load is usually in the range of 0.85-0.90, which means that the consumption of reactive power is typically about half of the active power generation. This aspect is taken into account in the design of the size of the capacitor bank. In order to be able to produce reactive power to the grid, the size of capacitor bank should thus be larger than the amount of reactive power consumed by the generator.

In the present implementation, a standard DIgSILENT SVC component is used to model the capacitor bank instead of a number of individual capacitors as used in earlier models [7]. The SVC component is a standard component in DIgSILENT and has the advantage of being an effective and easier way to simulate a capacitor bank consisting of several capacitor steps of the same size.

The standard SVC component is a combination of a shunt capacitor bank and a thyristor controlled reactance (TCR). The thyristor controlled reactance is usually used for a continuous control of reactive power. However, the compensation unit in wind turbines consists only of capacitors. Thus the TCR part of the standard SVC component is deactivated in the design of the present SVC control.

A discrete control of SVC is implemented using the dynamic simulation language DSL of DIgSILENT – see Fig. 15. The capacitors in the capacitor bank can be switched on and off individually by the control system, depending on the load situation, in response to changes in the reactive power demand.

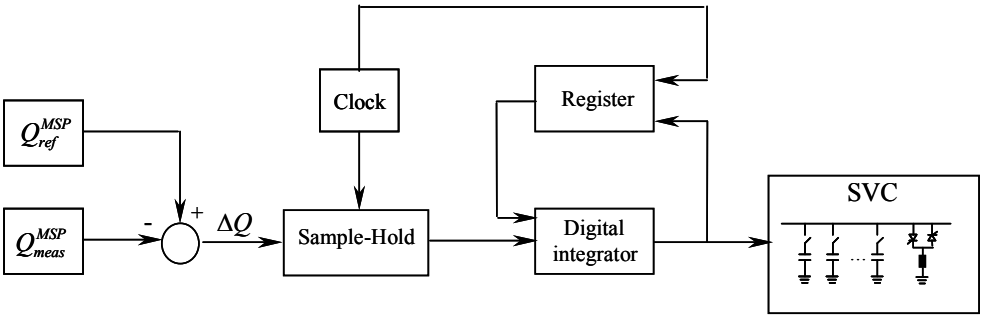

Fig. 15. Designed SVC control for the active stall wind turbine.

The difference ΔQ between the measured reactive power Q_{meas}^{MSP} on the low voltage side of the step-up transformer at the Main Switch Point MSP (see Fig. 15) and an imposed reference reactive power Q_{ref}^{MSP}, is used inside a sample-hold block. This block stores its sampled input signal at the output until the next rising edge of the clock signal appears. The clock supervises furthermore a register, which memorizes the number of capacitors, which have been switched on at the previous clock period. For each clock period, based on the new updated and the old loading situation, a digital integrator determines the required number of capacitors.

The control system of SVC has to solve a dilemma: it must be able to switch the capacitors fast in order to be able to support the grid but on the other hand it should not

attempt to control the 3p fluctuations in the reactive power consumption of the induction generator due to the wind fluctuations. The traditional wind turbines with directly connected induction generators are equipped with standard capacitor banks using mechanical contactors, which are typically controlled in intervals of 1-10 minutes. This control is not fast enough in the case when the turbine has to support the grid. However, if the capacitors are switched more often using mechanical contactors, the transients due to the switchings will reduce the lifetime of the capacitors and contactors too much. To provide a faster control possibility, new wind turbines are using thyristor switches instead of mechanical contactors, which can reduce the switching transients significantly and thus make it possible to switch the capacitor much more often without reducing the lifetime significantly.

As an example, the active stall controlled Bonus wind turbines in Nysted offshore wind farm in Denmark are equipped with such a dynamic phase compensation unit, using thyristor switches. Another similar dynamic phase compensation unit was tested on a wind turbine by Sørensen et.al.[14]. This test concluded that the dynamic phase compensation technology should not be used to remove the 3p fluctuations in reactive power, because the transients caused by the many capacitor switchings appeared to cause more flicker than could be removed by dynamically compensating the 3p reactive power fluctuations.

The control system of the capacitor bank has thus to switch the capacitors fast in order to be able to support the grid, but on the other hand it should not attempt to control the 3p fluctuations in the reactive power consumption of the induction generator.

In the present work, the fast switching of the capacitors is ensured by the clock time 20 ms, while the insensitivity to 3p fluctuations in the wind speed is realized by implementing a hysteresis in the digital integrator. The output of the digital integrator is sent directly to the SVC component and thus the required number of capacitors is switched on or off. The hysteresis has been used instead for a low pass filter in order to keep a very fast response to large changes in the reactive power reference. This is regarded as important for the ability of the wind turbines to support with voltage control.

3.1.4 Simulation results – active stall wind turbine

Different scenarios are simulated to illustrate the performance of the grid support power controller and of the fault ride-through control strategy for the active stall wind turbine. The controller's performance is assessed and discussed by means of a set of simulations of a 2 MW active stall wind turbine.

Fig. 16 and Fig. 17 present simulation results of the proposed power control strategy of the active stall wind turbine, shown in Fig. 13 and Fig. 15, respectively. The active stall wind turbine is simulated at an average wind speed of 11 m/s and a turbulence intensity of 20%. This operational point for the wind turbine corresponds to a transition operational regime for the wind turbine, between power optimization and power limitation regime, where the 3p fluctuation (three times the rotational frequency) is strong.

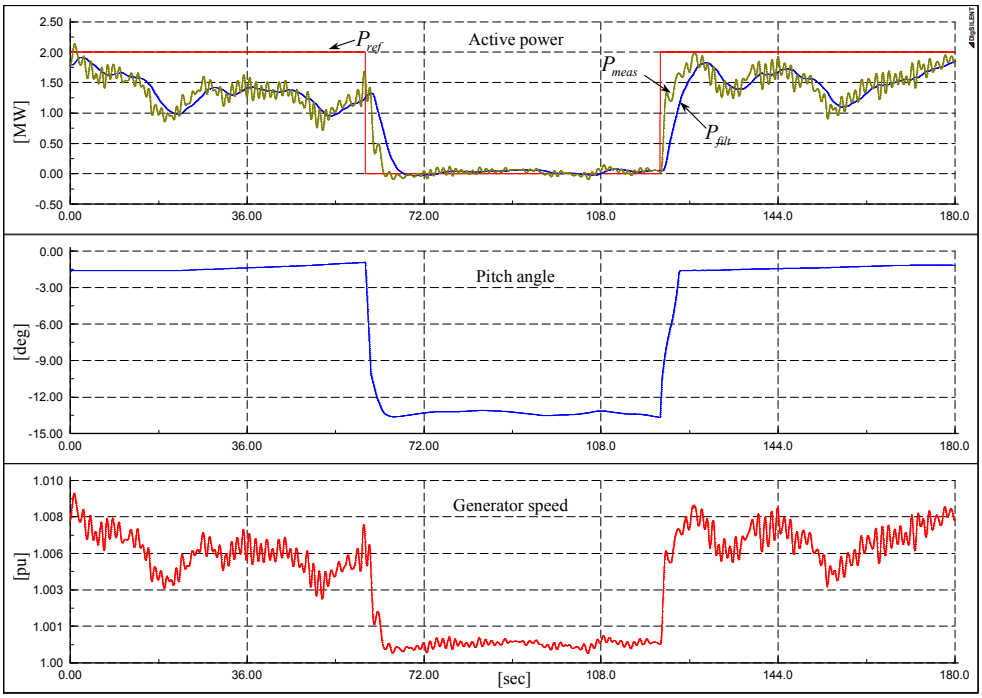

Fig. 16. Power reference response of an active stall controlled wind turbine.

Fig. 16 shows the reference power P_{ref}, the measured power P_{meas} at the MSP and the filtered measured power P_{filt} used in the controller, together with the pitch angle and generator speed, respectively. As expected for an active stall wind turbine, the 3p fluctuation is present in the measured electrical power P_{meas}. In order to illustrate the performance of the active stall wind turbine controller, the following sequence is

assumed. The first 60 sec, the power reference is set to the rated power (i.e. 2 MW). The power reference is then stepped down to 0 MW and after 120 sec it is stepped back again to 2 MW.

In the first and last 60 sec of the simulation, by setting the power reference equal to the rated power for a wind speed less than the rated wind, the wind turbine has to produce maximum possible power. In this case the pitch angle is set by the upper limit of the controller given by the "optimal pitch" look-up table – see Fig. 13. The wind turbine is then ordered to work in the power limitation mode when the power reference is set to 0 MW. In this control mode, the turbine has to produce less than it is capable of and therefore the power controller starts to actively drive the measured power to the power reference. The controller has been tuned so that the pitch angle changes smoothly from one steady state operational point to another without any overshoot. A reduction of the power production implies a more negative pitch angle and a smaller generator speed (slip). The demand of producing 0 MW is achieved while the wind turbine operates close to the border between generator and motor modes.

Fig. 17 gives a more detailed view on the power and the pitch angle in the moment when the power reference is stepped down to 0 MW. The new power reference is reached in 4-5 seconds. The change in the pitch angle is limited by the pitch rate limiter $\pm 8\,\mathrm{deg}/s$, which exists in the actuator.

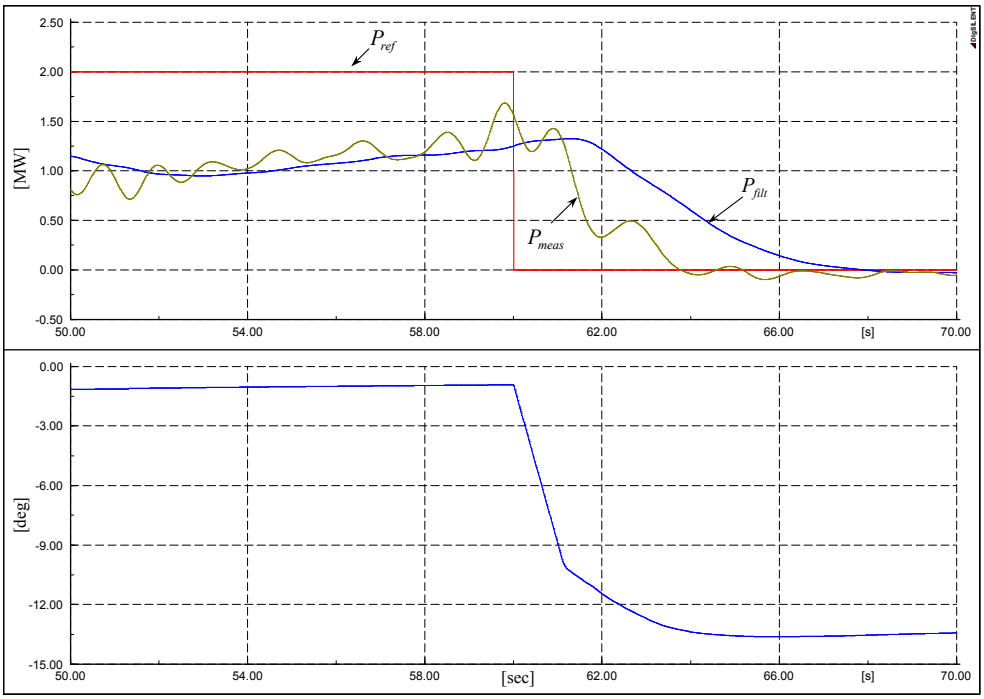

Fig. 17. Detailed view of the power reference responses illustrated in Fig. 16.

Fig. 18 shows how an active stall wind turbine equipped with fault ride- through capability behaves during a grid fault. It is assumed that the wind turbine operates at 12 m/s, corresponding to a rated power operation. A 3 phase short circuit closest to the wind turbine, i.e. on 10kV busbar, that lasts for 100ms is simulated. Fig. 18 shows the generator stator voltage, generator speed, pitch angle and the mechanical power of the wind turbine. As expected, the generator voltage drops right after the grid fault and recovers to its initial value when the fault is cleared after 100 msec. During grid fault, the turbine accelerates as the aerodynamic torque is no longer balanced by the electromagnetic torque of the generator. Notice that, as soon as the fault is detected, the normal operation control strategy is switched off and replaced by the open loop fault operation controller, which has to reduce the power production to a predefined level. The pitch angle ramps down to a fault operation pitch set point. The change in the pitch angle is limited by the pitch rate limiter existing in the servo mechanism. As soon as the fault is cleared and the voltage is recovered to the required range, the wind turbine continues still running at reduced power for still few seconds, before it ramps up the mechanical power of the rotor. The pitch system ramps then up the pitch angle to its normal operation conditions value.

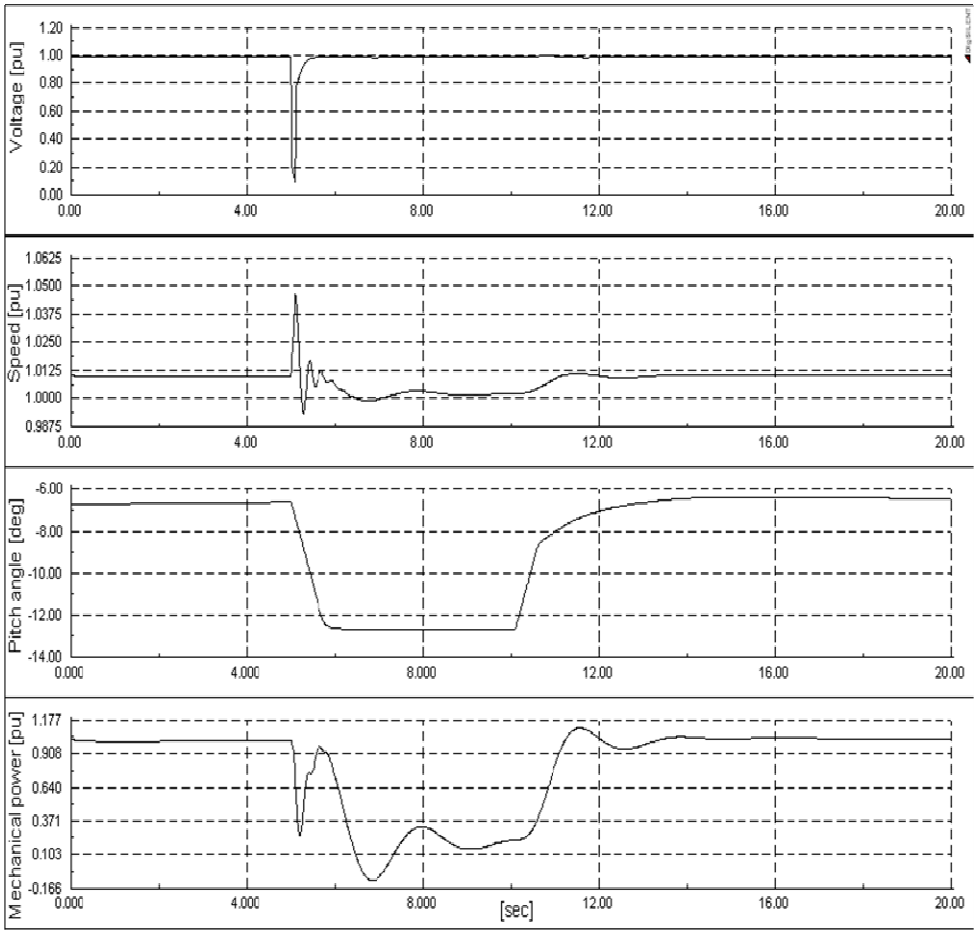

Fig. 18. Fault ride-through capability of active stall wind turbine.

Fig. 19 illustrates the simulation results for the reactive power control, sketched in Fig. 15. The simulation case is the same as shown in Fig. 16.The reactive power at the MSP is controlled to zero by switching on or off a certain number of capacitors. In the present simulation a capacitor bank consisting of 12 steps with 0.1 MVar is used. A clock with 20 ms sampling period ensures a necessary fast switch of the capacitors. With this fast sampling period, as seen in Fig. 19, the reactive power is changed immediately by capacitor switchings as soon as the reactive power exceeds the hysteresis interval ±150 kVar. Fig. 19 also shows the number of capacitors switched during the simulation. Notice that, as expected, a step down in the active power reference implies a reduction of the reactive power demand and, as a result, the number of connected capacitors is decreased.

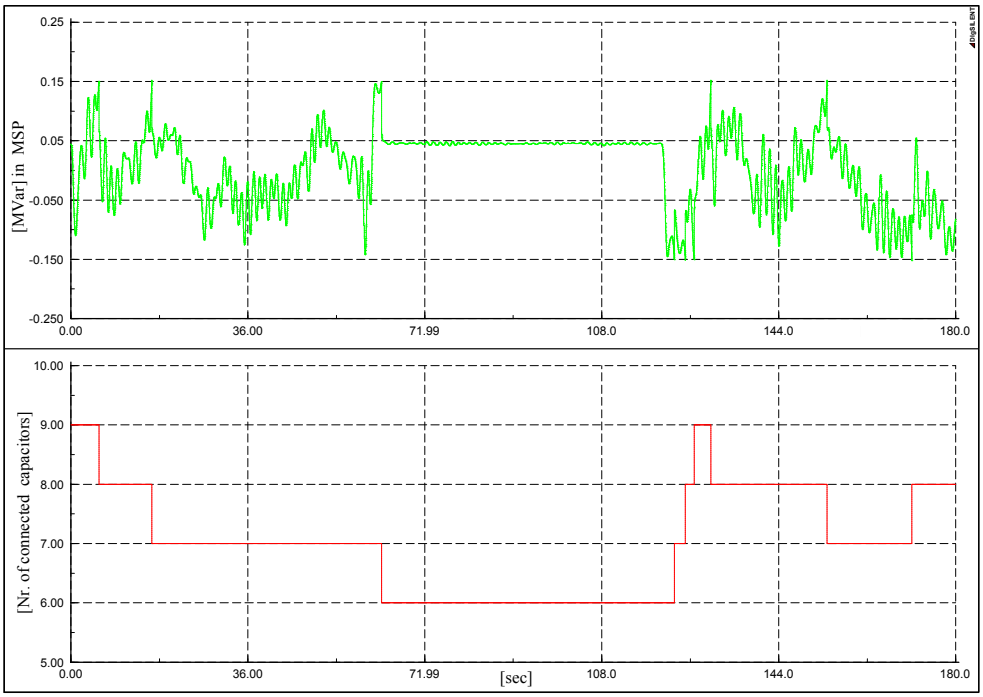

Fig. 19. Reactive power control for the active stall controlled wind turbine.

Fig. 20 illustrates the response of the active stall wind turbine at different steps in the power reference. It is assumed that the wind turbine is simulated at high wind speed, approximately 16m/s, including turbulence with rotational sampling. Initially, the power setpoint is the rated power, i.e. 2MW. The power reference is then stepped down i two steps 1 1MW and back again. Notice that the new setpoint is reached in 4-5 seconds.

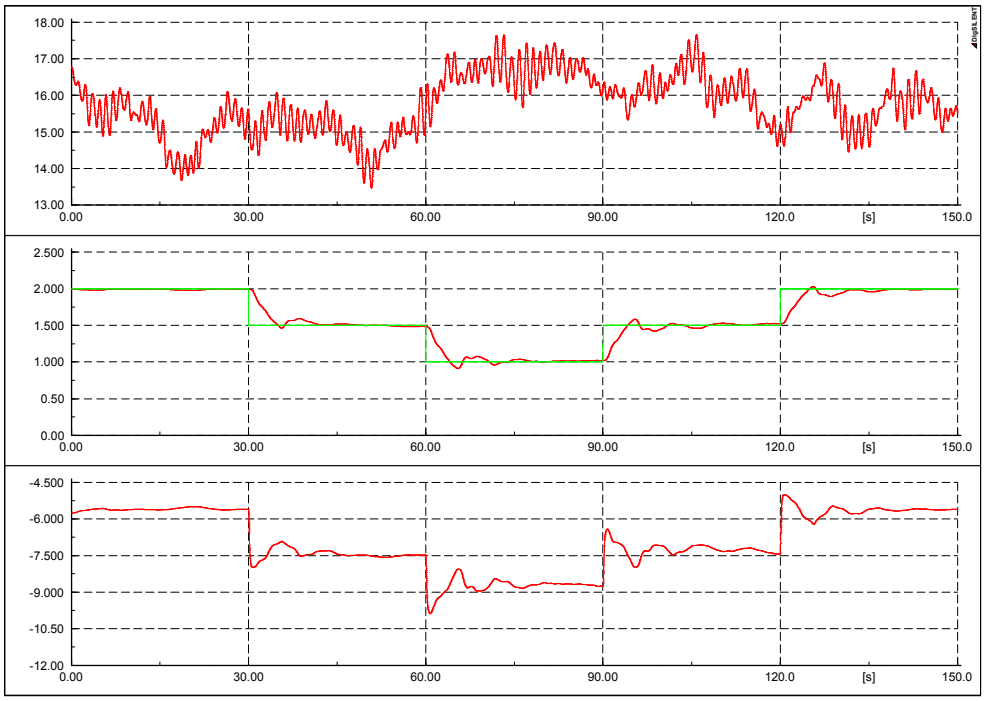

Fig. 20. Power reference response of active stall wind turbine.

The focus in the next simulations is on the wind farm controller performance in the PCC of the active stall wind farm. Therefore the simulation results only at the wind farm level are presented. Fig. 21 illustrates the performance of the wind farm power controller, when the active power demands from the grid operators is stepped down and up to different setpoints. The reactive power reference for the whole wind farm is kept to zero. The wind turbines in the wind farm are driven by different turbulent winds with 9 m/s mean speed value and 10% turbulence intensity. Fig. 21 shows the estimated available power, the power demand, the power reference and the measured power in the PCC of the wind farm. In order to test the performance it is assumed that the power demand from the operators is first stepped down from 6 to 2, 1 and 0, respectively, and then stepped up vice versa.

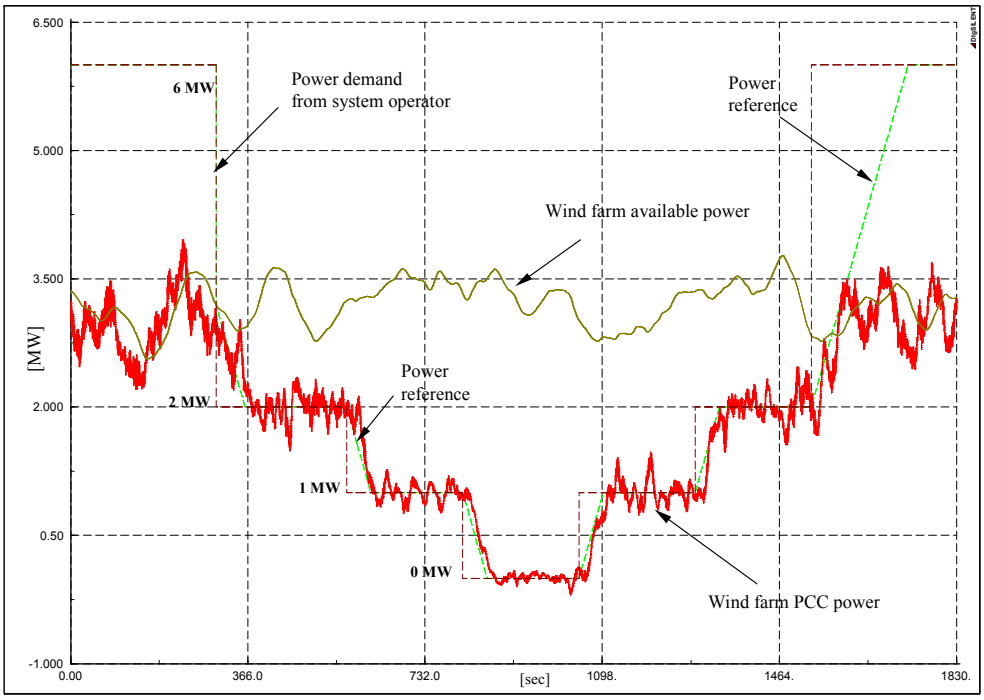

Fig. 21. Wind farm response in balance control with stochastic wind speed of 9m/s and turbulence intensity of 10%.

The first and last 300 sec, the wind farm performs a normal operation and it has to produce maximum power. Notice that in this operation mode, the power reference is set to the rated power of the whole wind farm. The wind farm controller is designed in such a way that in normal operation, it allows the wind farm to produce more than the wind farm estimated available power, if this is possible. The production is thus not restricted to the estimated available power and therefore unnecessary pitch activity at each wind turbine is avoided. Note in Fig. 21, that in the first and last 300 sec, the wind farm has the possibility to produce more than the estimated available power. At the wind turbine level this is reflected by a low pitch activity, the pitch angle being kept nearly constant to the optimal pitch value.

The simulation results show a good performance of the control system. The adjustment upwards and downwards of the wind farm production is performed with a power ramp rate limiter of about $\pm 1.2\ MW / min$. In power limitation mode the wind farm production follows properly the wind farm elaborated power reference, taking the power ramp rate limiter into account. Notice that the power fluctuations decrease at lower power references. The demand of producing 0 MW is achieved properly by the wind farm. At

the wind turbine level this is reflected by a slight oscillation in the machine's speed between generator and motor modes.

Fig. 22 illustrates the performance of the wind farm controller, when the reactive power demand from the grid operator is stepped up and down to different set points. There are two graphs: the first shows the whole sequence while the second provides a detailed view on the reactive power response at a step moment in the reactive power demand. The wind turbines are again driven by different turbulent winds with 9 m/s mean speed and 10% turbulence intensity. It is assumed that the wind farm is ordered to have maximum active power production. In order to test the performance of the reactive power wind farm controller, it is assumed that the reactive power demands from the operator are stepped up from 0 to 1, 2 and 3 respectively and then stepped down vice versa. Notice that the adjustments upwards and downwards of the wind farm reactive power production are performed very quickly as long as the size of capacitor bank permits that. The new reactive power reference is reached in less than 0.5 seconds. This quick performance is attractive from a grid support point of view. At a wind speed 9 m/s, each wind turbine generator produces around 1.1 MW and consumes about 0.5Mvar. This means that the whole wind farm consumes about 1.5 MVar. As each wind turbine presents a capacitor bank with 12 steps, each of 0.1 MVar, it means that for a wind speed about 9 m/s, the wind farm has a reactive power reserve of about 2 MVar. This is clearly illustrated in Fig. 22, when the 3 MVar reactive power demand cannot be reached.

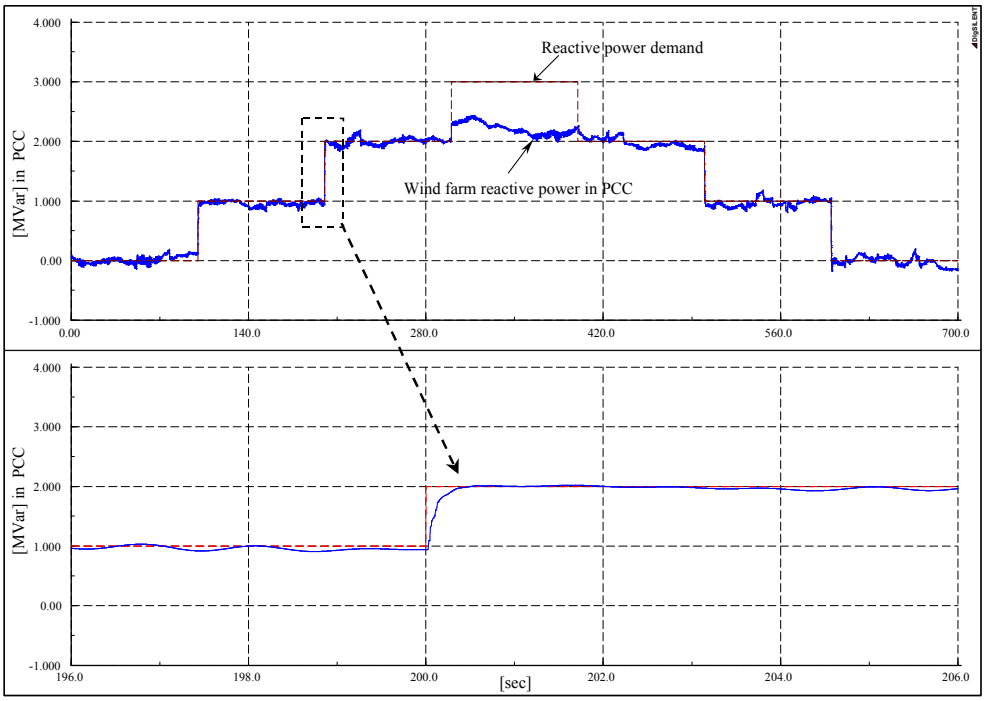

Fig. 22. Reactive power response for the wind farm.

3.2 Variable speed PMSG

A typical configuration of a variable speed wind turbine based on a multi-pole permanent magnet synchronous generator (PMSG) is illustrated in Fig. 23. It consists of:

- Wind turbine mechanical level:
  - Aerodynamics
  - Gearless drive train
  - Pitch angle control
- Wind turbine electrical level:
  - Multi-pole permanent magnet synchronous generator (PMSG)
  - Full-scale frequency converter and its control

In this configuration, the synchronous generator is connected to the grid through a full-scale frequency converter system that controls the speed of the generator and the power flow to the grid. The full-scale frequency converter system consists of a back-to-back voltage source converter (generator-side converter and the grid-side converter connected through a DC link), controlled by IGBT switches. The rating of the converter system in this topology corresponds to the rated power of the generator plus losses. The

use of such a converter enables the PMSG to keep its terminal voltage on a desired level and to adjust its electric frequency according to the optimized mechanical frequency of the aerodynamic rotor, independently of the fixed electric frequency and the voltage of the AC grid. The electric frequency fe at the PMSG terminals is the product of the mechanical frequency fm of the wind turbine rotor and the number of generator pole-pairs p:

$$f_e = f_m \; p \qquad [Hz] \tag{9}$$

where the mechanical frequency f_m of the generator rotor is related to the turbine rotor speed ω_m:

$$\omega_m = 60 \; f_m \qquad [rpm] \tag{10}$$

As illustrated in Fig. 23, the aerodynamic rotor of the wind turbine is directly coupled to the generator without any gearbox, i.e. through a gearless drive train. The permanent magnets are mounted on the generator rotor, providing a fixed excitation to the generator. The generator power is fed via the stator windings into the full-scale frequency converter, which converts the varying generator frequency to the constant grid frequency.

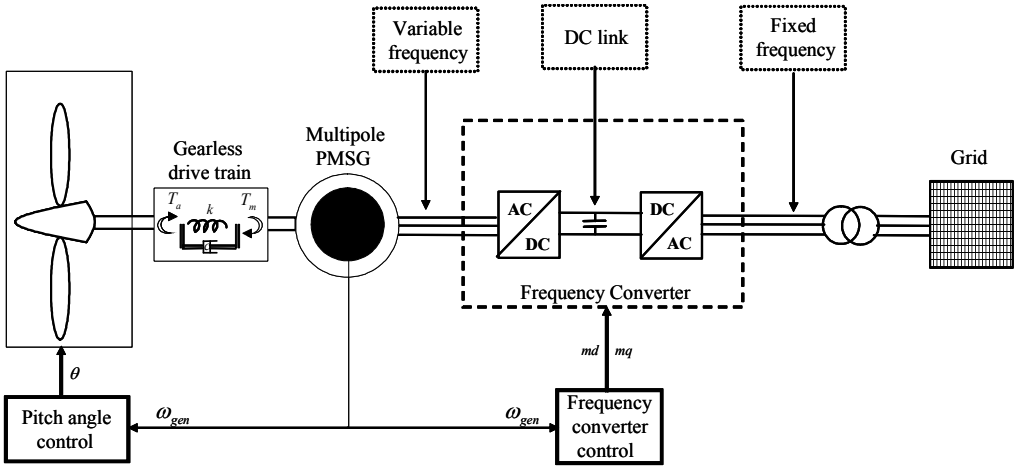

Fig. 23. Variable speed multi-pole PMSG wind turbine configuration.

3.2.1 PMSG wind turbine control during normal operation

The control system consists of two co-ordinated controllers: the wind turbine controller, i.e. pitch angle controller, and the frequency converter controller. Both controllers are using information about the generator speed. Contrarily fixed speed wind turbines, where the power flow to the grid is dependent on the aerodynamical power that drives the wind turbine, in variable speed wind turbines the power flow to the grid and thus the generator speed are controlled by the frequency converter according to an optimal power characteristic. The pitch controller controls the generator speed as well, but it is operational only at high wind speeds.

Since the PMSG is connected to the grid through the back-to-back converter, only the active power of the PMSG is transferred to the grid. The reactive power cannot be exchanged through the DC link in the converter system. However, the grid-side converter, whose electric frequency and voltage are fixed to the grid, can be set to control the reactive power/voltage on the grid.

The pitch angle control is realised by a PI controller with antiwind-up, using a servomechanism model with limitation of both the pitch angle and its rate-of-change, as illustrated in Fig. 24. The pitch angle controls the generator speed, i.e. the input in the controller is the error signal between the measured generator speed and the reference generator speed. The pitch angle controller limits the rotor speed when the nominal generator power has been reached, by limiting the mechanical power extracted from the wind and thus restoring the balance between electrical and mechanical power. A gain scheduling control of the pitch angle is implemented in order to compensate for the nonlinear aerodynamic characteristics [15]

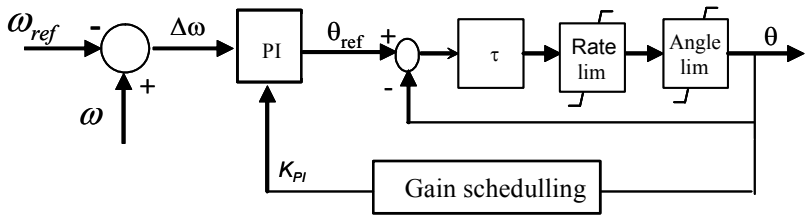

Fig. 24. Pitch angle control.

Similar to DFIG wind turbines, the PMSG wind turbines behavior is strongly dependent on the frequency converter control both in normal and fault operation conditions.

Frequency converters are usually controlled utilizing vector control techniques [16]. Briefly, vector control allows decoupled control of both active and reactive power. The idea is to use a rotating reference frame based on an AC flux or voltage and then to project currents on this rotating frame. Such projections are usually referred to as the d and q components of their respective currents. With a suitable choice of reference frames the AC currents appear as DC quantities in the steady state. For flux-based rotating frames, changes in the q component will lead to active power changes, while changes in the d component will lead to reactive power changes. In voltage-based rotating frames (and thus 900 ahead of flux-based frames) the effect is the opposite.

The frequency converter is a standard built-in model in the DIgSILENT library [17]. Its control is not a standard model in the DIgSILENT library and therefore it has to be implemented as a user-written model in the dynamic simulation language of DIgSILENT.

The control of the converter can be realized using different strategies:

- The generator-side converter controls traditionally the active power flow P_{grid} to the grid. Besides this, it has also to control the generator reactive power Q_{gen} or the generator stator voltage U_S. However, instead of the active power flow P_{grid}, the generator-side converter can also control the DC-link voltage U_{DC}. The control of the active power and of the DC-link voltage is strongly related to each other, as the active power can be fed into the grid as long as the DC-link voltage is kept constant.
- The grid-side converter controls typically the DC-link voltage U_{DC} as well as the reactive power flow Q_{grid} to the grid. Again, instead of the DC-link voltage U_{DC}, the grid-side converter can also control the active power flow P_{grid} to the grid.

In this investigation, the proposed full-scale converter control is modeled on a generic level, without focusing on any particular design of a manufacturer. As illustrated

in Fig. 25, the control uses an AC voltage oriented reference frame, i.e. d-axis to control the active current, while q-axis to control the reactive current.

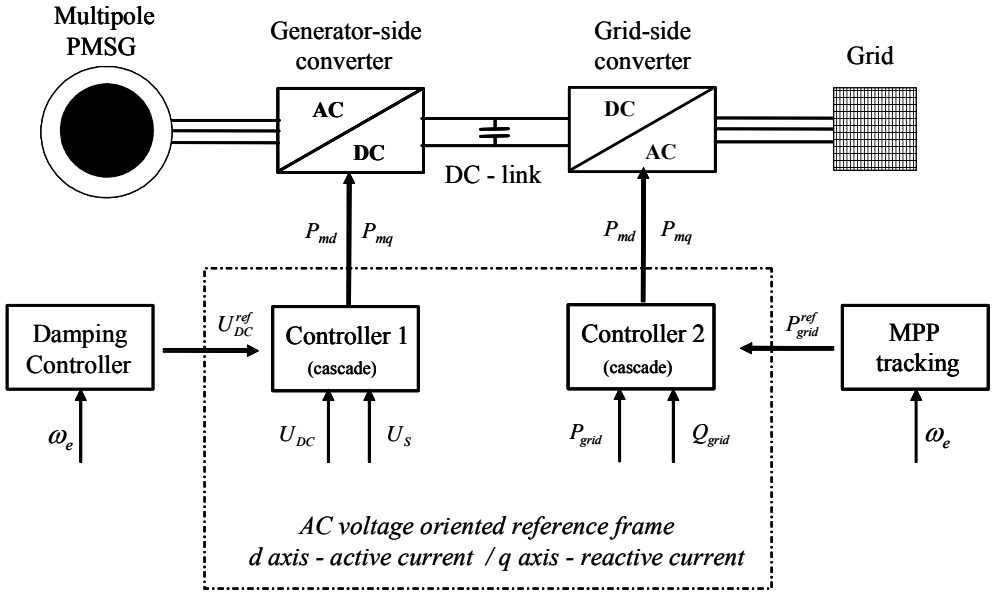

Fig. 25. Power converter control strategy of the variable speed multi-pole PMSG wind turbine.

It consists of the following controllers:

- Damping controller:
  - Ensures a stable operation of the wind turbine, by damping the torsional oscillations excited in the drive train and reflected in the generator speed ω_e.
- Generator-side converter controller (controller 1):
  - Keeps constant the DC-link voltage U_{DC} and controls the generator stator voltage U_S to its rated value in the stator voltage reference frame. The advantage of controlling the generator stator voltage U_S to its rated value is that the generator and the power converter always operate at the rated voltage, for which they are designed and optimized.
- Grid-side converter controller (controller 2):
  - Controls independently the active P_{grid} and the reactive Q_{grid} power to the grid in the grid voltage reference frame

Similar to the control of DFIG wind turbines [15], the control of the generator-side converter and the grid-side converter in variable speed multi-pole PMSG wind turbines is also based on two control loops in cascade: a very fast inner current controller regulating the currents to the reference values that are specified by the outer slower power controller. The current controller provides reference signals in d- and q- axis (P_{md} and P_{mq}) for the PWM-controlled power converter.

The reason of using a damping controller is due to the fact that a multi-pole PMSG wind turbine with full-scale converter has no inherent damping. This implies that any small speed oscillation excited by mechanical or electrical load changes, can be amplified causing self-excitation, high mechanical stress of the drive train and even instability if no external damping controller is applied. A damping controller, implemented as illustrated in Fig. 26, is acting similar to a power system stabilizer, [18]. Its goal is to influence the generator electrical torque in such a way that it counteracts the speed oscillations and ensures a stable operation of the wind turbine. The idea of the proposed damping controller is to use the DC capacitor as a short-term energy storage, i.e. the speed oscillations are buffered and reflected in an oscillating defined DC-link voltage reference U_{DC}^{ref}. This oscillating reference, to which the DC-link voltage signal is controlled, generates a generator torque component, which counteracts and damps the speed oscillations.

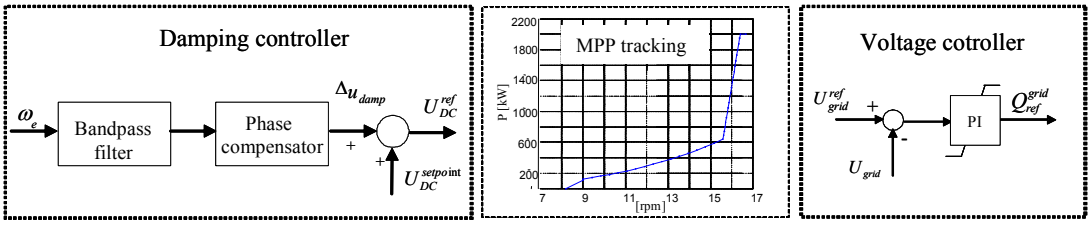

Fig. 26. Damping controller, maximum power point (MPP) characteristic and voltage controller.

The generic control of generator-side converter is illustrated in Fig. 27. It controls the DC-link voltage U_{DC} and the generator stator voltage U_S in the stator voltage oriented reference frame (SVRF). Hence, the DC voltage is controlled by the d-component of the stator current, while the stator AC stator voltage is controlled by the q-component of the stator current.

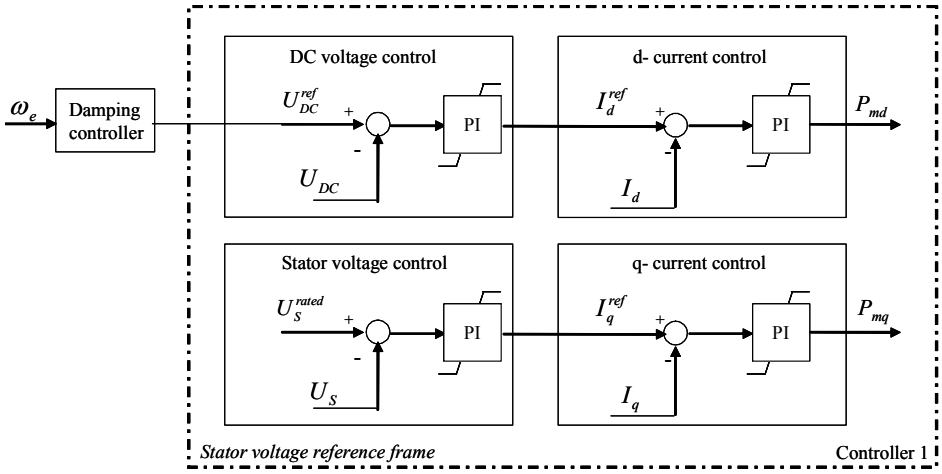

Fig. 27. Generator-side converter control (controller 1).

The stator voltage U_S is controlled to its rated value U_S^{rated}. This strategy provides a robust control of the generator as it avoids the risk of overvoltage and saturation of the converter. The disadvantage is that it implies a variable reactive power demand from the generator, which must thus be delivered by a power converter with an increased rated power.

The DC-link voltage U_{DC} is controlled to its reference value U_{DC}^{ref}. This reference signal is provided by the damping controller and oscillates with the right frequency and phase angle, which generates a torque that dampens the speed oscillations. Notice that even though the idea is to keep the DC-link voltage constant and to ensure thus the power transport from the PMSG terminals to the power grid, small variations of the DC-link voltage are however allowed since the electrical damping of the system is necessary.

The generic control of the grid-side converter is illustrated in Fig. 28. The grid-side converter controls independently the active power P_{grid} and the reactive power Q_{grid} in the grid voltage reference frame. Hence, the active power P_{grid} is controlled by the d-component of the converter current whereas the reactive power Q_{grid} is controlled by the q-component of the converter current.

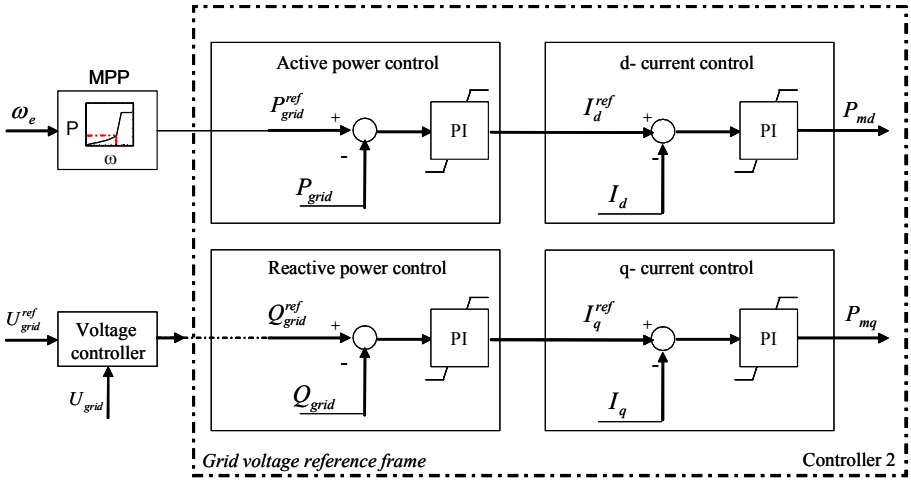

Fig. 28. Grid-side converter control (controller 2).

When there is no particular active power demand from the system operator, the reference P_{grid}^{ref} for the active power is given by the maximum power point characteristic (MPP look-up) table, illustrated in Fig. 26, as function of the optimal generator speed. The reference Q_{grid}^{ref} for the reactive power is typically set to zero, if no reactive power support is demanded. However, in the cases when the grid voltage is disturbed from its rated value and voltage grid support is demanded from the wind turbine, the reactive power reference Q_{grid}^{ref} can be provided by a voltage controller, as illustrated in Fig. 28. Such a voltage controller is realized by a PI controller with antiwind-up and it controls the grid voltage to its rated value. The input of the controller is the error signal between the measured grid voltage and the rated grid voltage.

3.2.2 PMSG wind turbine control during grid fault operation

The overall control of the PMSG wind turbine during grid fault operation is illustrated in Fig. 29 and described in details in [19].

Notice that the control uses an AC voltage oriented reference frame, i.e. d-axis to control the active current, while q-axis to control the reactive current. This means that in the generator-side converter's control, the DC-link voltage U_{DC} is controlled by the d-component of the stator current $\hat{I}_d$, while the AC stator voltage U_S is controlled by the q-component of the stator current $\hat{I}_q$. In the grid-side converter's control, the active

power P_{grid} is controlled by the d- component of the converter current $\breve{I}_d$ whereas the reactive power Q_{grid} is controlled by the q-component of the converter current $\breve{I}_q$.

Besides the reference signal for the stator voltage, all other reference signals for the power controller level are given by an outer control stage, as illustrated in Fig. 29. The reference signal for the generator stator voltage U_S is chosen to be its rated value. The advantage of controlling the generator stator voltage U_S to its rated value is that the generator and the power converter always operate at the rated voltage, for which they are designed and optimized and over voltages in the converter can be avoided. The outer control stage contains a damping controller, a maximum power tracking characteristic and a voltage controller – as illustrated in Fig. 29. Their design and performance have been presented in details in [20], and therefore only their main function is shortly addressed in the following.

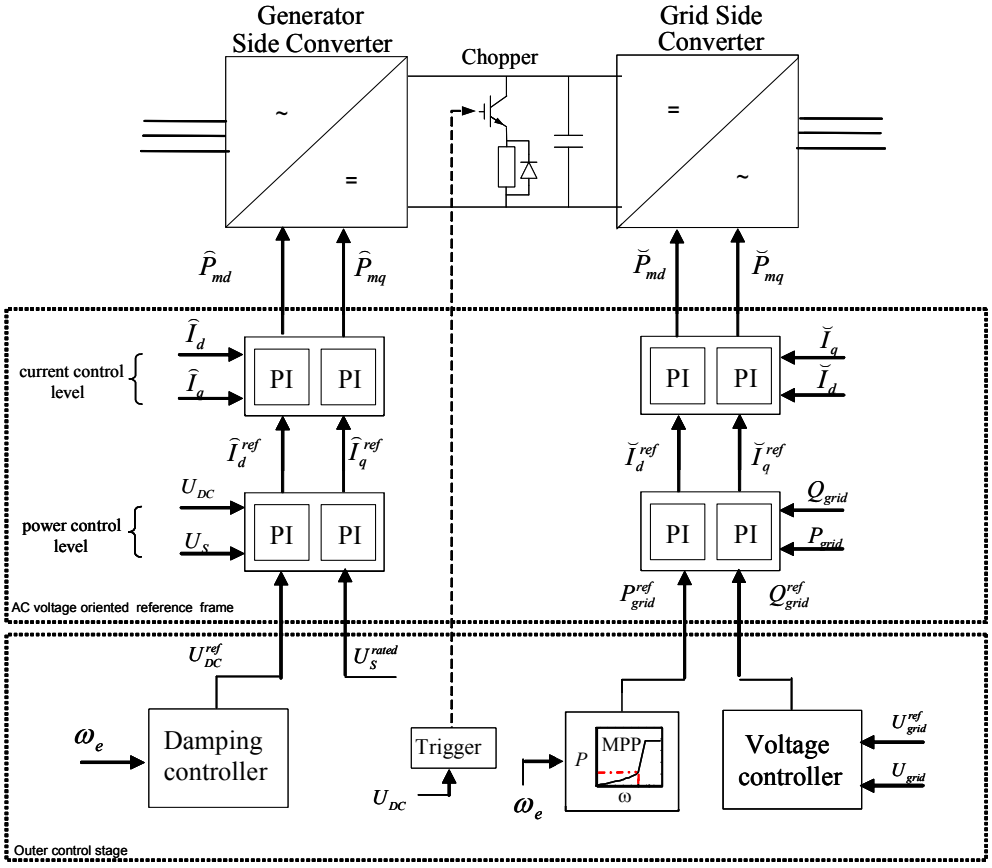

Fig. 29. Converter control strategy used in this work.

If there is no particular active power reference specified by the power system operator, the reference P_{grid}^{ref} for the active power control is given by the maximum power point (MPP) characteristic, illustrated in Fig. 29, as function of the optimal generator speed. This speed-power characteristic drives the turbine automatically in the operating point with the highest aerodynamic efficiency.

Notice that, since the PMSG generator is connected to the grid through a full-scale converter, only the active power of the generator is transferred to the grid. As the reactive power of generator cannot be exchanged through the DC-link in the converter system, the grid-side converter, whose electric frequency and voltage are fixed to the grid, can be set to control the reactive power/voltage on the grid. Notice that the reactive power production of the grid-side converter is thus independent by the reactive power set point of the generator, being limited only by the grid-side converter rating.

The reference Q_{grid}^{ref} for the reactive power is typically set to zero, if no reactive power support is demanded from the wind turbine. However, in the cases when the grid voltage is disturbed from its rated value and voltage grid support is demanded from the wind turbine, the reactive power reference Q_{grid}^{ref} can be assured by implementing a voltage controller, as illustrated in Fig. 29. Such a voltage controller is realized by a PI controller with antiwind-up and it controls the grid voltage to its rated value. Depending on the difference between the measured grid voltage and the reference voltage, the voltage controller demands thus the grid-side converter controller to provide or to consume reactive power in order re-establish the grid voltage level.

In the control strategy presented here, sketched in Fig. 29, the fault ride-through capability of PMSG wind turbine is directly integrated in the control design. In this control strategy, besides the stator voltage, the generator-side converter has to control the DC-link voltage. As the generator-side converter is not directly connected to the grid, and thus not affected during grid faults, it is able to fulfill its task to control the DC-link voltage undisturbed, also during faults. Meanwhile, as the grid-side converter is directly affected by grid faults, it can transfer less power to the grid than in normal operation conditions. As a consequence, the generator-side converter control reduces the generator power and thus the power flow to the DC-link, by decreasing the stator current, in order

to keep constant the DC-link voltage. Notice that the power imbalance, otherwise present in the DC-link during grid faults when the traditional control strategy is used, is transferred in this case to the generator. The power surplus is buffered in rotational energy of the large rotating masses. The power imbalance is thus reflected in the acceleration of the generator, which, in case when the generator speed increases above its rated value, is directly counteracted by the pitch controller, illustrated in Fig. 24. Notice that, due to the sudden loss of electrical power, the drive train system acts like a torsion spring that gets untwisted. It starts therefore to oscillate. These torsional oscillations of the drive train are quickly damped by the designed damping controller

Notice that the simple reversal of the converter's functions in the new control strategy compared to the traditional one, makes it thus possible for the multi-pole PMSG wind turbine concept equipped with the new control strategy to ride-through during grid faults, without any additional measures, such as chopper or cross-coupling control between the generator-side converter and grid-side converter.

Nevertheless, a chopper can be however used to enhance even more the fault ride-through capability of a multi-pole PMSG wind turbine equipped with the new control strategy. The use of a chopper in this case can reduce the amplitude of the oscillations in the shaft torque and thus the mechanical stress of the drive train system during grid faults.

3.2.3 Simulation results – PMSG wind turbine

Different scenarios are simulated to illustrate the performance of the grid support power controller and of the fault ride-through control strategy for a variable speed PMSG wind turbine. The controller's performance is assessed and discussed by means of a set of simulations of a 2 MW PMSG wind turbine.

Fig. 30 presents simulation results where the multi-pole PMSG wind turbine assists the power system. The capability to control independently the active and reactive power production to the grid is also illustrated. The wind turbine is simulated at an average wind speed of 11m/s and a turbulence intensity of 10%. This operation point corresponds to a transition operational regime for the wind turbine, between power operation and power limitation regimes. In order to illustrate the performance of the wind turbine's control system, the following sequence is assumed. During the first 80 s, the wind turbine has to produce maximum active power. In this case the pitch angle is set to zero as the wind

turbine works in the power optimization regime, while the speed tracks the slow variations in the wind speed. The power reflects the optimal power according to the generator speed and the MPP look-up table. The time period between 30 and 60s a reactive power demand of 1MVar is required from the wind turbine. Notice that the generated active power is not altered by the step in the reactive power demand, its variations being only due to the turbulent wind. In the time period between 80 and 170s, the active power reference is first stepped down to 1MW, then after 30s down to 0MW and then it is stepped back again to 1MW after 30s and then finally back to maximum power demand at the time 170s. In this control mode the turbine has to produce less than it is capable of and therefore the grid-side converter controller starts to actively drive the measured power to the imposed power reference. A reduction of the power production implies as expected an increased pitch angle and generator speed. The time period between 200 and 230s, the wind turbine is demanded to absorb 1MVar from the grid - a request which is also very well accomplished.

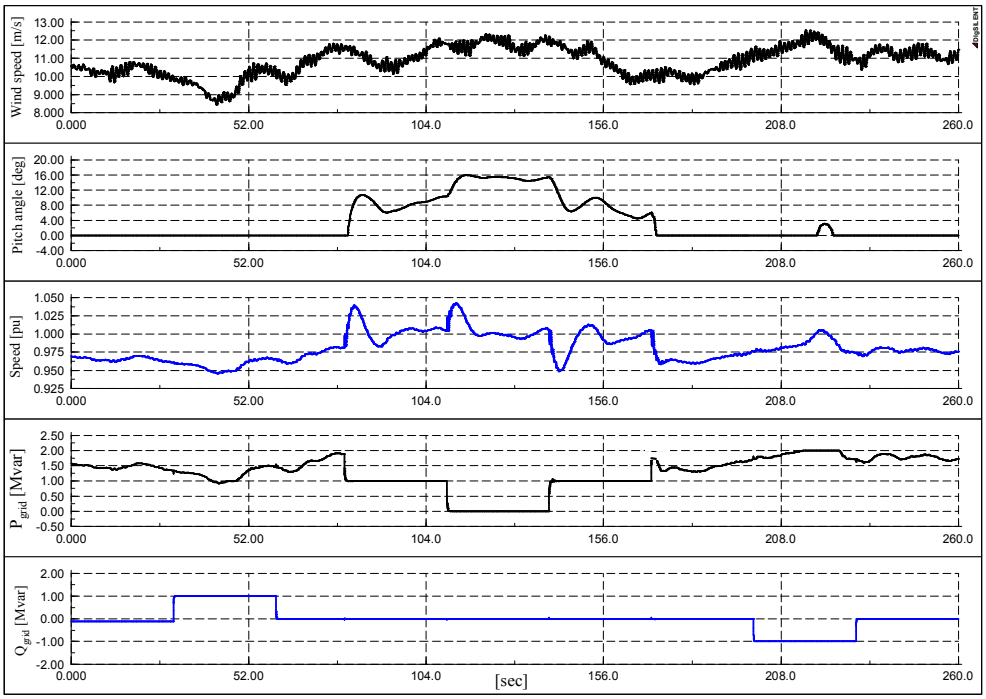

Fig. 30. Power grid support. Simulation sequence: during 0 - 80s maximum active power demand; during 30 – 60s reactive power demand of 1MVar; at time 80s active power demand of 1MW; at time 110 s active power demand of 0MW; at time 140s active power demand of 1MW; during 170 – 260s maximum active power demand; during 200-230s reactive power demand of -1MVar.

The simulation results indicate good performance of the presented control system. The specified references both for the active and reactive power are achieved properly. This illustrates that if it is required, the multi-pole PMSG wind turbine can operate as a conventional power plant, i.e. it can produce or absorb reactive power and it can adjust actively its active power production according to system operator demands.

To assess the performance of the voltage controller, presented in Fig. 28, a simulation is performed with two reactive power sinks (one of 1MVar and the other of 1.5MVar) connected at the MV terminal of the PMSG wind turbine and disconnected after 1 sec, successively.

The grid voltage and the reactive power supplied to the grid by the grid-side converter are illustrated in Fig. 31 for the situations with and without voltage controller, respectively. It is assumed that the 2MW PMSG wind turbine operates now at its rated capacity (i.e. at wind speeds higher than 12m/s), as this is worst for voltage stability.

Notice that the connection of each reactance implies as expected a drop in the grid voltage U_{grid}. The voltage drop is about 22% when the 1MVar reactance is connected and about 30% when the second 1.5MVar reactance is connected later. When no voltage control is enabled (case 1 in Fig. 31), no reactive power support is delivered to the grid by the grid-side converter. The voltage drop is not compensated by reactive power and the voltage recovers to its nominal value only when the reactance is disconnected.

On the other hand, when the voltage controller is used (case 2), the grid-side converter supports the grid by supplying reactive power – as illustrated in Fig. 31. The voltage controller notices the deviation in voltage and commands more reactive power. The increased reactive power supplied by the grid-side converter re-establishes the grid voltage to 1pu in less than 100ms when the first 1MVar reactance is connected. Notice that the supplied reactive power is higher than the value of the connected reactance 1MVar. The reason is that the converter also has to compensate for the reactive power absorbed by the transformer placed between the grid-side converter and the PCC. The 2MW PMSG wind turbine connected to the grid through the 2.5MVar converter has a reactive power reserve about 1.5MVar when it operates at its rated capacity, as it is the present case of 12m/s wind speed. Notice that the voltage is not completely re-established

when 1.5MVar is connected even though the voltage controller is enabled. The reason for this is that the reactive power reserve of 1.5MVar of the converter is reached in this case.

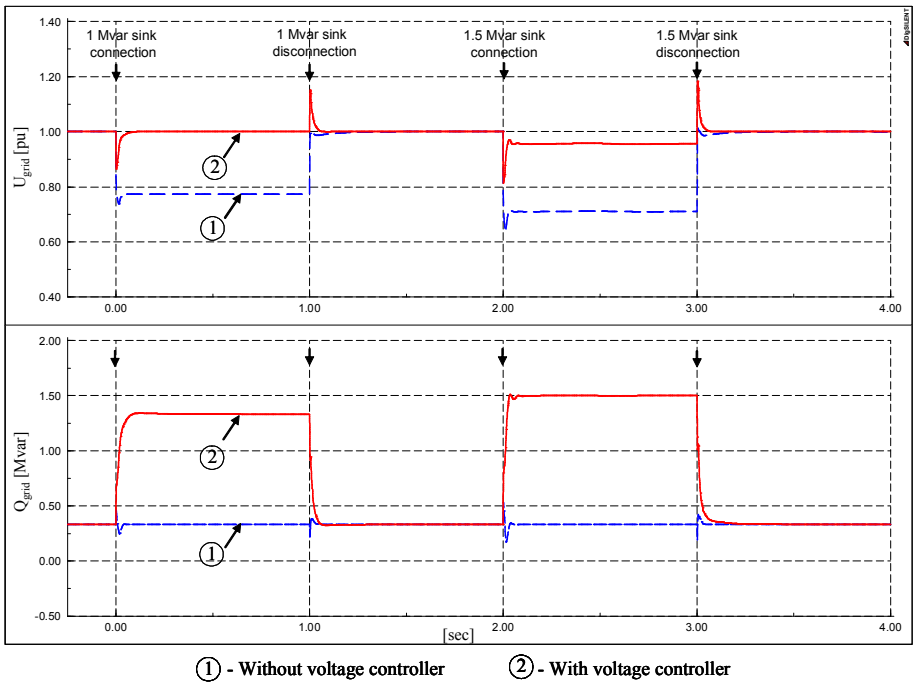

Fig. 31. PMSG voltage controller performance ((1) – without voltage control (2) with voltage control) -when a reactive power sink of 1Mvar and 1.5Mvar respectively, is connected and disconnected.

In the moment when each reactance is disconnected the voltage increases suddenly and the voltage controller reduces quickly the voltage to its nominal value by absorbing reactive power.

Fig. 32 and Fig. 33 illustrates firstly how the full-scale converter multi-pole PMSG wind turbine equipped with the new control strategy is able to ride-through grid faults without any additional measure and secondly how the use of a chopper can enhance the turbine's fault-ride through capability even further.

A 100 ms three phase short circuit is considered to occur at the high voltage terminal of the 2-windings transformer of the PMSG wind turbine. The PMSG wind turbine is connected to a grid, which is modeled as a Thevenin equivalent. It is assumed in the simulation that the voltage controller is disabled and that the wind turbine operates at its rated power first without any chopper attached. As illustrated in Fig. 32, the voltage drop occurs at the grid fault instant. Due to this drop, the grid-side converter can only transfer

a reduced amount of active power P_{grid} to the grid during the fault. However it is able to continue to control the reactive power to its initial reference value. Notice in Fig. 32, which during the grid fault the generator power and the power inserted in the grid have a similar characteristic. On the other hand, the grid power is kept constant after the fault has been cleared, while the generator power presents an oscillated behavior, as expected, which is however quickly damped, i.e. in less than 4 sec, by the damping controller. Meanwhile, when no chopper is used, the generator-side converter has to reduce the generator power, in order to be able to keep the DC-voltage constant. This action leads to a power imbalance between the reduced generator power and the unchanged aerodynamic turbine power. As result, the generator starts to accelerate and the drive train gets untwisted and starts to oscillate, as illustrated in Fig. 32.

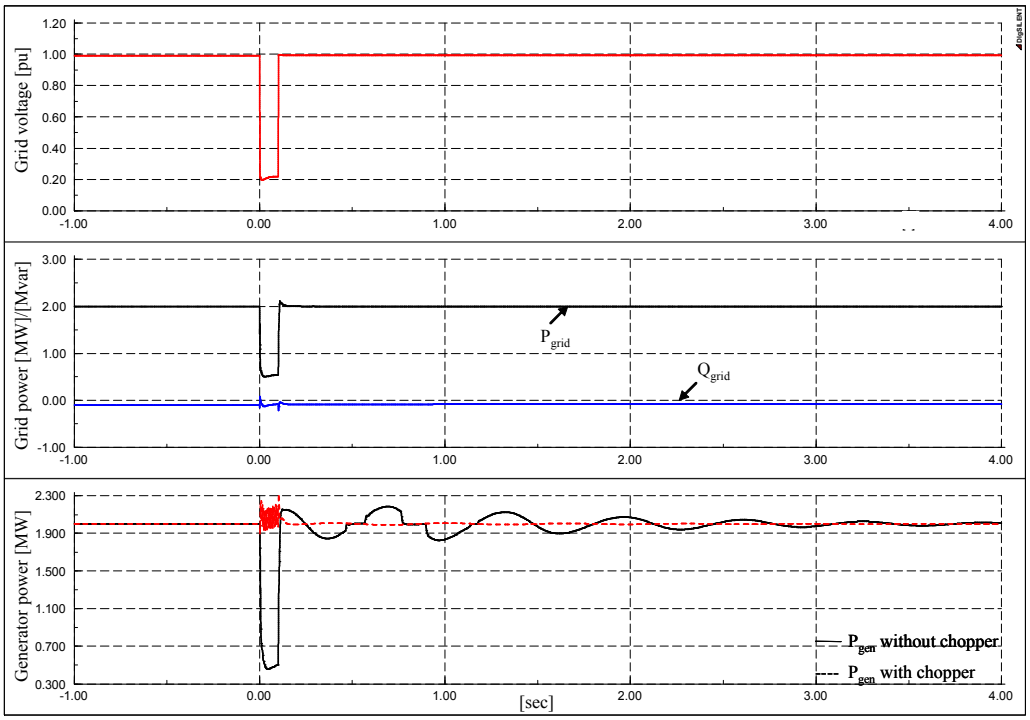

Fig. 32. Fault ride-through capability of full-scale converter multi-pole PMSG wind turbine equipped with the alternative control strategy.

The acceleration of the turbine is less than 2%, due to the large inertia of the turbine's rotor. The torsional oscillations in the drive train are visible both in the mechanical torque, generator speed and the DC-link voltage. Notice that they are quickly damped by the damping controller.

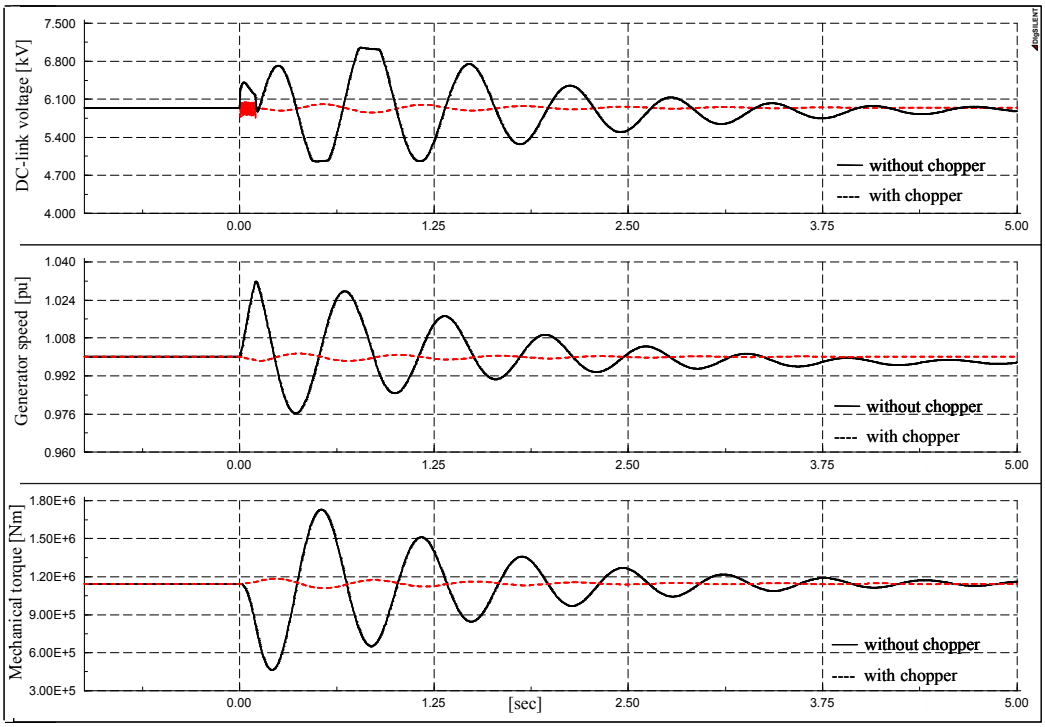

Fig. 33. Grid fault impact on the DC-link voltage, generator speed and on the shaft torque with and without chopper.

The simulations in Fig. 32 and Fig. 33 illustrate clearly that the wind turbine equipped with the new control strategy, is able to ride-through grid faults without any additional measures. In addition to this, the figures show also that the use of a chopper during a grid fault, when the new control strategy is applied, can enhance the turbine's fault ride-through capability even further. Notice that, when a chopper is used, the surplus power in the DC-link is burned in the chopper and, as shown in Fig. 32, it is therefore not necessary to reduce the generator power. Fig. 33 shows how the generator acceleration and drive train oscillations are significantly reduced when a chopper is used. It is also clearly illustrated that the chopper reduces effectively the grid fault impact on the wind turbine mechanical stress (i.e. smaller oscillations in the shaft torque) and enhances even further the PMSG wind turbine's fault ride-through capability.

In order to illustrate the PMSG wind farm voltage grid support capability, a worst case for the voltage stability is considered. It is thus assumed that, during the grid fault, the PMSG wind farm operates at its rated capacity. The wind farm is modeled with a one-machine approach based on the aggregation technique.

In Fig. 34, the voltage, the active power and the reactive power of the PMSG wind farm in the wind farm terminal (WFT) are illustrated. Two situations are compared: with and without voltage control of the PMSG wind farm, respectively. In order to achieve and illustrate the worst case for voltage stability, it is assumed that the power reduction control of the active stall wind farm is completely disabled during this first simulation.

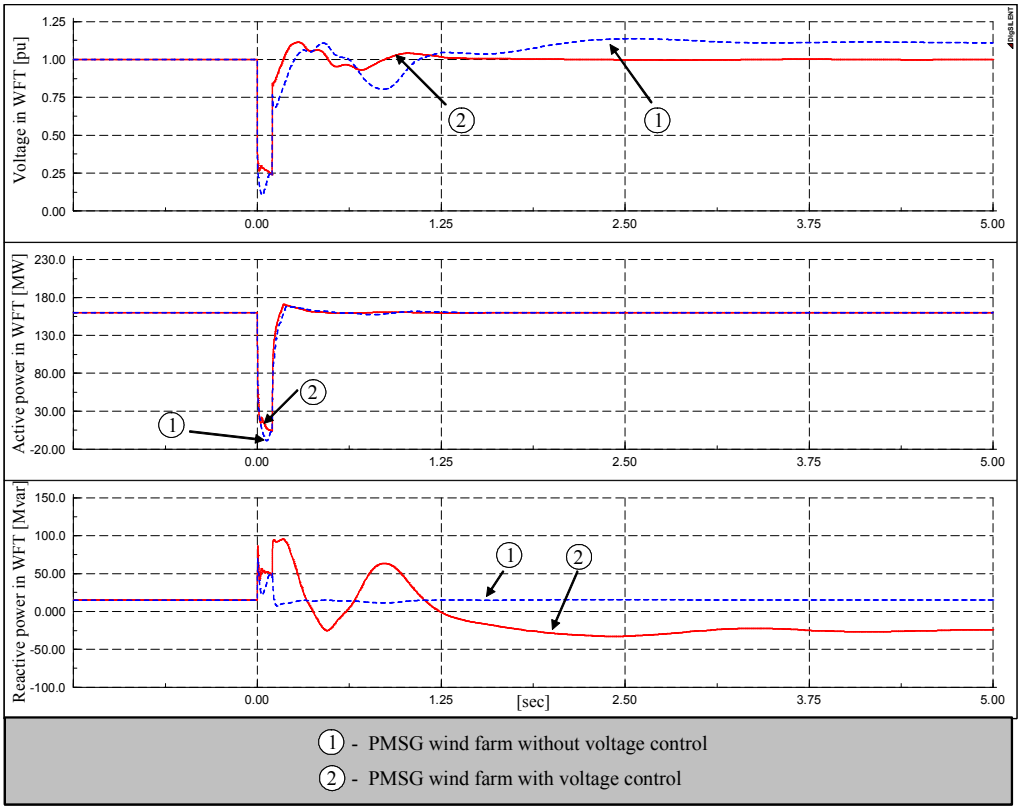

Fig. 34. PMSG wind farm terminal (WFT) with and without voltage control when the power reduction control of the active stall wind farm is disabled.

Notice that the grid fault causes a severe voltage drop at the wind farm terminal. As expected, the influence of PMSG wind farm's voltage control is visible both during the fault and after the fault is cleared (i.e. the voltage level is improved in both cases). When no voltage control is enabled, the grid voltage oscillates longer and stabilizes to a higher voltage level after the fault is cleared. This can be explained both by the reactive power surplus existent in the system as result of the on-land wind turbines disconnection and by the fact that, as result of the fault clearance (tripping Line 4), the transport of the active power from the wind farms to the grid is done through a higher resistance transmission line. Fig. 34 shows that, when the voltage control is enabled, the existing reactive power

surplus in the system after the fault is absorbed by the PMSG wind farm. The PMSG wind farm equipped with voltage control manages thus to re-establish quickly the grid voltage to 1p.u. by controlling the reactive power supply. Notice that, as expected, there is no significant effect of the voltage control on the active power production.

3.3 Variable speed DFIG

A DFIG system is essentially a wound rotor induction generator with slip rings, with the stator directly connected to the grid and with the rotor interfaced through a back-to-back partial-scale power converter. The DFIG is doubly fed by means that the voltage on the stator is applied from the grid and the voltage on the rotor is induced by the power converter. The converter consists of two conventional voltage source converters (rotor-side converter RSC and grid-side converter GSC) and a common dc-bus, as illustrated in Fig. 35.

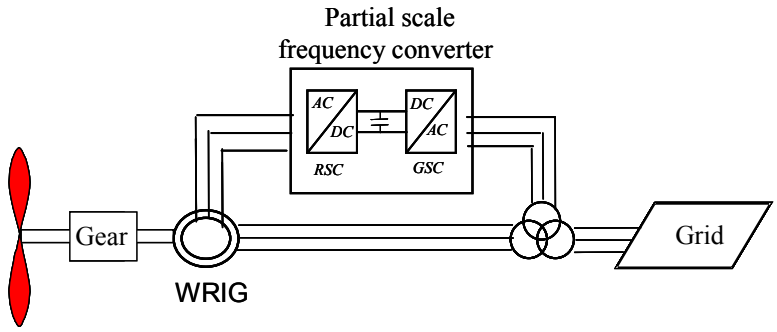

Fig. 35. DFIG wind turbine configuration.

The objective of the rotor side converter (RSC) is to control independently the active power of the generator and the reactive power produced or absorbed from the grid. The objective of the grid side converter (GRC) is to keep the dc-link voltage constant regardless of the magnitude and the direction of the rotor power and to guarantee a converter operation with unity power factor (zero reactive power). This means that the grid side converter exchanges only active power with the grid, and therefore the transmission of reactive power from DFIG to the grid is done only through the stator [21]. The behavior of the generator is governed by these converters and their controllers both in normal and fault conditions.

3.3.1 DFIG wind turbine control during normal operation

Fig. 36 sketches the overall control system of a variable speed DFIG wind turbine implemented in DIgSILENT. Two control levels using different bandwidths can be distinguished:

- Doubly-fed induction generator (DFIG) control level
- Wind turbine control level

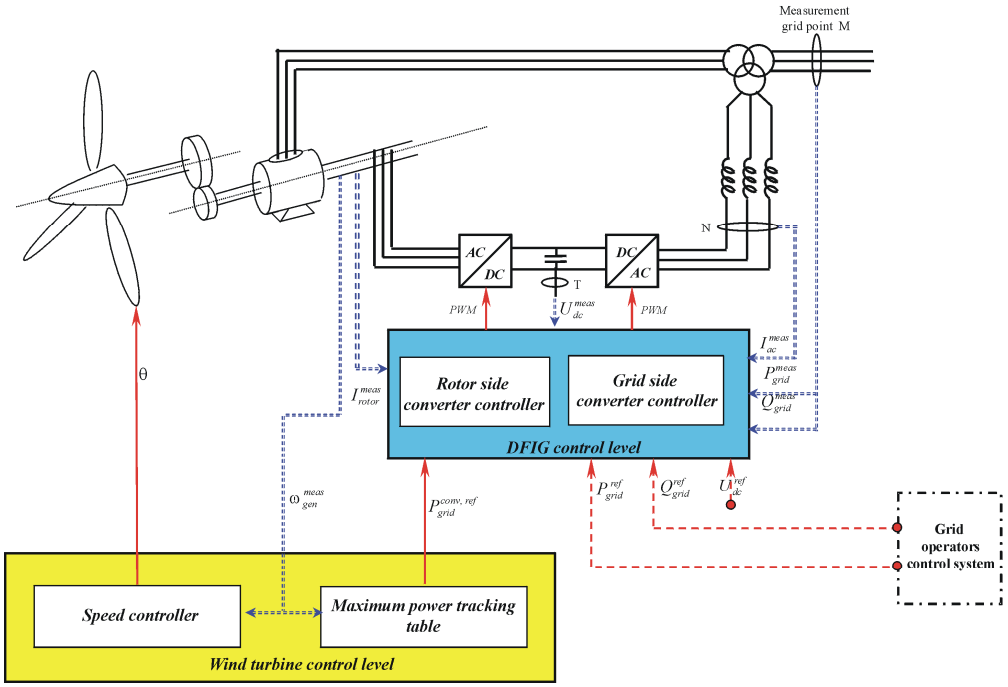

Fig. 36. Overall control system of variable speed wind turbine with doubly-fed induction generator.

The DFIG control, with a fast dynamic response, contains the electrical control of the power converters and of the doubly-fed induction generator. The DFIG control contains the controllers of the rotor side converter and grid side converter.

The wind turbine control, with slow dynamic response, provides reference signals both to the pitch system of the wind turbine and to the DFIG control level. It contains two controllers:

- Speed controller - has as task to control the generator speed at high wind speeds i.e. to change the pitch angle in order to prevent the generator speed becoming too. At low wind speeds, the pitch angle is kept constant to an optimal value. A gain scheduling control of the pitch angle is implemented in order to compensate for the existing non-linear aerodynamic characteristics.

- Maximum power tracking controller – generates the active power reference signal for the active power control loop, performed by the rotor side converter controller in DFIG control level. This reference signal is determined from the predefined characteristic $P-\omega$ look-up table, illustrated in Fig. 37, based on filtered measured generator speed. This characteristic is based on aerodynamic data of the wind turbine's rotor and its points correspond to the maximum aerodynamic efficiency.

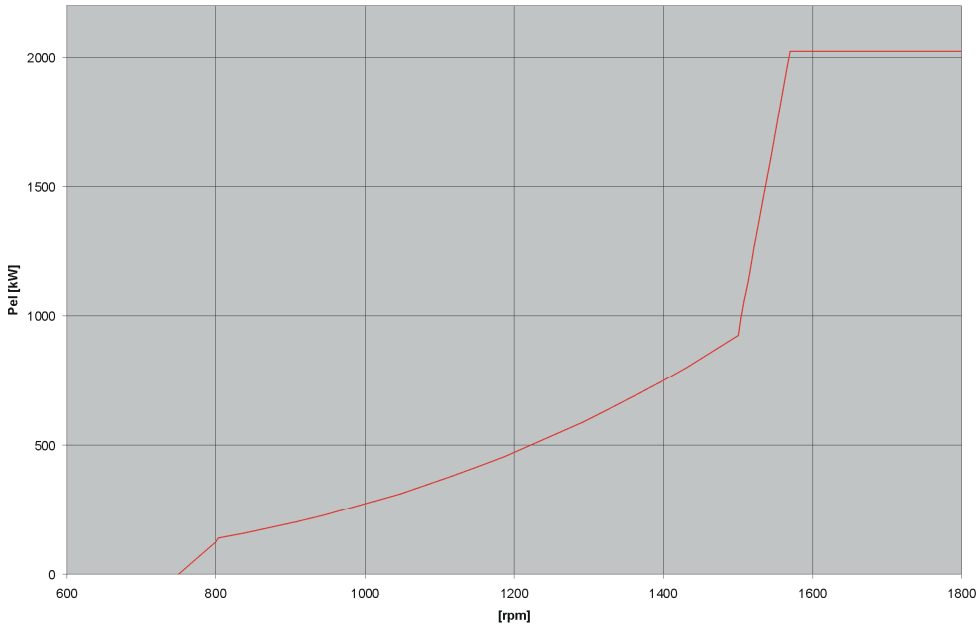

Fig. 37. Power-omega characteristic used in the maximum power-tracking controller.

Both the speed controller and the maximum power-tracking controller are active in the power limitation strategy, while only maximum power tracking controller is active in the optimization power strategy. In the case of high wind speeds there is a cross coupling between these two controllers.

Fig. 38 illustrates explicitly the speed controller, the maximum power tracking controller and the rotor side converter controller. The grid side converter controller does not interact directly with the wind turbine controller, and therefore it is shown as a "black box".

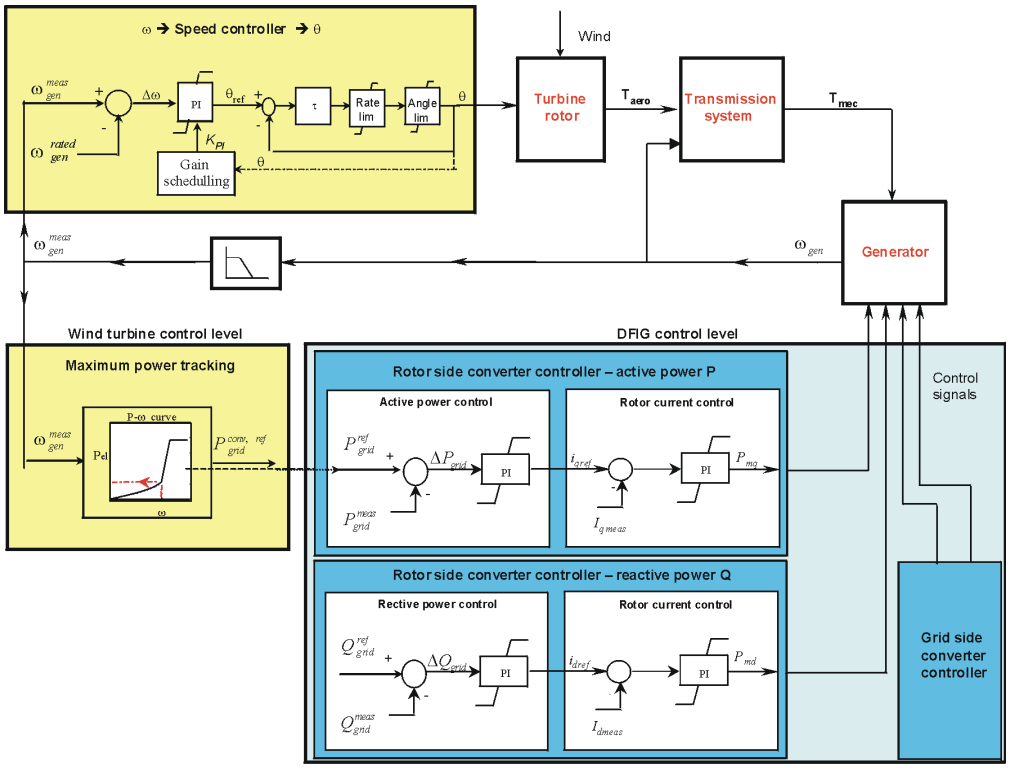

Fig. 38. DFIG wind turbine control during normal operation.

In the rotor side converter control, there are two independent control braches, one for the active power control and the other for reactive power control. Each branch consists of 2 controllers in cascade.

Notice that all these controllers, except maximum power tracking controller, are basically PI controllers. Both the speed controller and the maximum power tracking have as input the filtered measured generator speed. The generator speed is measured and a low-pass filter is used to avoid that the free-free frequency in the transmission system is amplified through the control system.

The DFIG control structure, illustrated in Fig. 38, contains the electrical control of the power converters, which is essential for the DFIG wind turbine behavior both in normal operation and during fault conditions.

Power converters are usually controlled utilizing vector control techniques [16], which allow de-coupled control of both active and reactive power. The aim of the RSC is to control independently the active and reactive power on the grid, while the GSC has to keep the dc-link capacitor voltage at a set value regardless of the magnitude and the direction of the rotor power and to guarantee a converter operation with unity power

factor (zero reactive power). As illustrated in Fig. 38, both RSC and GSC are controlled by a two stage controller. The first stage consists of very fast current controllers regulating the rotor currents to reference values that are specified by a slower power controller (second stage).

The control performance of the DFIG is very good in normal grid conditions. DFIG control can, within limits, hold the electrical power constant in spite of fluctuating wind, storing thus temporarily the rapid fluctuations in power as kinetic energy.

The active and reactive power set-point signals for the second stage controllers of the converters in Fig. 38, are depending on the wind turbine operational mode (normal or fault operation) signals. For example, in normal operation:

The active power set-point P_{ref}^{grid} for the rotor-side converter is defined by the maximum power tracking point (MPT) look-up table. The reactive power set-point Q_{ref}^{grid} for the rotor-side converter can be set to a certain value or to zero according to whether or not the DFIG is required to contribute with reactive power.

The grid-side converter is reactive neutral (i.e. $Q_{ref}^{GSC} = 0$) in normal operation. This means that, in normal operation, the GSC exchanges with the grid only active power, and therefore the transmission of reactive power from DFIG to the grid is done only through the stator. The dc-voltage set-point signal U_{dc} is set to a constant value, independent on the wind turbine operation mode.

The use of the partial-scale converter to the generator's rotor makes DFIG concept on one hand attractive from an economical point of view. On the other hand, this converter arrangement requires advanced protection system, as it is very sensitive to disturbances on the grid.

DFIG wind turbine control during grid fault operation

The grid fault is affecting both the mechanical and the electrical part of the wind turbine. During a grid fault, voltage and power at the wind turbine terminal drop and thus the power in the DFIG drops, too. This results in an acceleration of turbine and generator, which is counteracted by the speed controller, i.e. by the pitch angle control, which thus serves as an over speed protection. Moreover, when the electrical power drops the drive train will start to oscillate.

During grid faults, the electrical torque is significantly reduced, and therefore the drive train system acts like a torsion spring that gets untwisted. Due to the torsion spring characteristic of the drive train, the mechanical torque, the aerodynamical torque and thus the generator speed start to oscillate with the so-called free-free frequency:

$$f_{osc} = \frac{1}{2\pi} \cdot \sqrt{\frac{k}{J_{eq}}}$$

where Jeq is the equivalent inertia of the drive train model, determined by:

$$J_{eq} = \frac{J_{rot} \cdot n_{gear}^2 \cdot J_{gen}}{J_{rot} + n_{gear}^2 \cdot J_{gen}}$$

As these torsional oscillations may influence the converter operation both during grid faults and a short while after the grid faults have been removed, their modeling by using at least a two-mass model for the drive train system is essential. Furthermore, these torsional oscillations can even be excited and become undamped at a fast converter control [22]. Due to this reason a damping controller is implemented as shown in Fig. 39, which actively damps any torsional oscillations of the drive train and prevents instability of the system and substantially reduces the mechanical stresses of the turbine.

Without any protection system, the concern in DFIG is usually the fact that large grid disturbances can lead to large fault currents in the stator due to the stator's direct connection to the grid. Because of the magnetic coupling between the stator and the rotor and of the laws of flux conservation, the stator disturbance is further transmitted to the rotor. High voltages are thus induced in the rotor windings that on their turn cause excessive currents in the rotor as well. Furthermore, the surge following the fault includes a "rush" of power from the rotor terminals towards the converter.

Since the stator-rotor ratio of the DFIG is designed according to the desired variable speed range, in the case of grid faults it might not be possible to achieve the desired rotor voltage in order to control the high rotor currents. This means that the converter reaches fast its limits and as a consequence, it looses the control of the generator during the grid fault [23]. As the grid voltage drops in the fault moment, the GSC is not able to transfer the power from the RSC further to the grid and therefore the additional energy goes into charging the dc bus capacitor, i.e. dc bus voltage rises rapidly.

A protection system of the DFIG converter is thus necessary to break the high currents and the uncontrollable energy flow through the RSC to the dc-link and thus to minimize the effects of possible abnormal operating conditions. The protection system monitors usually different signals, such as the rotor current, the dc-link voltage and when at least one of the monitored signals exceeds its respective relay settings, the protection is activated.

A simple protection method of the DFIG under grid faults is to short circuit the rotor through a device called crowbar. The crowbar protection is external rotor impedance, coupled via the slip rings to the generator rotor instead of the converter. The function of the crowbar is to limit the rotor current.

When the crowbar is triggered, the rotor is short circuited over the crowbar impedance, the rotor-side converter (RSC) is disabled and therefore the DFIG behaves as a conventional squirrel cage induction generator (SCIG) with an increased rotor resistance. The independent controllability of active and reactive power gets thus unfortunately lost. Since the grid-side converter (GSC) is not directly coupled to the generator windings, there is no need to disable this converter, too. The GSC can therefore be used as a STATCOM to produce reactive power (limited however by its rating) during grid faults.

An increased crowbar resistance improves the torque characteristic and reduces the reactive power demand of the generator at a certain speed [24]. By the addition of the external resistance (crowbar resistance) in the rotor circuit during grid faults, the pull-out torque of the SCIG generator is moved into the range of higher speeds. The dynamic stability of the SCIG generator is thus improved by increasing the external resistance[22].

3.3.2 Fault ride-through

In normal operation the active power set-point P_{ref}^{grid} for the RSC control is defined by the maximum power tracking point (MPT) look-up table, as function of the optimal generator speed – see Fig. 39. This means that for each wind speed there is only one generator speed resulting in maximum aerodynamic coefficient C_p. However, in case of

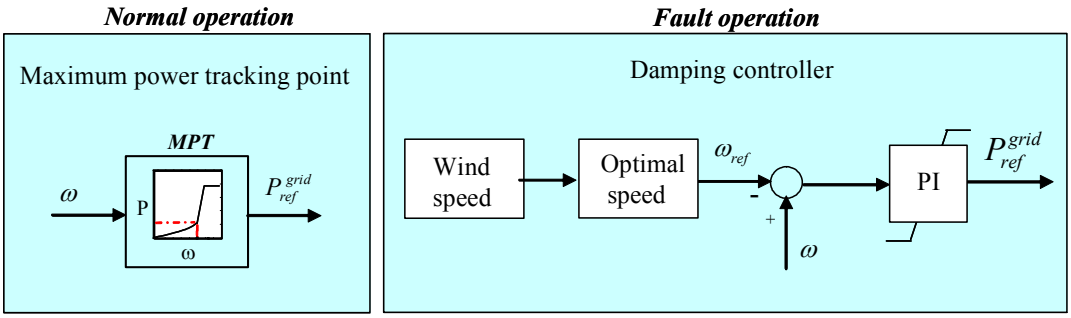

Fig. 39. Definition of active power set-point for normal and fault operation, using MPT and damping controller respectively.

grid faults, the generator speed variation is not due to the wind speed change but due to electrical torque reduction. This means that, in the case of grid faults the active power set-point P_{ref}^{grid} has to be differently defined, i.e. as the output of a damping controller. Such a controller has as task to damp the torsional excitations which are excited in the drive train owing to the grid fault.

Different control schemes can be applied to damp these torsional oscillations. In this work, the damping controller suggested by [22] is adopted. As illustrated in Fig. 39, the PI damping controller produces the active power reference signal P_{ref}^{grid} based on the deviation between the actual generator speed and its reference. The speed reference is defined by the optimal speed curve at the incoming wind. The damping controller is tuned to actively damp the torsional oscillations excited at a grid fault in the drive train system. [25] shows that absence or insufficient tuning of this PI controller may lead to self-excitation of the drive train system and to a risk of tripping as protection against vibrations in the mechanical construction.

The pitch control system is not able to damp the torsional oscillations, because of several delay mechanisms in the pitch [26]. The pitch control damps the slow frequency variations in the generator speed, while the damping controller is able to damp the fast oscillations in the generator speed.

During a grid fault, the tasks of RSC and GSC can be changed, depending on whether the protection system (i.e. crowbar) is triggered or not. In the case of less severe grid faults (i.e. not triggered crowbar) or reactive power unbalance in the system, the RSC and the GSC have the same tasks as in normal operation. In the case of severe fault

(i.e. triggered crowbar), a specific grid support strategy has to be designed and developed.

3.3.3 Grid support

The technical specifications for the wind turbines, as defined by the power system operator, require wind turbines to behave as active components and to support the grid. In this paper, the attention is mainly drawn to the DFIG voltage grid support during grid faults.

In general, different possible voltage control strategies exist for regulating voltage at the terminals of DFIG wind turbines. The voltage can in principle be controlled by either the RSC, [27], or the GSC, [28], or by both of them, [22]. There it is limited information in the literature about the latter voltage control method. The attention in this paper is therefore drawn to the voltage control strategy, where the reactive power contribution is performed by both converters in a co-ordinated manner. The idea is that the RSC is used as default reactive power source, while the GSC is used as a supplementary reactive power source during the blocking of the RSC.

At a severe grid fault, if the generator is not tripped, the DFIG wind turbine has to continue its operation with a short circuited generator, trying to sustain grid connection. When the crowbar is triggered, the RSC is blocked. In such situation, the RSC's controllability is lost and the DFIG grid support capability is thus strongly reduced. A solution to enhance the DFIG grid support capability during grid faults is to design a control strategy where the grid voltage (reactive power) control is taken over by the GSC. The GSC does not block at a grid fault, but it continues its operation as STATCOM as long as the RSC is blocked. When the crowbar is removed, the RSC starts to operate and the GSC is set again to be reactive neutral. The remove of the crowbar protection, and thus the re-start of the RSC can be performed according different criteria, such as the magnitude of the grid voltage or of the rotor currents. A too soon RSC restarting may cause tripping of the converter again at the fault clearance.

As illustrated in Fig. 40, the DFIG voltage grid support strategy is implemented in this work as an extension of the DFIG control structure used in normal operation and presented in Fig. 38.

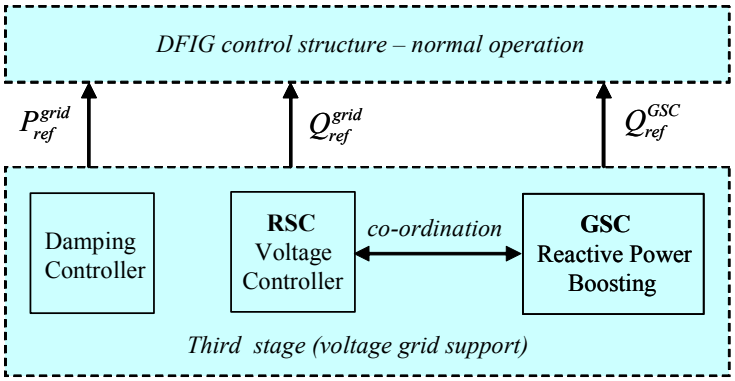

Fig. 40. Extended DFIG control structure for voltage grid support during grid faults.

An additional third control stage, having as task to improve the DFIG voltage grid support capability during grid fault, is thus added to the DFIG control structure used in normal operation, [23]. This third (voltage) control stage, used in the case of fault operation and illustrated in Fig. 40, provides the reference signals for the second stage controllers. This control stage contains three controllers, such as a damping controller, a rotor-side converter (RSC) voltage controller and a grid-side converter (GSC) reactive power boosting.

The damping controller, illustrated in Fig. 39, is attenuating the oscillations in the drive train produced by the grid fault. It ensures the fault ride-through capability of the wind turbine, i.e. avoids an eventual wind turbine grid disconnection due to undamped oscillations in the generator speed. The RSC voltage controller controls the grid voltage as long as the RSC is not blocked.

The GSC reactive power boosting (a supplementary reactive power controller) generates a reactive power reference signal Q_{ref}^{GSC} for the GSC voltage control, in the case when RSC is blocked. The implemented reactive power boosting provides a zero reactive power reference when the RSC is active, and a maximum reactive power of the GSC (1p.u.) as reference value in the case when the RSC is blocked. This means that the GSC contributes with its maximum reactive power capacity for grid support under severe grid faults.

As illustrated in Fig. 40, a co-ordination between the RSC and GSC voltage control is implemented. During the grid fault, some of the controllers have to be disabled, while others are enabled. The enabling (start-up) of the controllers requires to be treated with some care to avoid discontinuities and to minimize the loads on wind turbines. Such

discontinuities could eventually lead to prolonged transients and, implicitly, to subsequent operations of the crowbar protection.

3.3.4 Simulation results – DFIG wind turbine

Different scenarios are simulated to illustrate the performance of the grid support power controller and of the fault ride-through control strategy for the variable speed DFIG wind turbine. The controller's performance is assessed and discussed by means of a set of simulations of a 2 MW DFIG wind turbine.

Simulation results for normal operating conditions are given in Fig. 41 and verify the designed control strategy. Fig. 41 illustrates the wind speed, the pitch angle, the generator speed as well as the active and reactive power production in case of turbulent wind with a mean wind speed of 12 m/s and a turbulence intensity of 10 %. The signals of pitch angle, speed and active power reflect the stochastic character of the wind and are tracking the slow variations of the wind speed. For wind speeds below rated wind (approx 12 m/s) the power and speed are adapted to the point of maximum aerodynamic efficiency. For wind speeds above rated wind the pitch mechanism is active and the power is limited to its rated value. However, independent of the fluctuations of the wind, active and reactive power can be controlled to imposed reference values. Inspired by [12], the control system is set to follow a specified sequence: In the time period between 30 s and 60 s a reactive power demand of 0.5 MVar is required from the turbine. Notice, that the active power production is not influenced by the step in reactive power. Between 80 s and 170 s the active power reference is stepped down first to 1 MW and then to 0 MW and is then stepped up back again. The turbine is however only capable to follow this reference if the wind speed is sufficiently high. Notice, that a reduced reference power implies higher changes in pitch angle and generator speed. Finally between 200 s and 230 s the wind turbine is demanded to absorb 0.5 MVar reactive power from the grid, which is also very well accomplished. Figure 6 points out, that the designed control strategy of the variable speed wind turbine model with DFIG is able to control active and reactive power independently to specific imposed reference values, exactly as a conventional power plant does.

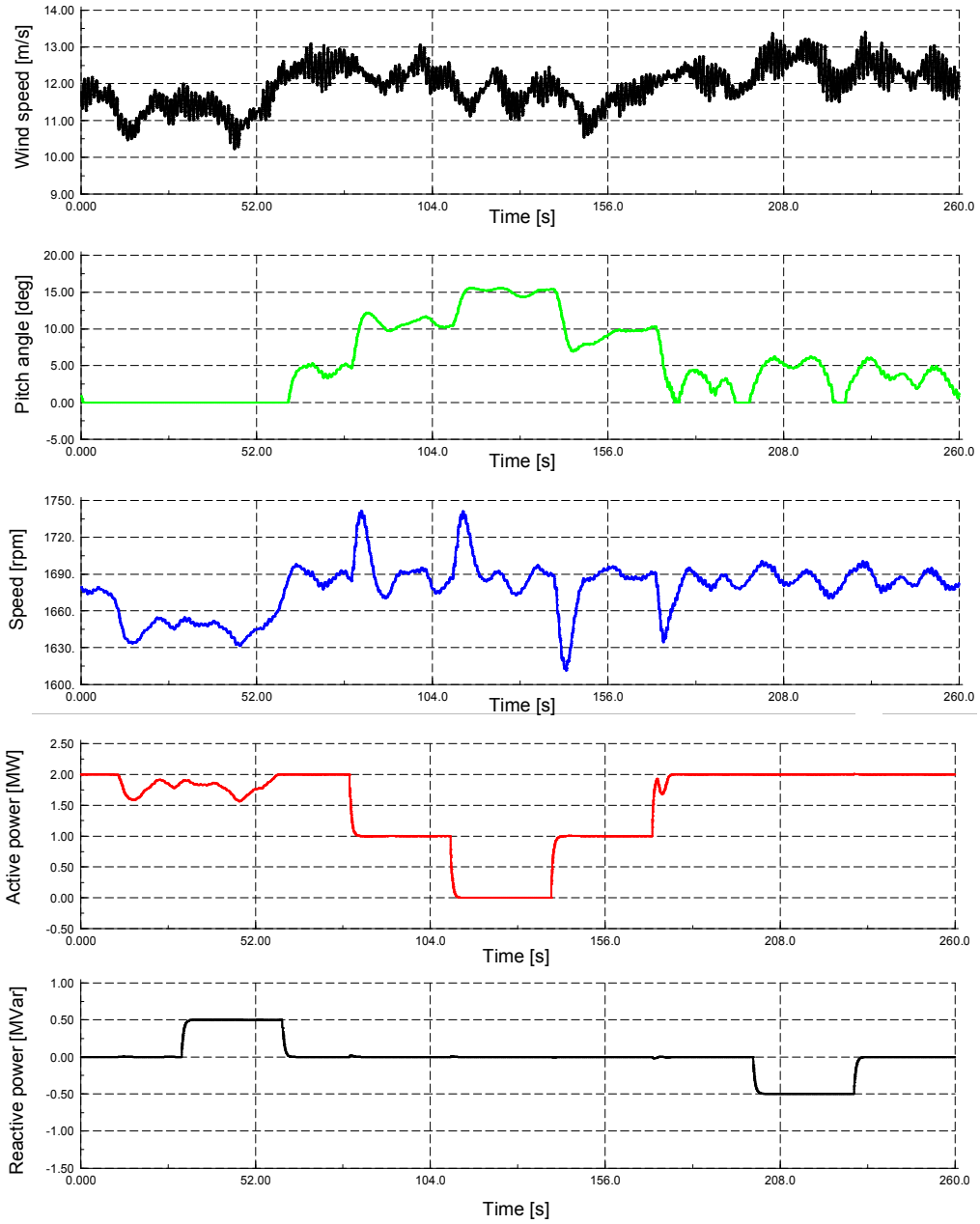

Fig. 41. Control of active and reactive power of DFIG.

Fig. 42 shows the simulation of a normal operation of a 6MW variable speed DFIG wind farm, when it is ordered to performed balance control, delta control, the power gradient limiter and the reactive power control. The wind turbines in the wind farm are driven by different turbulent winds, with 9 m/s mean speed value and 10% turbulence intensity. Fig. 42 illustrates both the available and the actual active power and the reactive power measured in the PCC of the wind farm, when the system operators require

different control actions. In order to test the wind farm controller, the following active power control functions sequence is proposed:

The first 100 sec the wind farm has to produce maximum power. Notice that the actual power follows the available power as long as the ramp limiter permits that.

The time period between 100 sec and 420 sec a delta control is imposed. The wind farm has to operate with a 0.5 MW constant reserve capacity.

The time period between 200 sec and 320 sec a balance control is imposed. The wind farm is ordered to regulate downwards to 2 MW. Notice that in this period, both the delta and the balance control are active at the same time. The adjustment upwards and downwards of the wind farm production is performed with a ramp limitation about ±1.2 MW/min.

The time period between 420 sec and 700 sec maximum power production is again ordered. The reactive power reference for the whole wind farm Q_{ref}^{WF} is set to zero the first 560 sec. A step in the wind farm reactive power demand to 1 MVar is then applied at 560 sec and the previous active power control functions sequence (1-4) is repeated. Notice that the generated active power is not altered by the step in the reactive power demand, its variations being only due to the turbulent wind. The simulation results show a good performance of the control system. The specified references both for the active and reactive power are achieved properly.

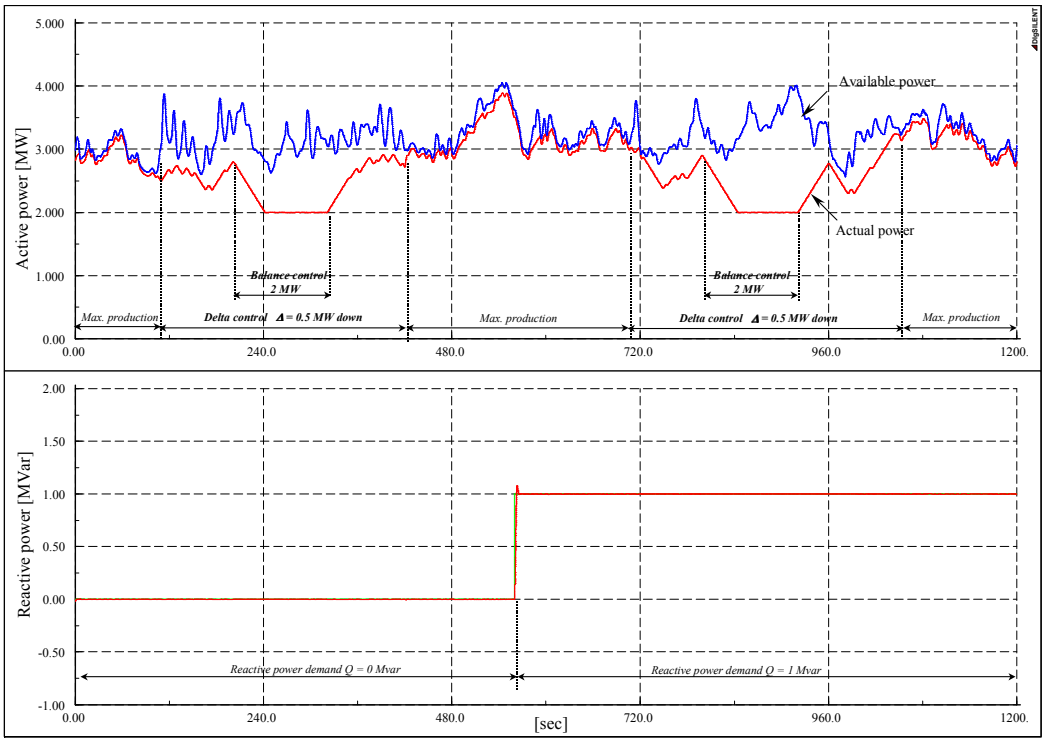

Fig. 42. Wind farm control level: maximum production, delta control, balance control, ramp limiter. At time 560 sec the reactive power reference is changed from 0 Mvar to 1 Mvar.

Fig. 43 illustrates the effect of the damping controller in case of a 100 ms three phase grid fault at the high voltage terminal of the 3-windings transformer of a 2MW DFIG wind turbine. It is assumed that the wind turbine works at its rated power at the fault instant. As the fault operation is small compared to the wind speed fluctuations, the wind speed can be assumed constant in the grid fault simulations. The generator speed and the mechanical torque are illustrated for the situations with and without damping controller respectively.

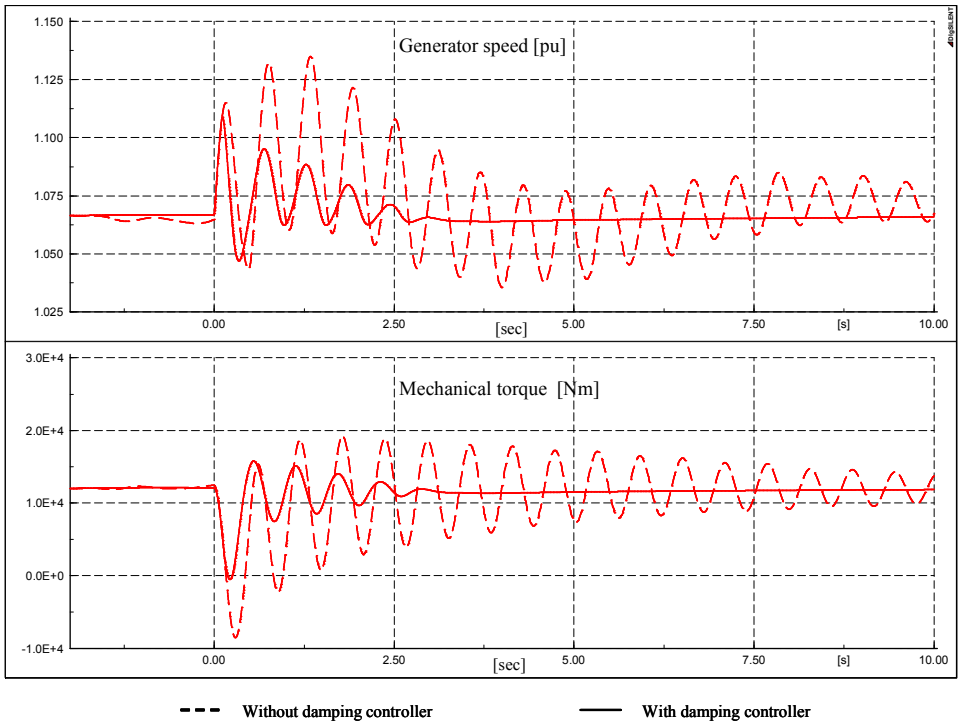

Fig. 43. Damping controller effect.

Note that without the damping controller, the torsional oscillations excited by the grid fault are only slightly damped still 10 seconds after the grid fault incident. It is clearly visible that the oscillations are quickly damped over few seconds when the damping controller is used. Furthermore the amplitude of the mechanical torque is much smaller when using the damping controller. Moreover, in contrast to the case when no damping controller is used, the mechanical torque crosses only once through zero when the damping controller is used, and therefore the mechanical stress of the drive train is substantially reduced in this case. The damping controller is thus minimizing the grid fault effect both on the mechanical and on the electrical side of the turbine. The protection system together with the damping controller enhances thus the DFIG fault ride-through capability.

In order to illustrate the DFIG voltage grid support capability, a worst case for the voltage stability is considered. It is thus assumed that, during the grid fault, the DFIG wind farm operates at its rated capacity. The wind farm is modeled with a one-machine approach based on the aggregation technique.

Fig. 44 illustrates the voltage, the active and the reactive power of the DFIG wind farm in the wind farm terminal (WFT), for the situations with and without DFIG voltage grid support respectively.

As expected, the influence of voltage grid support is visible both during grid fault, when the GSC operates as STATCOM and supplies reactive power, and after the disconnection of the crowbar, namely when the RSC controls the voltage on the grid. When no DFIG voltage grid support is enabled, the grid voltage oscillates as expected. After a while, it stabilizes to a higher voltage level. This aspect can be explained both by the reactive power surplus existent in the system as result of the on-land wind turbines' disconnection and by the fact that, as result of the fault clearance (tripping Line 4), the transport of the active power from the wind farms to the grid is done through a higher resistance transmission line.

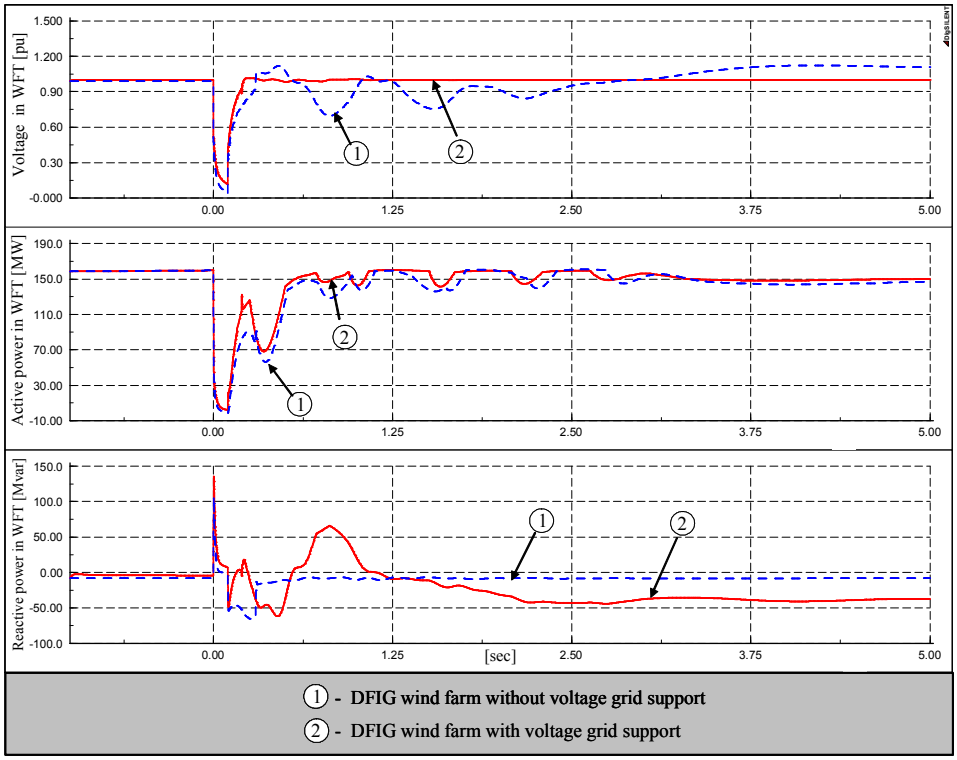

Fig. 44. DFIG wind farm terminal with and without voltage control when the power reduction of the active stall wind farm is disabled.

Fig. 44 shows that the existing reactive power surplus in the system is absorbed by the DFIG, when the voltage grid support control is enabled. Note that the DFIG voltage

control re-establishes the grid voltage to 1p.u. very quickly without any fluctuations. No significant effect of the voltage control appears on the active power production. However, there it is a slight improvement in active power when voltage control is used. The small “drops” in the power, visible in both cases just after the fault is cleared, are generated by the damping controller used to damp torsional oscillations in the generator speed of the DFIG after the grid fault. Similarly to Fig. 43, these oscillations are damped over few seconds. The initial level of the active power is reached after few more seconds.

4. Dynamic security and FRT

Emphasis in this section is given on Rhodes power system dynamic security and on fault ride-through (FRT) capability of large wind farms, which are expected to be connected in the island in the reference year 2012.

An analysis of the secure operation of non-interconnected systems, under high wind power penetration during normal operation and different variable wind and load profiles in the Rhodes power system will be described in details further below. The attention here is therefore drawn on the investigation in detail of the dynamic security aspect of non interconnected systems during serious disturbances, such as short circuit faults. The technical requirements set by the networks operators nowadays include various aspects, such as fault ride-through capability of wind turbines during faults, voltage-reactive power control and overall control of the wind farms as conventional power plants. Detailed models for the power system as well as for the wind farms are therefore essential for power system studies related to these issues, especially when applied to non interconnected systems with high wind power penetration. Three different wind turbine technologies – Active Stall Induction generator (ASIG), Doubly Fed Induction generator (DFIG) and Permanent Magnet Synchronous generator (PMSG) – are modeled in detail and the interaction with the power system is investigated. Unlike many previous studies [29], [30], this survey manages to deliver conclusions about the crucial dynamic security of power systems with high wind power penetration based on a set of simulations carried out with detailed models for different components of the system; three different types of conventional generators and three different types of wind turbine technologies are incorporated in the model. Discussion is made for the protection system and the load shedding following faults.

The investigation in this case study is carried out through a set of simulations based on the detailed models for the power grid of the island, the wind farms and their control, which have been implemented in the dedicated power system simulation program Power Factory from DIgSILENT, [2].

The technical requirements of network operators are becoming more onerous. Especially in isolated power systems, like Rhodes power system, these requirements have to be

carefully designed as a rapidly increased wind power penetration can pose serious dynamic security issues, due to low system inertia and relatively low spinning reserve.

There have been numerous publications illustrating the capability of wind farms to contribute to system stability during disturbances, [31], [32]. Nevertheless, in most of these studies, simplified models are used for either the power system or the wind farms. In this article, detailed models for all different components of the system are used to evaluate with maximum accuracy the dynamic security margins posed by the increasing wind power penetration. In order to allow for wind power penetration to be expanded beyond the usual 20-30% of the peak annual load for non-interconnected systems, different key aspects as voltage and frequency stability, power system inertia and protection relays settings have to be thoroughly analyzed.

Today, most modern power systems include different wind turbine technologies, covering a wide range from older generation fixed speed wind turbines up to new variable speed ones. This study includes the most three commonly available wind turbine designs in the market today and investigates their capability to contribute to the stability of the power system they are connected to.

The modeling of Rhodes power system and of the wind farms, which are expected to be online in the island by the year of study 2012, have already been described above. The attention here is drawn on the additional control features designed for different wind turbine technologies, such as the fault ride through capability, power reduction operation and voltage-reactive control.

The section is organized as follows. Wind farms modeling and control issues, especially during grid faults, are addressed with focus on the specific three wind turbine technologies available on Rhodes power system in the reference year 2012. A set of results, based on simulations with sever short circuit in the grid, is then illustrated and discussed, with focus on the most crucial variables, which reveal the wind farms impact on the grid, i.e. voltage and frequency. The system frequency variations and the resulting load shedding are discussed in addition to the frequency relay settings applied to systems like Rhodes. In the last part, conclusions of the work are presented and the overall study is summarized, focusing on the dynamic security aspects related to power systems with specific characteristics as the ones for Rhodes power system.

The security of autonomous power systems like Rhodes with a rapidly increasing wind power penetration is strongly dependent on the fault ride-through capability of wind farms installed in the island. This is therefore addressed in the following. The critical effect of these additional control aspects on the transient response of the power system during disturbances is assessed and illustrated through a set of simulation results.

4.1 Wind farms' fault ride-through capability

4.1.1 Fault ride through of DFIG wind turbines

The main electrical components as well as the mechanical parts and the controllers of a DFIG wind turbine, which considered in the model, are presented above, and described in more detail in [33], [35]. In this section, the attention concentrates on the fault ride through capability of DFIG wind turbines.

The specific converter arrangement in the DFIG configuration requires advanced protection system, because of the high inrush stator and rotor currents during grid faults. The protection of the converter against overcurrents, but also of the generator rotor and the dc-link against overvoltage is ensured via the so called crowbar. In principle, the crowbar is external rotor impedance, coupled via the slip rings to the generator rotor, as illustrated in Fig. 45. When the crowbar is triggered, the rotor side converter (RSC) is disabled and bypassed, and therefore the independent controllability of active and reactive power gets unfortunately lost. Since the grid side converter (GSC) is not directly connected to the generator windings, where the high transient currents occur, this converter is not blocked by the protection system during grid faults. When the crowbar is removed, the RSC is enabled again to control independently the active and reactive power.

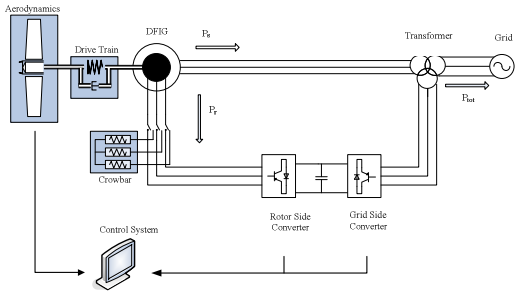

Fig. 45. System configuration and control of a DFIG wind turbine equipped with crowbar protection.

In normal operation of a DFIG wind turbine, the active power reference for the rotor side converter is given by the maximum power tracking (MPT) point characteristic as function of the optimal generator speed [33]. In the case of a grid fault, this power reference is defined as the output of a damping controller [34], [35]. The damping controller is attenuating the oscillations in the drive train produced by the grid fault. It ensures the fault ride-through capability of the wind turbine, i.e. avoids an eventual wind turbine grid disconnection due to undamped oscillations in the generator speed. When a fault is detected, the definition of the power reference is thus switched between the normal operation definition (i.e., MPT) and the fault operation definition (damping controller). Notice that the pitch control system is not able to damp the torsional oscillations, because of several delay mechanisms in the pitch [35]. The pitch control damps the slow frequency variations in the generator speed, while the damping controller is able to damp the fast oscillations in the generator speed. The effect of the damping controller both on the electrical and the mechanical parts of the turbine is illustrated in section IV.

4.1.2 Fault ride-through of PMSG wind turbines

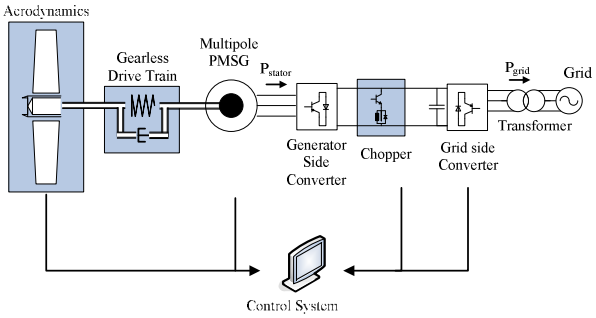

Fig. 46. System configuration and control of a direct driven PMSG wind turbine.

A multi-pole PMSG wind turbine (see Fig. 46) is connected via a full-scale frequency converter to the grid and therefore in principle can easily accomplish fault ride-through and support the grid during faults. The presence of the full-scale converter makes it possible for this wind turbine configuration to absorb or produce larger amounts of reactive power than DFIG wind turbine configuration does in general and especially during grid faults. As the converter decouples the generator from the grid, the generator and the turbine system are not directly subjected to grid faults in contrast to the direct grid connected wind turbine generators.

The control strategy followed in this study for the PMSG wind turbines is described in [36], [37]. As the generator side-converter is not directly connected to the grid, its performance is not affected during grid faults. It is therefore able to fulfill its task in controlling the DC-link voltage undisturbed also during faults. Meanwhile, as the grid-side converter is directly affected by grid fault, it cannot deliver the expected active power when subjected to low voltage during faults. The generator-side converter starts then to reduce the generator power by decreasing the stator current in order to keep the DC-link voltage constant. The power surplus is transformed in rotational energy of the rotor mass, which start thus to accelerate. If the speed gets higher than the rated, the pitch controller acts to limit the acceleration.

As described in [37], the torsional oscillations in the drive train system during faults, owing to the torsional spring behavior of the system following the sudden loss of electrical power, are damped by a damping controller.

This control strategy allows PMSG wind turbine configuration to ride-through grid faults without any additional measure. However, it is shown in [37] that the presence of a chopper in the system can even more enhance the fault ride-through capability of the turbine. The chopper includes a resistance and a power electronic switch, placed in parallel to the capacitor in the DC-link. When the DC-link voltage increases over a critical value the chopper is triggered and the surplus power is consumed in the chopper resistance. The capacitor discharges and the DC-link voltage decreases. As it is shown in section IV, the use of a chopper can have an additional benefic effect on the wind turbine mechanical stress.

4.1.3 Fault ride-through of ASIG wind turbines

The fault ride-through capability of an ASIG wind farm, and thus its stabilization at a short circuit fault, can be achieved by reducing the wind turbine power production for duration of few seconds from the moment of fault occurrence.

In this work, the ASIG wind turbine control strategy during grid faults is implemented based on [38]. The idea is that during the fault, the ASIG wind turbine normal controller is switched off and replaced by a control strategy to reduce directly the mechanical power of the rotor to a predefined level. The ordering of power reduction is given for example when the monitoring of the grid voltage indicates a fault occurrence. When the grid fault is cleared, the wind turbine continues running at reduced power for still few seconds, after which it starts to ramp up the mechanical power of the rotor and re-establish the control for ASIG wind turbine normal operation conditions. The simulation results in case of ordered power reduction are presented in the next section.

4.2 SIMULATION RESULTS

In this section, different simulation results are presented in order to illustrate the dynamic response to severe grid faults both of the overall Rhodes power system and of each wind turbine technology presented in the paper. The simulations, presented in the following subsection, are carried out in the condition of the Maximum Wind Power Penetration scenario (SCEN3), as this case is supposed to be the worst case scenario for the dynamic security of the system. Wind power penetration reaches 30% of the peak annual load in this scenario - SCEN3 - , limit which represents the margin for secure operation in autonomous systems.

In each simulation a severe three-phase short circuit grid fault is applied in the moment t=1 sec, in the transmission grid at the middle of the line connecting one of the two conventional power stations to the power system. The fault lasts for 100 ms and gets cleared by tripping the relays of the faulty line (see simplified net diagram below). It should be noted that the fault location is close to the busbars where the wind farms equipped with DFIG and PMSG wind turbines are located.

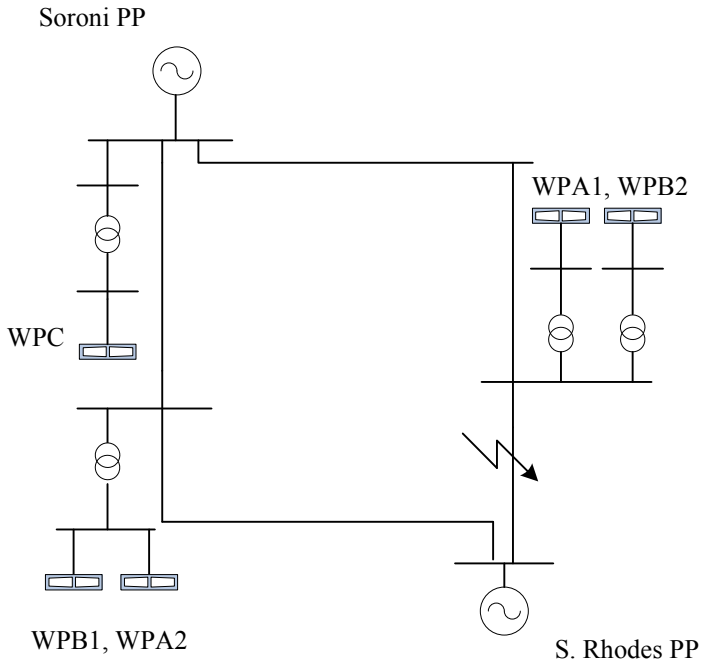

Fig. 47. Simplified net diagram of Rhodes power system.

It is assumed that during the grid fault and the maximum penetration scenario, the wind turbines on the island operate almost at half of their rated capacity.

The majority of the wind farms are close to the fault location and the stress imposed to the converters and the generators is considered very strong.

4.2.1 Rhodes power systems response to the grid fault in SCEN3

Beside the system frequency, Fig. 48 shows the response of the rotor speed for all five different wind farms in the p.u. system. Notice that, as the ASIG wind turbine is directly connected to the grid, its rotor speed has the same behavior as the system frequency. When the event occurs, both the system frequency and the rotor speed of the ASIG wind turbine increase, mainly due to the reduction of the power inserted into the power system during a fault. The increase in the rotor speed is due to the fact that the wind turbine rotor accumulates rotating energy, as result of the imbalance between the mechanical power and the no electrical power that is exported into the system during the fault. Meanwhile, the conventional generators try to compensate for the power reduction into the system by accelerating and thus by increasing the frequency system. Notice in Fig. 48, that the rotor speed of the PMSG wind turbines is entirely isolated from the grid frequency, while in

the DFIG configuration there is a partial correlation between the rotor speed and the system frequency.

.

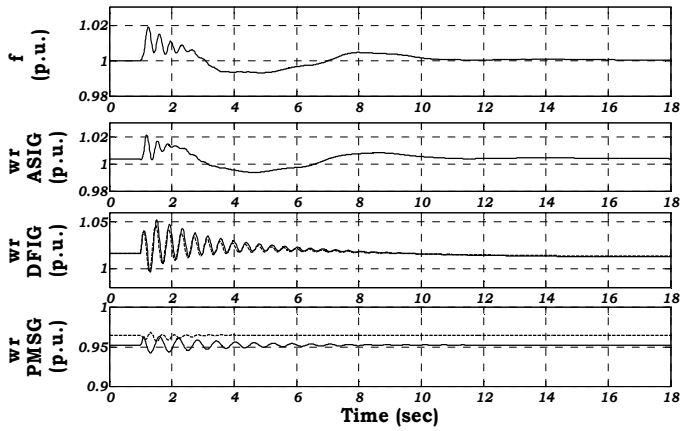

Fig. 48. System frequency and rotor speeds in p.u. for different wind turbines in the Rhodes power system during three phase short circuit – system frequency, ASIG rotor speed, DFIG rotor speed, PMSG rotor speed

This correlation between the rotor speed and the system frequency in fixed speed wind turbines is also crucial during frequency deviations in the system, such as sudden change of generation or load, i.e. when the system frequency drops, the rotor of the fixed speed wind turbine also decreases and the kinetic energy of the rotating mass is delivered to the system contributing to the primary control service, traditionally operated by conventional generators through droop control [39], [40].

Fig. 49 illustrates the voltage in the point of common coupling (PCC) of each individual wind farm. Notice that the voltage drops down to 0.1 p.u. in the PCC of variable speed wind farms (WPA1, WPA2, WPB1 and WPB2), and to 0.2 pu for WPC. As mentioned before, it is assumed that the wind farms have fault ride-through capability, i.e. they are able to remain connected and withstand the high inrush currents which follow sudden drops in voltage.

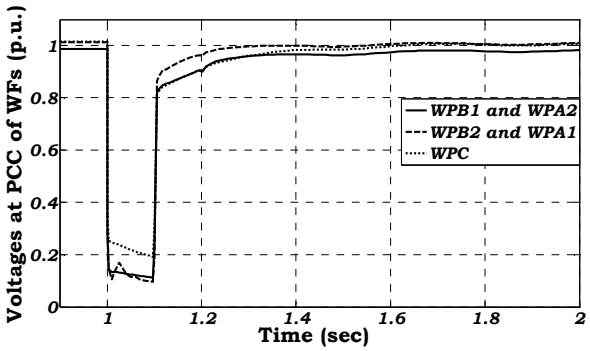

Fig. 49. Voltages at the PCC of all wind farms during three phase short circuit grid fault.

Immediately after the fault clearance, the voltage does not recover to its nominal value but reaches a slightly lower level (see Fig. 49). The reason for that will be explained in more detail in the following when the operation of the protection system of the wind turbines is described.

The dynamic response to grid faults of each wind turbine configuration present in the island is presented in the following. Typical signals, which are relevant to illustrate the response, such as the grid power, mechanical torque, generator speed and the reactive power of the turbines are illustrated.

4.2.2 DFIG wind turbines' response to the grid fault

Fig. 50 -Fig. 53 reveal the behavior of the DFIG wind turbines in one of the wind farms in the Rhodes power system during the fault, with or without damping controller.

It should be noticed that the illustrated active and reactive power correspond to the whole wind farm (WPA1), while the other signals refer to only one wind turbine.

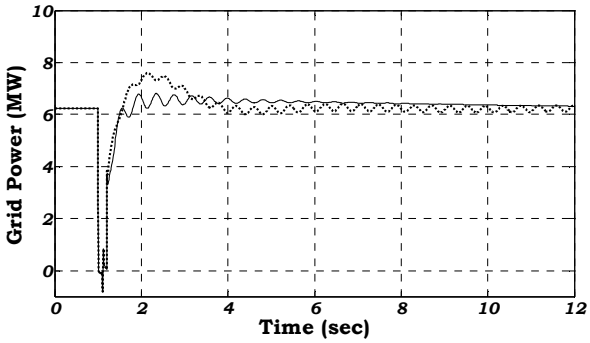

Fig. 50. Active power during the fault for wind farm with DFIG wind turbines – solid line, with damping controller, dashed line, without damping controller.

The sudden drop of the voltage leads to drop in the stator and rotor flux, which result in decrease of the active power delivered by the wind turbine. The electromagnetic torque is also dropping, and as the drive train acting as torsion spring gets untwisted during fault, the mechanical torque drops too, as shown in Fig. 51.

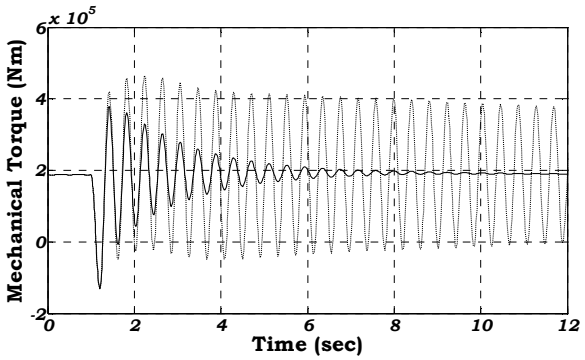

Fig. 51. Mechanical torque during the fault for DFIG wind turbine – solid line, with damping controller, dashed line, without damping controller

However, the mechanical torque drops slower than the electromagnetic torque and therefore the generator starts to accelerate (Fig. 52). The high inrush currents, which follow the voltage drop, trip the crowbar protection system. The rotor side converter (RSC) is blocked and the generator behaves as a conventional squirrel cage induction generator.

Notice that the effect of the damping controller, which acts directly on the active power reference signal, is very crucial. This controller damps actively the torsional excitations in the drive train system following the grid fault. When no damping controller is used, both the oscillations in the mechanical torque and in the generator speed remain undamped and could possibly lead to disconnection of the wind turbine by the protection system. The repeated crosses through zero of the mechanical torque, when no damping controller is used, indicate severe mechanical stress in the drive train. The comparison reveals therefore a positive effect of the damping controller on both the electrical and mechanical side of the wind turbine.

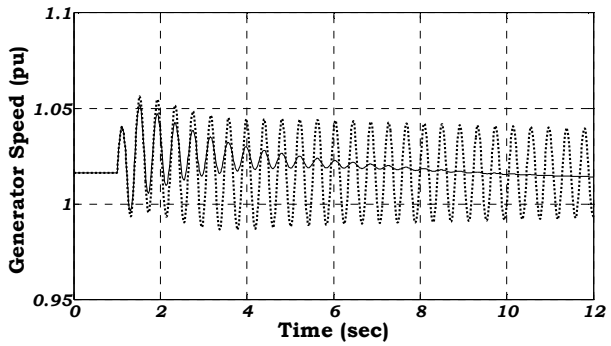

Fig. 52. Generator speed during the fault for DFIG wind turbine – solid line, with damping controller, dashed line, without damping controller.

During the fault, the voltage control of the grid side converter (GSC) demands the wind turbine to deliver reactive power to support the voltage at the PCC of the wind farm. The wind farm manages to provide with large amount of reactive power (Fig. 53). Notice that, as expected, the damping controller doesn't have significant effect on the reactive power. When the fault is cleared, the generator starts to absorb reactive power, as it is still behaving as squirrel cage induction generator as long as the crowbar is triggered. The RSC is still blocked and this delays the quick restoration of the voltage until the tripping of the crowbar protection system, as it was illustrated in Fig. 49.

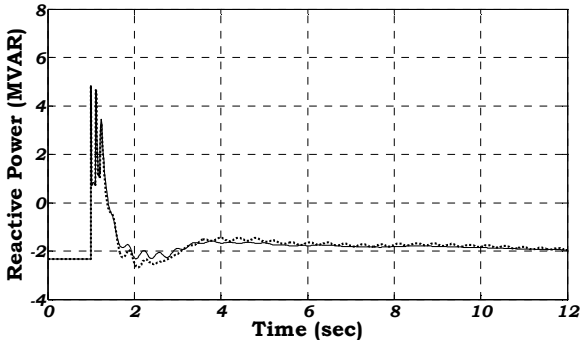

Fig. 53. Reactive power during the fault for wind farm with DFIG wind turbines.

4.2.3 PMSG wind turbines' response to the grid fault

Fig. 54 - Fig. 58 illustrate the fault ride-through capability of the PMSG wind turbines in wind farm WPB2, with and without chopper. It is shown how the use of a chopper can even more improve the response of the turbine during faults.

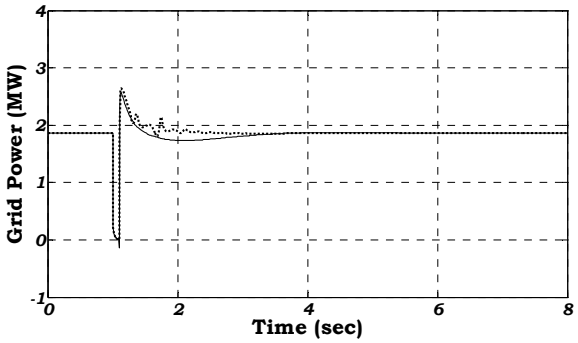

Fig. 54. Active power during the fault for wind farm with PMSG wind turbines – solid line, with chopper, dashed line, without chopper.

As illustrated in Fig. 54, during the fault, the grid-side converter cannot deliver to the grid the whole active power generated by the generator, but only a reduced amount of it. When no chopper is used, the generator power has a similar behavior as of the grid power, because it is reduced by the generator side converter, to be able to keep the DC-link voltage constant. Due to the imbalance between aerodynamic and electrical power during the fault, remains still the generator starts to accelerate. Meanwhile, the drive train gets untwisted and starts to oscillate. Fig. 55 illustrates the oscillations in the mechanical torque acting on the rotor mass.

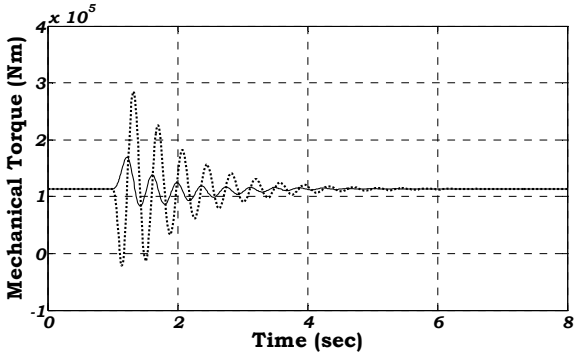

Fig. 55. Mechanical torque during the fault for a PMSG wind turbine – solid line, with chopper, dashed line, without chopper

Notice that contrary DFIG wind turbine, a PMSG wind turbine can ride through a grid fault without any additional measure, i.e. a chopper. However, the oscillations visible in the torque and the generator speed (see Fig. 55 - Fig. 56), are significantly reduced when a chopper is used. Besides the faster damping of the oscillations, the chopper helps also to decrease the peak torque and rotor accelerations following the fault, and to minimize the mechanical stress of the wind turbine.

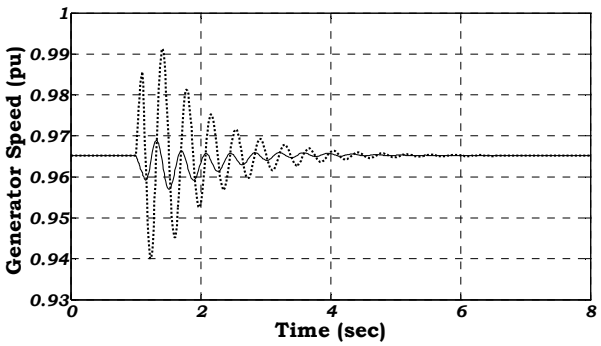

Fig. 56. Generator speed during the fault for a PMSG wind turbine – solid line, with chopper, dashed line, without chopper.

In addition to this, the use of a chopper reduces the oscillations in the DC-link voltage, as illustrated in Fig. 57. The surplus energy, which can not be delivered to the grid, is thus consumed in the chopper resistance.

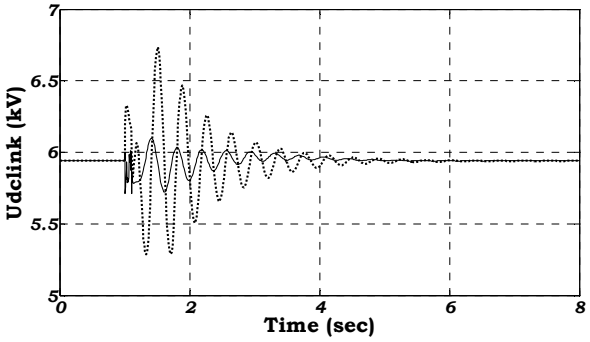

Fig. 57. DC-link voltage during the fault for a PMSG wind turbine – solid line, with chopper, dashed line, without chopper.

Notice in Fig. 58, that, as expected, the chopper does not have any effect on the reactive power response during the fault. The wind turbine controls the voltage at the PCC and delivers reactive power to support the voltage during the drop. Details about the implemented voltage control can be found in [37].

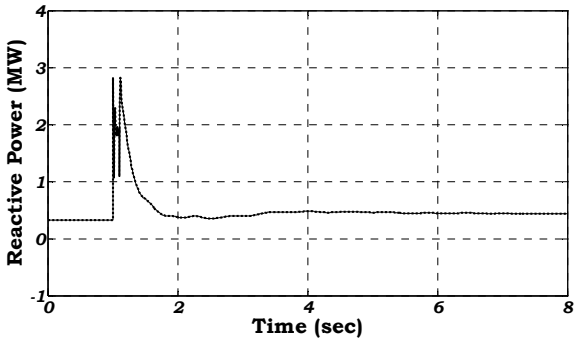

Fig. 58. Reactive power during the fault for a wind farm equipped with PMSG wind turbines – solid line, with chopper, dashed line, without chopper.

4.2.4 ASIG wind turbines' response to the grid fault

The wind farm equipped with ASIG wind turbines, although not very close to the fault location has to withstand the low voltage during the fault, and ensure uninterrupted operation. Fig. 59 - Fig. 65 illustrate in the following the behavior of ASWG wind turbine during grid faults.

Fig. 59 shows the active power delivered to the grid during the fault. After the clearance of the fault, the active power may still be reduced for a few seconds. As explained above, during the voltage drop, the active power delivered by the generator has to be reduced in order to make the turbine able to ride through the fault.

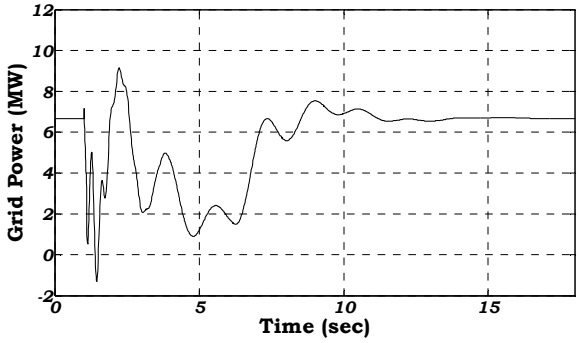

Fig. 59. Active power during the fault for a wind farm equipped with ASIG wind turbines

Although the inrush currents are high during the fault, the thermal constants of the induction generator are also quite high and the need for protection is reduced compared to the sensitive power electronics of variable speed wind turbines.

As expected, following the electromagnetic torque, the mechanical torque is also reduced both during and after the fault (see Fig. 60).

Fig. 61 shows the rotor speed of the ASIG wind turbine, which as mentioned before it reflects the power system frequency behavior during the fault. When the fault occurs, the speed is initially increased due to the acceleration of the conventional generators and after that it drops below nominal value.

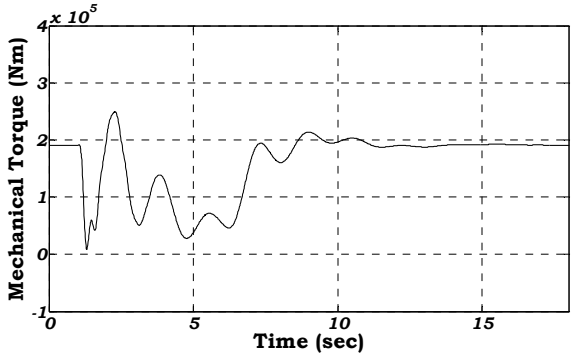

Fig. 60. Mechanical torque during the fault for a ASIG wind turbine.

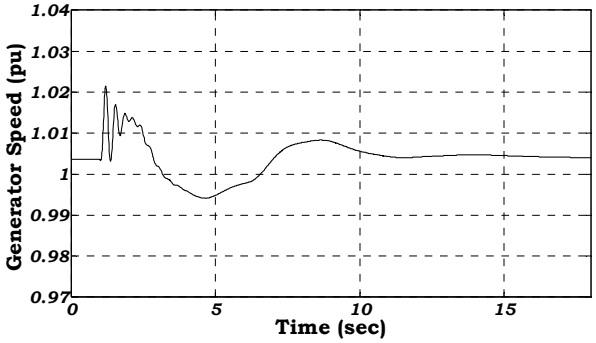

Fig. 61. Generator speed during the fault for a ASIG wind turbine.

The reduction of the wind turbine mechanical power is applied to assess the fault ride-through capability of the active stall wind farms. As shown in Fig. 62, this implies that the pitch is changing according to the ordered reduced power. Once the pitch angle of reduced power is reached, the turbine is still ordered to remain in this mode some few seconds after the clearance of the fault and then to start to ramp the pitch angle again to its initial normal operation value. Notice thus that, reducing the power has no effect during the fault but rather after the nominal voltage has been re-ensured.

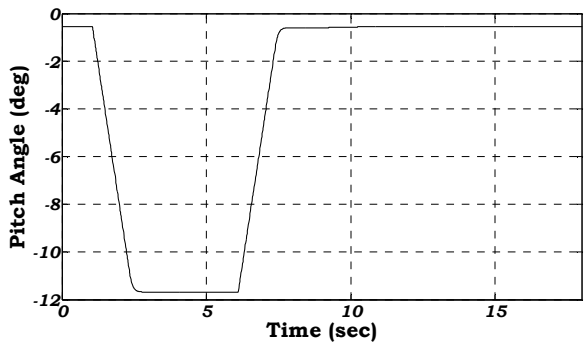

Fig. 62. Pitch angle during the fault for a ASIG wind turbine.

During the grid fault the ASIG wind turbine absorbs reactive power during the low voltage conditions. After the initial peak in the reactive power, shown in Fig. 63, the wind farm absorbs reactive power, threatening the voltage stability of the system. The reactive power in Fig. 63 is measured in the PCC, and includes the power delivered to the grid by the capacitor banks installed at the wind farm bus to reduce the negative effect on reactive power-voltage control of the system during severe faults.

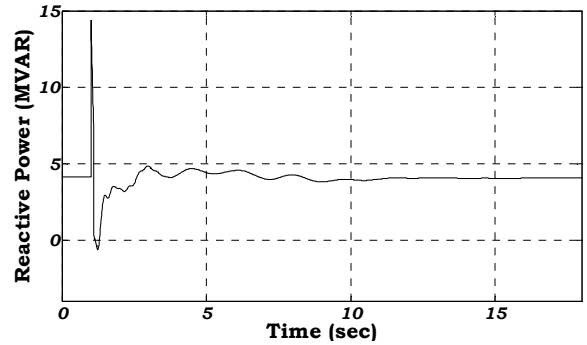

Fig. 63. Reactive power during the fault for a wind farm equipped with ASIG wind turbines.

4.2.5 System frequency response overview for different load scenarios with and without FRT in the wind farms

As it was already mentioned, these subsections intend to give an overview of the system frequency response to grid faults during different load scenarios and when the wind farms have or not fault ride- through controller. As it is mostly the case in many island grids, like Rhodes, there is still no grid code for the operation of the wind farms. Even today, the wind parks in isolated systems are allowed to trip during severe faults to avoid destruction of the power electronics and mechanical stress. The task to support the grid during faults, therefore, is assigned to the conventional generators and the spinning

reserve is also determined without taking into consideration the available wind power on the island.

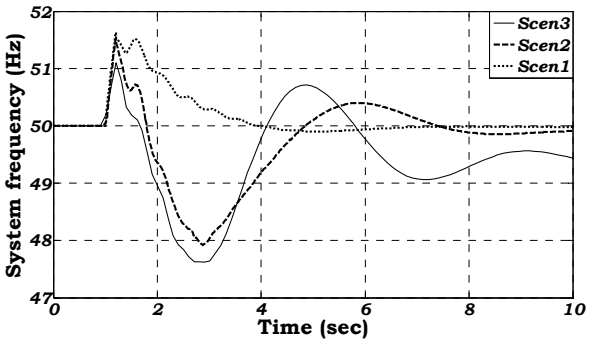

Fig. 64. System frequency during the fault when wind farms are tripped for three different scenarios

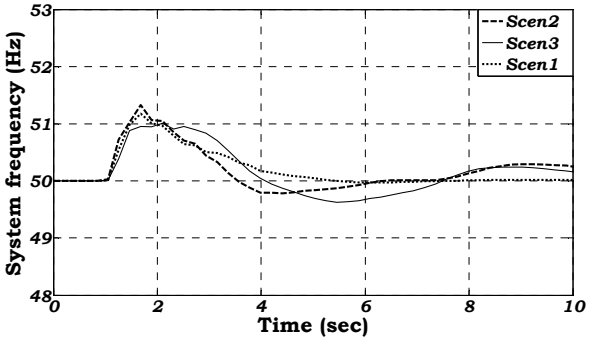

Fig. 65. System frequency during the fault when FRT is available for three different scenarios

Fig. 64 illustrates the grid fault's impact on the system frequency as it is today, namely when large wind farms connected to the island are tripped by their protection system during a grid fault, as they are not equipped with fault ride-through control. Notice that in these conditions, during SCEN3, i.e. Maximum Wind Power Penetration scenario, which has been mainly in focus in this session, the frequency of the system drops down to 47.6 Hz, reaching thus limits which are not considered accepted by the operators nowadays. This reduction in the frequency is caused by the loss of large amount of wind power in just few milliseconds after the voltage drop. The imbalance between active power production and consumption in the system leads thus to severe drop of the system frequency. When the frequency reaches the limits of the under frequency relays, the protection acting on the loads connected to the substations cuts off a

percentage of the connected load. For this scenario, the load shedding cause by such deep drop in frequency is 65.5 %, i.e. 54 MW of load is immediately disconnected.

Fig. 64 illustrates also the case of the Maximum Wind Power Production scenario (SCEN2), where the frequency drops down to 47.9 Hz due to the grid fault, implying a load shedding by 34% of the connected load. Although the wind farms are producing more in this scenario, the percentage of active power in the system coming from wind is less than the previous one. The minimum frequency is therefore slightly higher in this case, although still very low. The zone 47.5 Hz – 48.3 Hz is the frequency area where the under frequency protection relays are acting, meaning that in these frequencies even a small drop in frequency can lead to large load shedding. Notice that in the case of a Peak Load Demand scenario (SCEN1), the frequency does not drop below 49 Hz and the load shedding is therefore avoided. In this case, the wind farms provide with only 3% of the total production, so when the wind farms are tripping by their protection system, the loss of active power in the system is not so dramatic that can lead to significant frequency drop.

Fig. 65 illustrates the grid fault's impact on the frequency system in the case when it is assumed that the wind farms have fault ride-through capability, i.e. they are able to ride through the grid faults, without being tripping. Notice, that in this case, as the wind farms are able to remain connected to the grid during fault, the system frequency drop is significantly less. The frequency minimum in this case is for example 49.7 Hz for the Maximum Wind Power Penetration scenario (SCEN3) and the load shedding is actually avoided completely. The contribution of the fault-ride through capability in the frequency stability but also in the load shedding of power systems, like Rhodes, appears to make FRT crucial for the secure operation of the system.

Similar for SCEN3, the frequency in the other two scenarios, Peak Load Demand scenario and Maximum Wind Power Production scenario, does not drop below 49 Hz and the load shedding is again avoided.

These scenarios cover the possible operation range of the island system; therefore it is actually quite clear that when the wind farms are equipped with FRT capability, the load shedding following severe disturbances, like short circuit grid faults, can be successfully avoided ensuring the security of dynamic operation of the power system.

5. Frequency response to wind power fluctuations

This part addresses different grid integration issues of large wind farms in non-interconnected power systems with respect to secure operation during variable wind and load profiles. Today, the power systems all over the world need a dramatic and continuous restructuring, as different renewable energy technologies are going to replace some of conventional units in the near future. This means, that there is urgent need for accurate modeling of various different generation technologies and novel wind turbine control strategies to fulfill requirements set by the TSOs, in order to ensure the dynamic security of such power systems.

Especially referring to wind power, the fluctuating nature of wind power imposes serious challenges to system operators. Power system inertia, protection relays settings, voltage and frequency stability in autonomous power systems have to be carefully and thoroughly analyzed before the penetration margin levels are expanded.

In most of the cases, operation experience defines the accepted penetration levels keeping the margin at 25-30% of peak annual load. However, higher or lower values can actually be accepted depending on the combination of power generator technologies online, [5] – as it is the case of the specific power system under study here.

Modeling considerations of the power system under study are presented, especially speed governors and automatic voltage regulators of the conventional units. Defining accurate models of these system components is of vital importance for the overall system performance. Modeling and control issues for three different wind turbine technologies are described. The study case of Rhodes island is presented through simulations for various load and wind scenarios. The frequency fluctuations are calculated using wind time series based on measured and validated results, [41].

5.1. Wind farms modeling

Modern power systems include a variety of wind turbine technologies. The different response of each kind in dynamic phenomena requires separate and detailed modeling of each one. Three wind turbine technologies are considered here, namely Doubly Fed

Induction Generator (DFIG), Permanent Magnet Synchronous Generator (PMSG) and Active Stall Induction Generator (ASIG) based wind turbines.

In order to investigate the interaction between these large wind farms and the power system, an aggregated method for modeling the wind farms is used, [42], [43]. Such modeling approach is commonly used for power system studies, as it reduces substantially both the complexity of the system and the computation time, without compromising the accuracy of the simulation results.

Models for all these different wind turbine technologies are implemented, including the main components of each wind turbine configuration:

- Drive train and aerodynamics
- Pitch angle control system
- Control system
- Protection system

The system configuration, as well as some modeling and control issues for each wind turbine technology are described in the following section.

5.1.1 System configuration of variable speed DFIG wind turbine

The DFIG wind turbine configuration stands nowadays as the mainstream configuration for large wind turbines, [44]. To ensure a realistic response of a DFIG wind turbine, the main electrical components as well as the mechanical parts and the controllers have to be considered in the model. The model used in this study for the wind farms with DFIG wind turbines is described in detail in [33].

The DFIG system is essentially a wound rotor induction generator with slip rings, with the stator directly connected to the grid and with the rotor interfaced through a back-to-back partial-scale power converter [34]. The converter consists of two conventional voltage source converters (rotor-side converter RSC and grid-side converter GSC), and a DC-bus, as illustrated in Fig. 66.

A two-mass model is used to represent the drive train to illustrate the dynamic impact of wind turbines on the grid properly. A large mass for the wind turbine rotor and a small mass for the generator are thus connected by a flexible shaft characterized by stiffness and damping for the low-speed shaft. A simplified aerodynamic model, based on a two-

dimensional aerodynamic torque coefficient *Cq* table [34], is typically sufficient for such studies.

The control system consists of a pitch control system and an electrical control system of the converters. The pitch control system is realized by a PI controller with antiwind-up, using a servomechanism model with limitation of both the pitch angle and its rate-of-change. As the pitch angle controls directly the generator speed to its reference signal, this control is able to prevent over-speeding both in normal operations and during grid faults, by limiting the mechanical power extracted from the wind and thus restoring the balance between electrical and mechanical power.

The efficiency of the pitch control system is crucial for studies like in this work, where the response of the wind farms under variable and extreme wind conditions is vital from the power system perspective.

The electrical control system, depicted in Fig. 66, is essential for a good behavior of a DFIG wind turbine during both normal and grid fault operations. Decoupled control of active and reactive power is applied through vector control techniques [34], allowing for changes in the active and reactive power in the range of milliseconds. The RSC controls mainly the active and reactive power delivered to the grid, while the GSC ensures nominal voltage at the common DC-bus at unity power factor operation of the converter. As illustrated in Fig. 66 and described in details in [46]-[47], the control of the converters is based on cascade control loops: a very fast inner current controller regulates the currents to the reference values that are specified by the outer slower power controller.

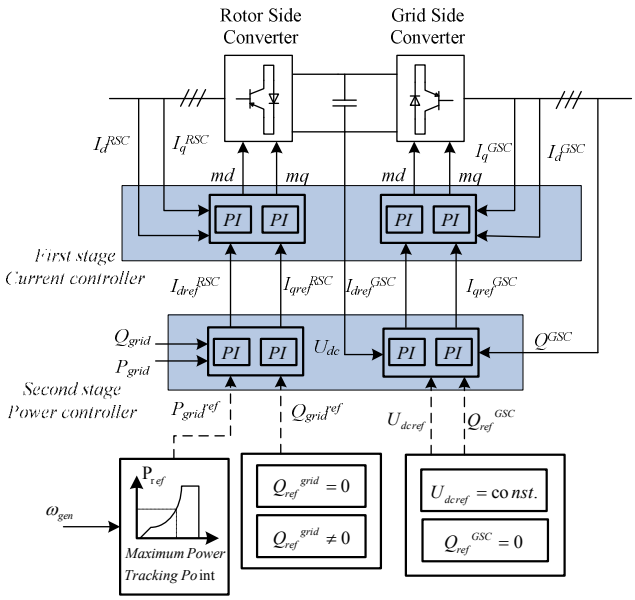

Fig. 66. Electrical control scheme for the DFIG wind turbine.

5.1.2 System configuration of variable speed PMSG wind turbine

Similar to the DFIG wind turbine configuration, the PMSG model consists both of a wind turbine mechanical level (i.e. aerodynamics, gearless drive-train and pitch angle control) and a wind turbine electrical level (i.e. multi-pole PMSG with a full-scale frequency converter and its control).

The synchronous generator is connected to the grid through a full-scale frequency converter system that controls the speed of the generator and the power flow to the grid. The full-scale frequency converter system consists of a back-to-back voltage source converter (generator-side converter and the grid-side converter connected through a DC link), controlled by IGBT switches. The rating of the converter system in this topology corresponds to the rated power of the generator plus losses. The presence of such a converter enables the PMSG to keep its terminal voltage on a desired level and to adjust its electric frequency according to the optimized mechanical frequency of the aerodynamic rotor, independently of the fixed electric frequency and the voltage of the AC grid.

The wind turbine mechanical level of PMSG (aerodynamics, drive train and the pitch control) is modelled similarly to that for the DFIG wind turbine. The generic control

strategy of the frequency converter for the PMSG wind turbine, as illustrated in Fig. 67, is described in details in [36].

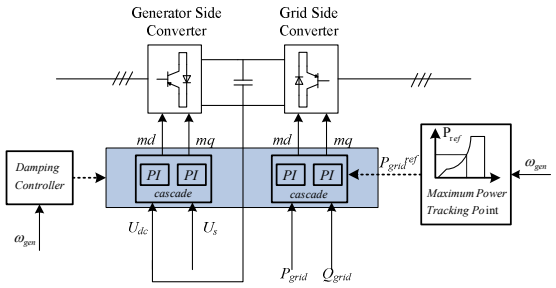

Fig. 67. Power converter control strategy for the variable speed wind turbine with multi-pole PMSG.

The damping controller ensures stable operation for the wind turbine, by damping the torsional oscillations excited in the drive-train and reflected in the generator speed ω_{gen}. The generator-side converter controller keeps DC-bus voltage U_{dc} constant and controls the generator stator voltage U_s to its rated value in the stator voltage reference frame. The advantage of controlling the generator stator voltage U_s to its rated value is that the generator and the power converter always operate at the rated voltage, for which they are designed and optimized. The grid-side converter controller controls independently the active P_{grid} and the reactive Q_{grid} power to the grid in the grid voltage reference frame. The controllers of the converter are also based on control loops in cascade, similarly to the DFIG control scheme.

5.1.3 System configuration of fixed speed ASIG wind turbine

The sub-models for aerodynamics, mechanical components and the squirrel cage induction generator in the ASIG wind turbine configuration are as described in [48].

The drive train is again represented by a two-mass model, similar to the other configurations. The turbine's power is controlled directly by the pitch controller through the pitch angle. The operation of the wind turbine is based on two control modes:

Power limitation - where the turbines power is limited to the rated power above rated wind speed. The stall effect is thus controlled by adjusting accordingly the pitch angle.

Power optimization - where the aerodynamic efficiency and thus the power output is maximized for wind speeds below rated wind speed. The pitch angle as function of the wind speed is shown in Fig. 68.

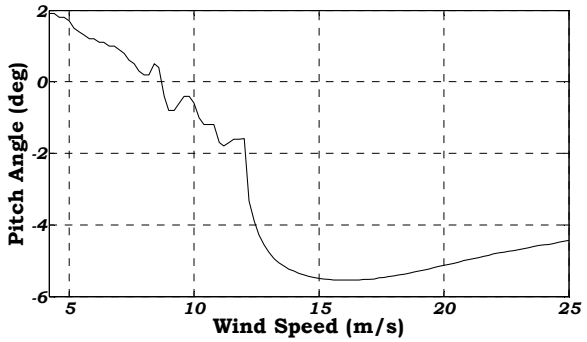

Fig. 68. Pitch angle as a function of the wind speed.

Notice that all three wind turbine configurations are using a gain scheduling procedure, [49], in their pitch control system in order to compensate for the existing non-linear aerodynamic characteristics. The fundamental principle of the gain scheduling feature is that the proportional controller of the pitch angle controller is varied so that the total gain of the system remains unchanged for all the operating points of the wind turbine.

5.2. Simulation results

In the following, two sets of simulations are carried out. The emphasis is made on the secure operation of the system under variable load and wind profiles. The goal of these simulations is to illustrate and evaluate the interaction between the five wind farms with Rhodes power system during different load scenarios and winds. The first set of simulations focuses on the dynamic response of the three types of wind farms configurations, considered in this article and on the impact on the system during deterministic wind speed steps. The second set of simulations is carried out in order to illustrate and evaluate the fluctuations that occur in the generator speed and the power of wind turbines in the presence of a turbulent wind. The attention is also drawn to the impact of these fluctuations on the power system of Rhodes and to the wind farm controller capability to ensure safe operation of the wind farms during different variable load and wind profiles.

5.2.1 Deterministic wind speed steps in wind farms

In the following, the response performance of each individual wind farm type during sudden steps in wind speed is assessed through simulations. It order to keep focus on the impact each wind farm type has on the power system, it is assumed that the steps in wind speed are applied for one wind farm at a time, while the wind speed for the others is considered to be constant. These step response simulations are especially interesting for a maximum wind power penetration scenario, i.e. SCEN3, as in this case the frequency of the system can vary significantly when sudden changes in wind speed occur. The wind speed changes cover different wind speeds from low up wind speeds to over the rated wind speed.

Fig. 69 and Fig. 70 show the results for the case when a set of wind steps is applied as input in the DFIG wind farm, WFA1. As mentioned, the wind speeds of the other wind farms are assumed constant during the simulation. As illustrated in Fig. 69, the wind speed is stepped-up every each 30sec.

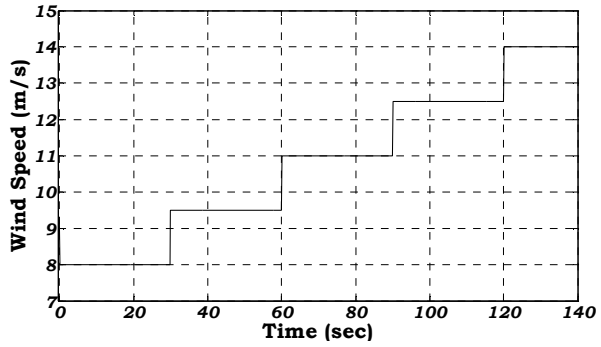

Fig. 69. Wind speed steps applied to WFA1 (SCEN3).

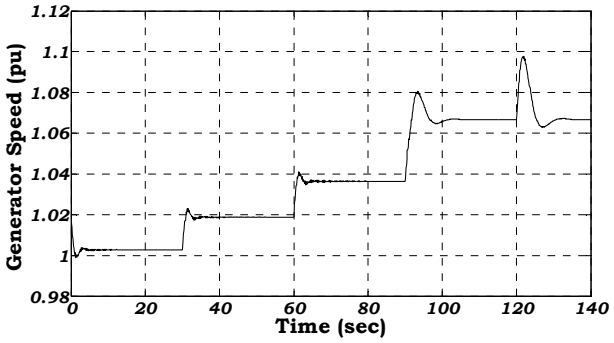

Fig. 70. Generator speed for a DFIG wind turbine in WFA1 (SCEN3).

Notice that, in power optimization (at wind speeds less than the rated speed - 12m/s), the Maximum Power Tracking (MPT) strategy succeeds to adapt the generator speed accordingly to the wind speed, in such a way that it is extracted the maximum power out of the wind. In power limitation (at wind speeds above the rated wind speed), the generator speed is kept at its rated value. As described in section 3.3, the converters controller controls the active power to the active power reference provided by the maximum power tracking look-up table. Notice that the generator speed is decoupled from the power system frequency.

At rated wind speed the wind farm produces 11 MW, which accounts for 13% of the demand. As illustrated in Fig. 71, the frequency of the system increases accordingly to the increased injected active power by the DFIG wind farm into the system. Notice that, the primary control of the conventional generators on the island manages to stabilize the frequency in less than 5 seconds, each time after a step in the wind speed. As the secondary control is not active in this time frame, the frequency reaches each time a new steady state value, which is not equal to 50 Hz. The frequency varies thus between 49.8 Hz and 50.25 Hz, which is an area where the under/over frequency relays are not activated. The impact in the system although visible in terms of frequency deviations is thus negligible.

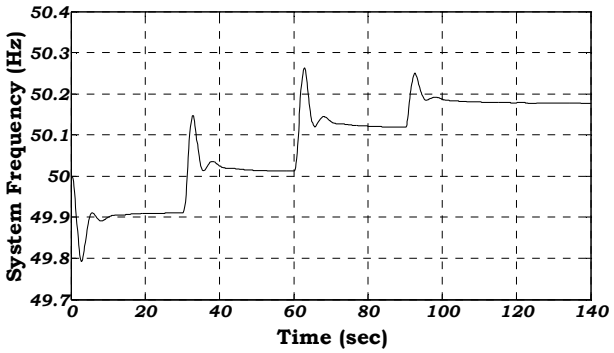

Fig. 71. System frequency for wind steps in WFA1 (SCEN3).

Fig. 72 illustrates which is the impact of wind speed changes applied to the DFIG wind farm (WFA1) on the generator speed of the wind turbines existing in the active stall wind farm WFC (see TABLE II). As expected, the fixed speed wind turbine equipped with induction generator acts as any other induction machine in the system, when sudden changes in frequency occur. Notice that the curves of the system frequency and of the

generator speed of an ASIG wind turbine are very similar. For example, in this case when there is an increase in system frequency, the turbine starts accelerating at a rate determined by the moment of inertia of the turbine plus all the masses connected to the shaft connecting the turbine and the generator mass. This leads to reduction of the electrical energy delivered to the grid, thus increasing the kinetic energy of the rotating mass. An opposite behavior appears when there it is a decrease in system frequency, as it is the case at time t=0 sec in Fig. 71. The active stall wind farm counteracts in these means the active power surged by the DFIG wind farm, by reducing its electrical power output.

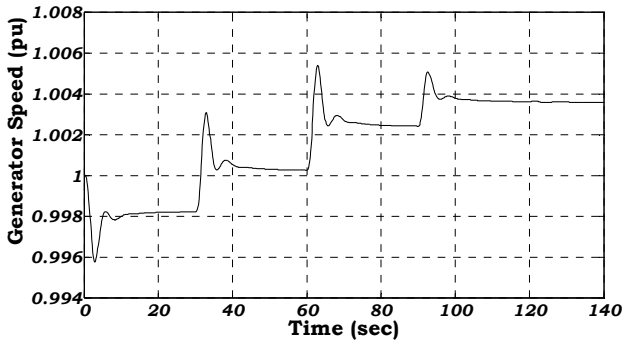

Fig. 72. Generator speed for ASIG wind turbine in WFC during wind steps in DFIG wind farm WFA1 (SCEN3).

Fig. 73 and Fig. 74 show the results for the case when a set of wind steps is now applied as input to the wind farm WFB1 equipped with permanent magnet synchronous generator wind turbines (see TABLE II).

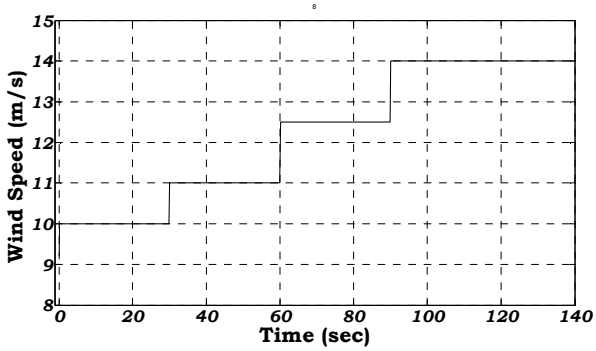

Fig. 73. Wind speed steps applied to WFB1 (SCEN3).

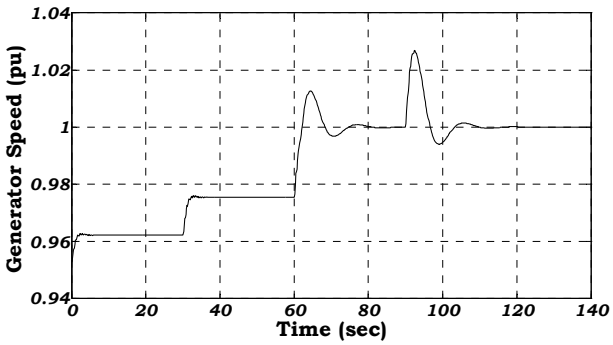

Fig. 74. Generator speed for a PMSG wind turbine in WFB1(SCEN3) .

Notice, that the response of the PMSG wind turbine, shown in Fig. 74, is similar to the of the DFIG wind turbine, illustrated previously. The generator speed of a PMSG wind turbine is as expected fully decoupled from the system frequency – see Fig. 74 and Fig. 75.

In power limitation, when the wind speed increases above the rated value, the wind farm WFB1 produces 18 MW i.e. 21% of the total demand. The frequency deviations shown in Fig. 75 are slightly larger than the ones shown in Fig. 71, although the range is still in a narrow range around the nominal 50 Hz.

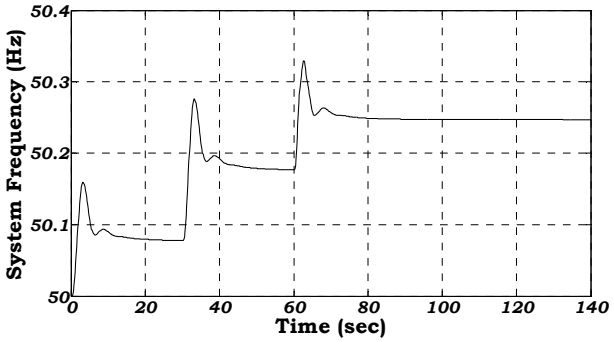

Fig. 75. System frequency for wind steps in WFB1 (SCEN3)

Fig. 76 illustrates the deviations of the generator speed in a ASIG wind turbine provoked this time by wind speed steps applied to a PMSG wind turbine. Notice that ASIG wind turbine reacts similar to the response presented in Fig. 72.

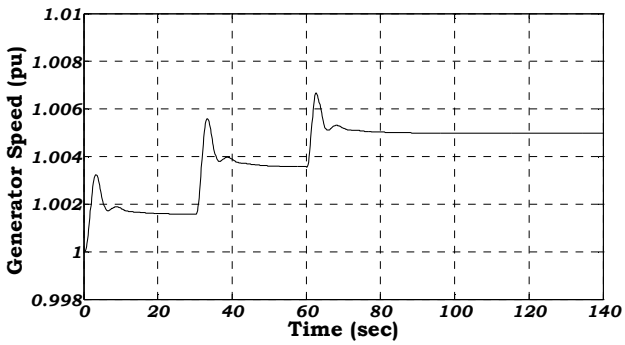

Fig. 76. Generator speed for ASIG wind turbine in WFC during wind steps in PMSG wind farm WFB1 (SCEN3).

5.2.2 Turbulent wind speed in wind farms

In the following, simulations with turbulent wind speed time series are presented and discussed. The goal of these simulations is to evaluate the fluctuations in the system frequency due to wind speed fluctuations during different load scenarios. It is assumed that all five farms are running with turbulent wind speed.

The wind turbine time series, which are inputs to the wind farms, are generated based on the wind speed fluctuation model developed by Sorensen et. al., [41]. This wind speed fluctuation model has been validated against wind speed measurements from large wind farms.

For each wind farm site and each wind and load scenario, different wind time series are generated for 10 minutes. The correlation between the wind speeds of the wind turbines in a wind farm is taken into account in the wind speed fluctuation model. The correlation aspect is even more important for such isolated power system as it is the case of Rhodes island. As the distances between the wind farms are quite small, the wind speeds seen by the wind farms can be highly correlated.

- *Results for SCEN1*

Fig. 77 illustrates the wind time series, which has been applied to the wind farms, during the load scenario with maximum load demand, i.e. SCEN1. Notice, that all wind farms are running in power optimization mode, as their wind speeds are below the rated wind speed.

In this scenario, the wind farms produce in total 7.5 MW, accounting only for 3% of the total demand. The system frequency fluctuations due to the wind speed fluctuations

are negligible, as illustrated in Fig. 78, thus the wind power impact on the power system is in this case very small. As expected, although visible, the fluctuations are of quite small magnitude and they are therefore not leading to problems in the system security.

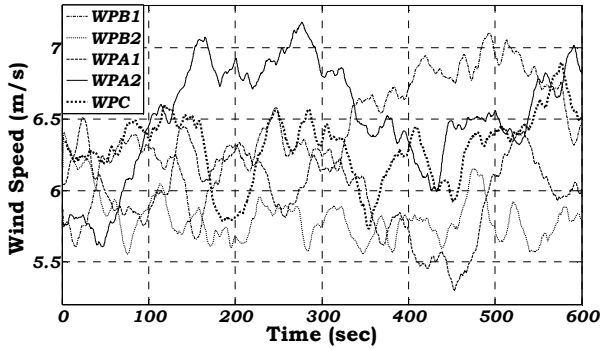

Fig. 77. Wind time series applied to the wind farms (SCEN1).

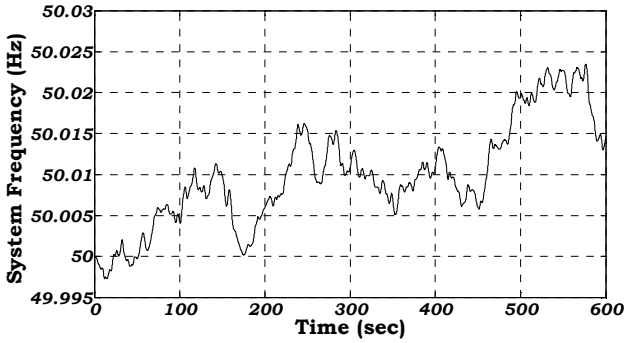

Fig. 78. System frequency for wind time series (SCEN1).

- *Results for SCEN2*

Fig. 79 illustrates the wind time series, which has been applied to the wind farms, during the load scenario with maximum wind power production, i.e. SCEN2.

Notice that in this SCEN2, the wind turbines operate in a narrow range around their rated capacity and it can thus be presumed that the wind power fluctuations' impact on the Rhodes power system to be more significant compared to the SCEN1.

Due to the highly correlated the wind speeds, the form that frequency fluctuations appear to have in Fig. 80, is not directly related to a specific wind time series, but rather to the combination of the active power fluctuations delivered by all five wind farms.

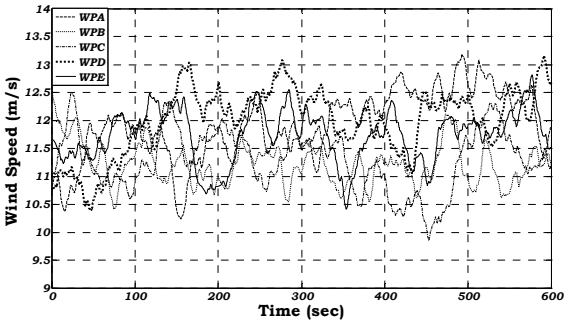

Fig. 79. Wind time series applied to the wind farms (SCEN2).

In this scenario, the wind farms produce in total 45.2 MW, which corresponds to 26% of the total demand. Notice that the system frequency, illustrated in Fig. 80, has very fast dynamic deviations in the range 49.96 Hz – 50.1 Hz, which is considered safe from the power system security point.

Even though the wind power penetration is significant in SCEN2, the frequency fluctuations are not considered large enough to impose security questions. The high correlation among the wind in all the wind farms is ensuring that the system frequency is not strongly dependent on a sudden drop or increase of the wind in only one wind farms. One of the most important factors influencing the frequency deviations – besides the parameters of the conventional units and their emergency rate of power undertake – is of course the size of each wind farm and the type of generator used.

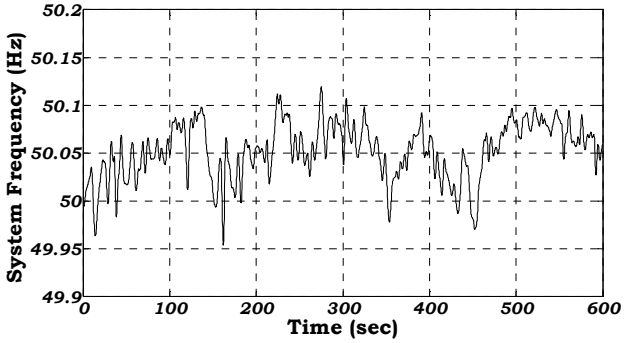

Fig. 80. System frequency for wind time series (SCEN2).

The following graphs show the performance during the scenario SCEN2 of two wind turbine technologies, i.e. ASIG wind turbine and PMSG wind turbine, which are picked-up to illustrate the behavior of a generic fixed and variable speed wind turbine,

respectively. Beside the wind speed, typical quantities, as generated power to the grid, generator speed and the pitch angle are illustrated.

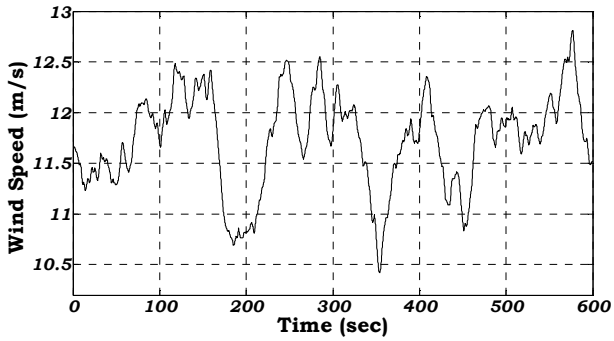

Fig. 81. Wind time series in ASIG wind farm WFC (SCEN2).

Fig. 81 illustrates the wind speed time series applied as input to an ASIG wind turbine inside wind farm WPC. Notice that the wind turbine is simulated at an average wind speed of about 11.5 m/s. This operational point corresponds to a transition operational regime for the wind turbine, between power optimization and power limitation regime.

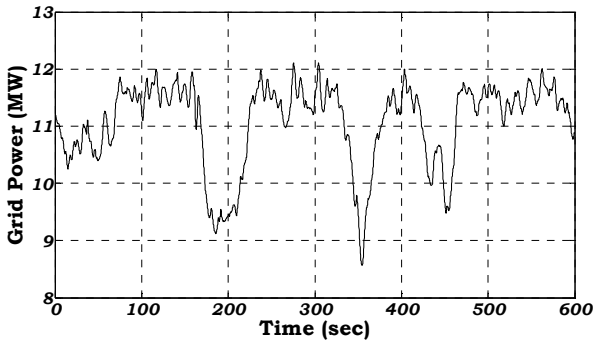

Fig. 82. Wind farm active power output for ASIG wind farm WPC (SCEN2).

The strong correlation between the wind speed fluctuations, active power output and generator speed is obvious in Fig. 81 -Fig. 83. As expected for a ASIG wind turbine, the 3p fluctuation in the wind is visible both in the active power output and the generator speed. It should be noticed that, in this scenario SCEN2, the ASIG wind farm produces around 6 % of the total demand.

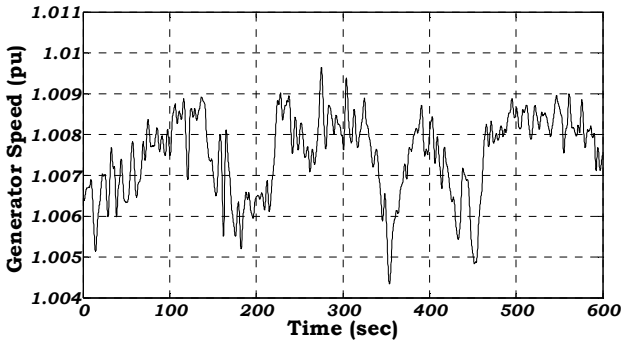

Fig. 83. Generator speed for ASIG wind turbine in wind farm WPC (SCEN2).

Fig. 84 shows the pitch angle of ASIG wind turbine during SCEN2. When the wind speed is less than the rated wind, the wind turbine produces maximum possible power. In this case, the pitch angle is equal with its optimal value, i.e. -1.7 deg. When the wind speed is above rated wind speed value, the pitch angle corresponds to the values which keep the turbine power to the rated power. Notice that the pitch system responds with delay due to the pitch rate limiter existing in the actuator. Despite the very fast wind speed deviations, the pitch control system manages to ensure smooth transition between the optimization and limitation range whenever the wind speed crosses the rated value.

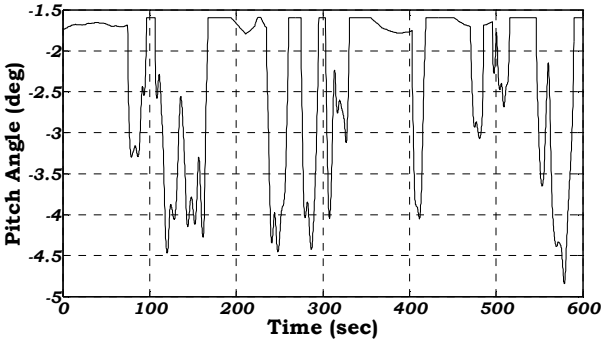

Fig. 84. Pitch angle for ASIG wind turbine in wind farm WPC (SCEN2).

Fig. 85 - Fig. 88 illustrate how the wind farm WFB2 equipped with PMSG wind turbines behaves during the scenario SCEN2. Fig. 85 shows the wind speed time series, which has been applied as input to a PMSG wind turbine inside wind farm WFB2.

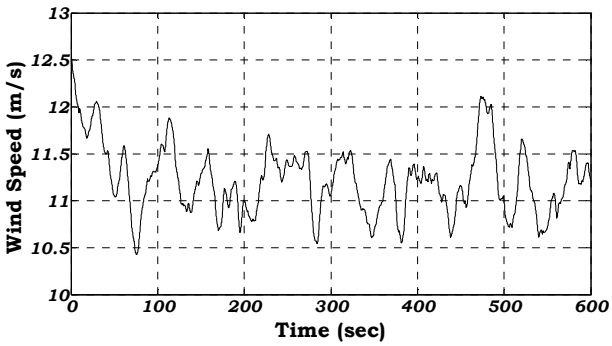

Fig. 85. Wind time series in PMSG wind farm WFB2 (SCEN2).

Similar to the ASIG wind turbine, discussed previously, the operation point of the PMSG wind turbine corresponds again to a transition operational regime for the wind turbine, between power optimization and power limitation regime.

This wind farm has rated capacity 3 MW, which stands for 1% of the total demand. As illustrated in Fig. 86, whenever the wind speed goes above the rated value, the pitch control manages to keep the active power output constant and equal to nominal power.

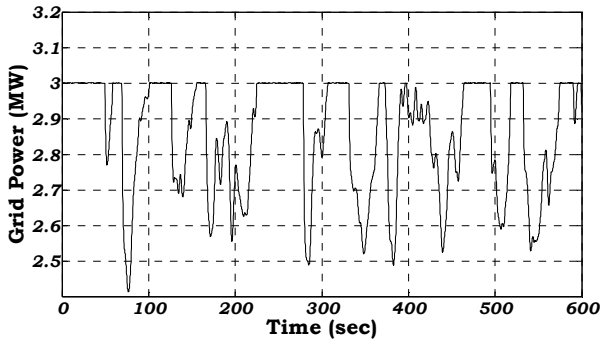

Fig. 86. Wind farm active power output for PMSG wind farm WPB2 (SCEN2)

Notice that the generator speed of the PMSG wind turbine is tracking the slow variation in the wind speed each time the turbine is running in the operation mode, while in power limitation mode, the speed controller tries to control the generator speed to its rated value.

The damping controller manages to damp the torsional oscillations in the drive train and ensures safe operation of the wind turbine. Compared to the results from the ASIG wind farm above, the fast deviations in the wind are filtered out from the electrical power. The generator is decoupled from the grid through the converter at its terminal and any rapid fluctuations in the wind are not influencing the power delivered to the grid. Fig.

88 gives the pitch angle, which is increased from its optimal value each time the turbine is running in power limitation mode.

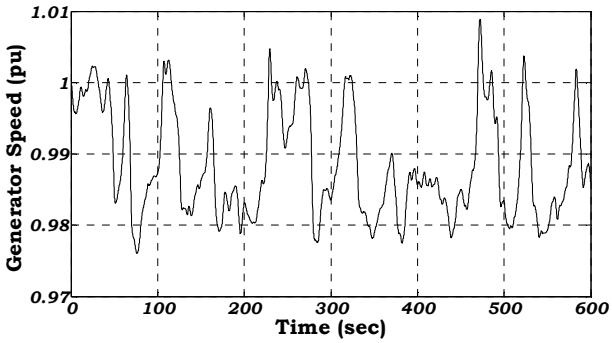

Fig. 87. Generator speed for PMSG wind turbine in wind farm WPB2 (SCEN2)

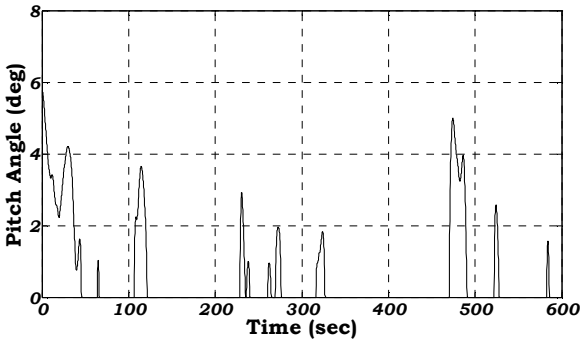

Fig. 88. Pitch angle for PMSG wind turbine in wind farm WPB2 (SCEN2).

- *Results for SCEN3*

In this scenario, the wind power penetration is maximum, reaching 32% of the total demand. The wind farms however are not producing as much as in SCEN2. This scenario is considered the worst case scenario, as the fluctuations in the wind may have serious impact on the power system operation.

Fig. 89 illustrates the wind time series, which has been applied to the wind farms, during the load scenario with maximum wind power penetration, i.e. SCEN3.

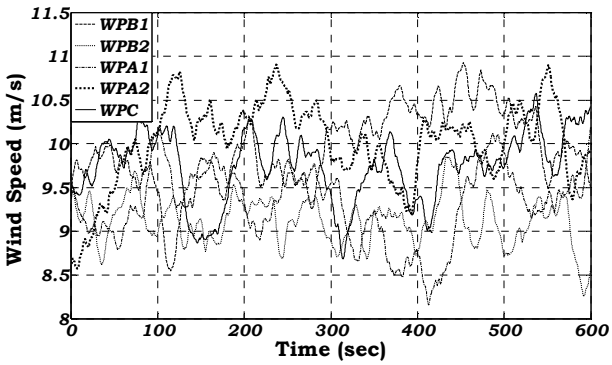

Fig. 89. Wind time series applied to the wind farms (SCEN3).

The range of operation for the wind turbines in this case covers the optimization area, where the control of the wind turbine has to ensure optimum power output.

As illustrated in Fig. 90, due to the wind fluctuations, the system frequency varies between 50 Hz and 50.25 Hz, which is considered safe for the system operation. Although the wind speeds in each wind farm may have sudden changes, as it is illustrated in Fig. 89, the overall response of the system is satisfactory, and the power outputs from the wind farms seem to counteract each other in the frequency impact. The system frequency deviates more in this case than in SCEN2 (see Fig. 80), which is due to the increased wind power penetration levels in this scenario. Nevertheless, the emergency rate of power undertaken by the conventional units is sufficient to overcome the rapid active power fluctuations produced by the wind farms on the island.

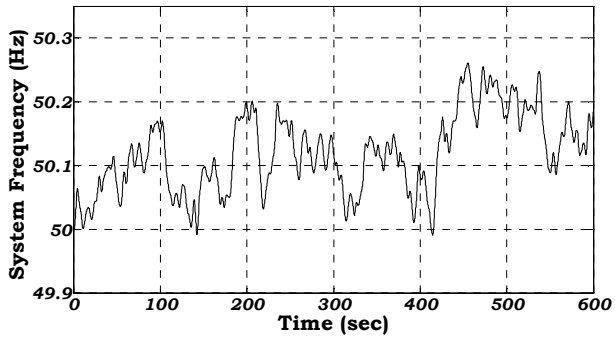

Fig. 90. System frequency for wind time series (SCEN3).

In the following, the attention is directed in details towards the performance of two wind turbine technologies during SCEN3, this time on a ASIG wind turbine and a DFIG wind turbine. Again typical quantities, as generated power to the grid, generator speed and the pitch angle are illustrated.

Fig. 91 illustrates the wind speed time series, which has been applied as input to the ASIG wind farm WPC. In scenario SCEN3, this wind farm produces around 7 MW i.e. 8 % of the total demand.

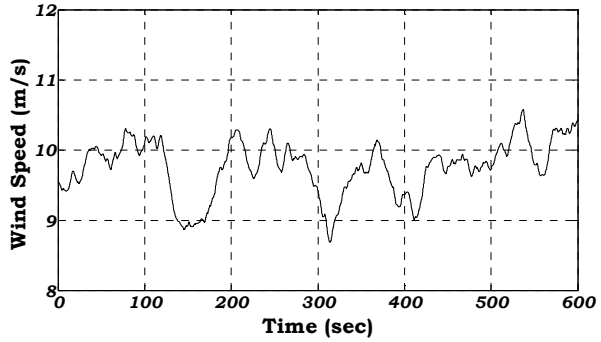

Fig. 91. Wind time series in ASIG wind farm WFC (SCEN3).

Notice in Fig. 91-Fig. 93 that the fluctuations in wind speed, active power output, generator speed are strongly correlated in this case, and the fast dynamic deviations are also here significant. Fig. 94 shows the pitch angle, which is reduced accordingly although restricted by the pitch rate limiter when the wind speed changes at very high rate.

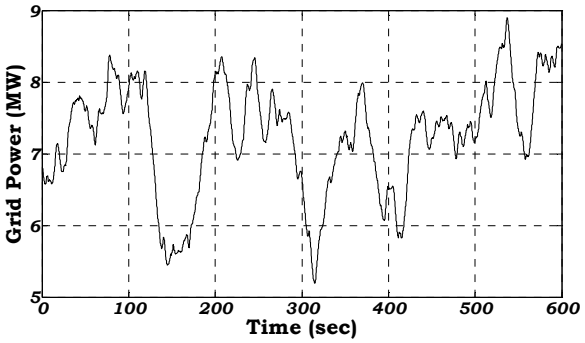

Fig. 92. Wind farm active power output for ASIG wind farm WPC (SCEN3).

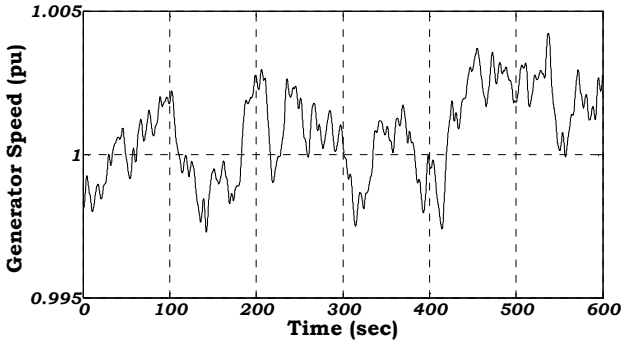

Fig. 93. Generator speed for ASIG wind turbine in wind farm WPC (SCEN3).

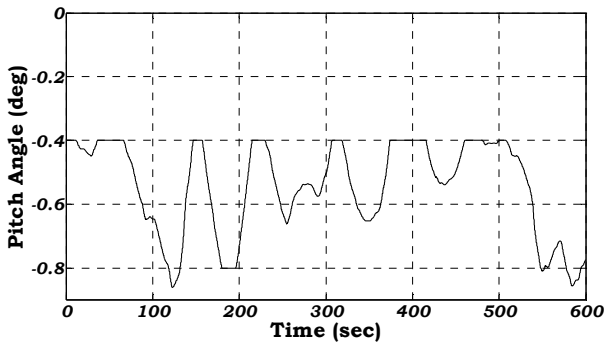

Fig. 94. Pitch angle for ASIG wind turbine in wind farm WPC (SCEN3).

The dynamic performance of the DFIG wind farm WPA1 during SCEN3 is in the following addressed in order to illustrate the efficiency of the designed models. This farm produces almost 6.5 MW i.e. 7.5% of the total demand. Fig. 95 shows the wind speed time series, which has been applied as input to the DFIG wind farm during SCEN3.

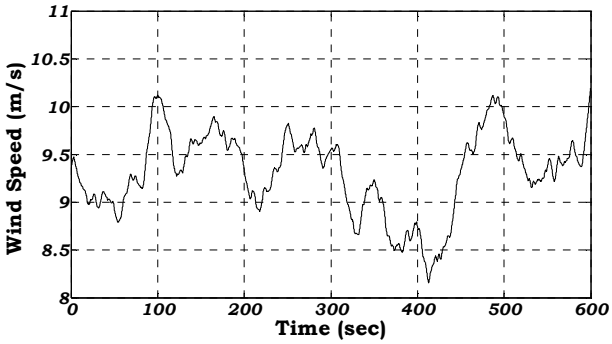

Fig. 95. Wind time series in DFIG wind farm WFA1 (SCEN3).

The Maximum Power Tracking (MPT) strategy, implemented in the RSC (rotor-side converter) of the DFIG system ensures optimum operation of the wind turbine maximizing the aerodynamic coefficient Cp in every wind speed. In this operational area for the DFIG wind turbines, small changes in the rotor speed result in significant changes in the active power output of the system. This is due to the fact, that the designed MPT characteristic is very stiff in this area.

Notice that, contrary to an ASWT wind farm, where the correlation between the system frequency and the wind turbine response is very strong, in the case of DFIG configuration the generator is partially decoupled from the system frequency, as seen in Fig. 90, Fig. 93 andFig. 97.

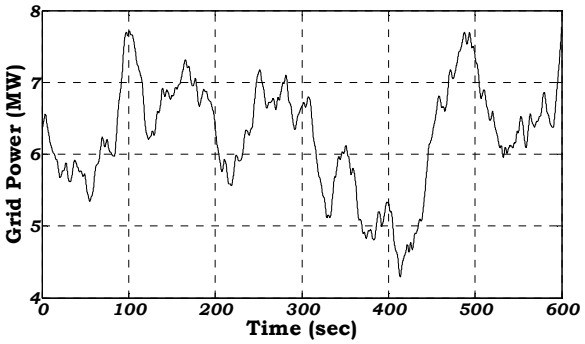

Fig. 96. Wind farm active power output for DFIG wind farm WPA1 (SCEN3).

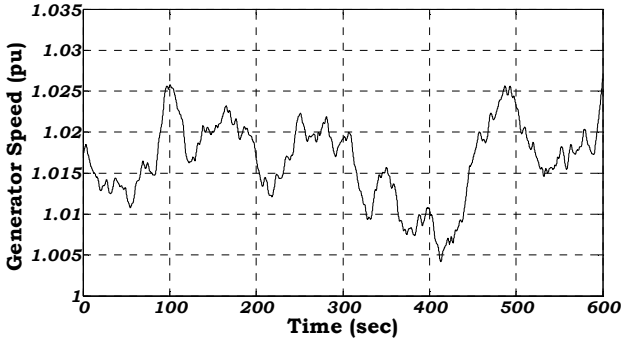

Fig. 97. Generator speed for DFIG wind turbine in wind farm WPA1 (SCEN3).

The generator is speed is continuously adapted to the wind speed in order to extract maximum power out of wind. As wind farm is running in optimization mode, the pitch angle is passive, being kept constant to its optimal value.

6. Frequency control of wind power

Increasing wind power penetration especially in non-interconnected systems is changing gradually the way grid frequency control is achieved. The technical requirements set by the networks operators include various aspects, such as fault ride-through of wind turbines during faults, voltage-reactive power control and overall control of the wind farms as conventional power plants. A key aspect of the operation of wind farms in autonomous power systems is the frequency control. This session presents the results from a study on the Rhodes power system already presented above, focusing on frequency control. The Rhodes power system has been used to address all the main issues related to system secure operation under different system conditions. The response of the wind farms in frequency disturbances is analyzed and the different characteristics of each wind turbine type related to frequency are described. Three different wind turbine configurations have been used – Active Stall Induction generator (ASIG), Doubly Fed Induction generator (DFIG) and Permanent Magnet Synchronous generator (PMSG). An auxiliary control has been designed for the DFIG type to enhance the capability to support the frequency control. The load shedding following severe frequency disturbances is calculated and the under/over-frequency protection relay settings are discussed under the novel system conditions. Results for different system conditions and control methods are presented and discussed focusing on the ability of modern wind turbine technologies to assist in frequency control in isolated power systems during severe disturbances in the production-consumption balance.

As wind power penetration increases in modern power systems, a variety of technical and regulatory issues regarding the interaction between large wind farms and power system is under constant discussion. The system operators are setting onerous requirements that that wind farms have to fulfill. Among these, voltage and frequency control play an important role. Frequency control has started to appear as emerging need under increasing wind power penetration conditions and due to the extended replacement of conventional generators by large wind farms in power supply. The impact of wind farms in frequency phenomena is even more vital in non-interconnected power systems, where the power system inertia is limited.

It is often the case, that when auxiliary services of wind turbines, like frequency control, are investigated, simple models are used for either the power system or the wind turbines. In this article, detailed model for all different components of the system were used to evaluate the system response in serious events with maximum accuracy. The dynamic security of power systems has to be carefully examined, before wind power penetration limits are expanded. The response of conventional units, the load dependency on frequency and voltage and the wind turbines' response during events that affect system frequency are some of the key aspects that have to be modeled in detail for this kind of investigations.

In this article the main issues of frequency control in isolated power systems, with high wind power penetration are investigated. Rhodes power system, includes three different types of conventional generators – namely gas, diesel and steam units – and three different types of wind turbines – Active Stall Induction generator (ASIG), Doubly Fed Induction generator (DFIG) and Permanent Magnet Synchronous generator (PMSG) wind turbines. This variety of components gives the chance for a wide range investigation of frequency issues for modern power systems.

Definitions regarding the frequency control in autonomous power systems are given and the protection relay system settings related to under/over frequency deviations are discussed. The response of different wind turbine technologies during frequency events is explained. Three different primary frequency control schemes implemented in the developed model are analyzed. Finally, the basic characteristics of the power system are given followed by a brief description of the available wind turbine technologies available on line in the system for the reference year 2012. Results from various simulations are discussed and the capability of modern wind farms to provide auxiliary frequency control is demonstrated.

6.1. Frequency definitions and protection system

In this section, some basic definitions on frequency are given to introduce the main issues regarding frequency control with emphasis on isolated power systems.

In the power system, frequency is the variable indicating balance or imbalance between production and consumption. During normal operation, the frequency should be

around the nominal value. The deadband which is considered as safe operation in most European grid codes is the zone $50 \pm 0.1\,\text{Hz}$, although the limits vary between the different system operators in Europe, mainly due to the different characteristics of each grid. The range $49 \div 50.3$ Hz is in general the dynamic security zone that in most of the cases is not allowed to be violated at any means, [50]. However, these safety margins for frequency deviations are often expanded in autonomous power systems, where system inertia is low, to avoid constant load shedding whenever the balance between production and consumption is lost.

In case of sudden generation loss or large load connection, the frequency of the frequency starts to drop. The two main system functions that ensure return of an unbalanced system to nominal frequency are:

- *Primary Control:* During the first 30-40 sec after the event leading to frequency deviation, the rotational energy stored in large synchronous machines is utilized to keep he balance between production and consumption through deceleration of the rotors. The generation of these units (often referred to as primary control units) is thus increased until the power balance is restored and the frequency is stabilized.
- *Secondary control:* After the primary response of the generators, a slow supplementary control function is activated in order to bring frequency back to its nominal value. The generators connected to the system are ordered to change their production accordingly either through an Automatic Generation Control scheme, either through manual request by the system operator – which is often the case in isolated systems like Rhodes.

These two main frequency control functions are illustrated in Fig. 98 for a sudden drop in system frequency.

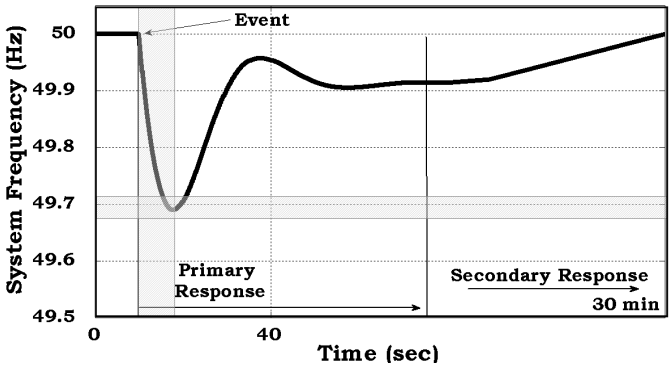

Fig. 98. Definitions of frequency control in power systems

The rate, at which the frequency changes following an event i.e. drops in Fig. 98, is depending on the so called inertia of the system thus the total angular momentum of the system which is the sum of the angular momenta of the rotating masses in the system i.e. generators and spinning loads. The frequency control implemented in this study tries to improve the system response in terms of initial Rate of Change of Frequency and minimum frequency (frequency nadir). Therefore, the discussion and also the results will emphasize the capability of wind farms to provide with primary frequency support in the first seconds after the event which causes the frequency deviation.

6.2. Response of wind turbines to frequency events

The replacement of conventional synchronous generators by wind farms in modern power systems with increased wind power penetration, changes the way traditional frequency control was treated in power systems. Wind turbines connected to the grid, depending on their configuration, have a different response to frequency deviations. In this Session, the relation between each wind turbine configuration and its response during frequency deviations is discussed and explained.

6.2.1 Response of ASIG wind turbines in frequency events

One of the most common wind turbine configurations in modern power systems is the standard fixed speed wind turbine based on induction generator connected to the rotor through a transmission shaft and a gearbox. The Active Stall Induction Generator wind turbine model developed to simulate the fixed speed wind turbines in this study is described in previous sections.

As described in [51], the induction machine based wind turbine inertia response is slower and lower than the conventional synchronous generator's response. This difference is mainly because of the reduced coupling of the rotational speed of the WT and the system frequency and of the lower inertia constant of the WT compared to a standard conventional generator connected to the grid.

However, in the case of a frequency drop, like the one illustrated in Fig. 98, the inertia response of the ASIG wind turbine is not negligible due to usual low nominal slips. The rotor of the ASIG is decelerating following the system frequency drop. The kinetic energy which was accumulated in the rotating mass is transformed into electrical energy delivered to the grid. The amount of the available kinetic energy is determined from the total angular momentum of the WT – thus the sum of the angular momenta of the electrical generator, the rotating blades and the gearbox – and the rotational speed. There are some studies estimating this available energy [52], [53] through rough estimations.

A comparison between the inertia response provided by the three different wind turbine configurations studied in this article is given in Fig. 99 for loss of the largest infeed in the system of Rhodes. When the frequency starts to drop, the ASIG provides with significant active power surge to the grid, thus, reducing the initial rate of change of frequency. The response of the DFIG and PMSG wind turbine types is explained further below. It is obvious that, fixed speed wind turbines have an intrinsic behavior that provides auxiliary service to the system during frequency imbalances, although they can not contribute to other services, i.e. voltage – reactive power control, in the same way the variable speed wind turbines can.

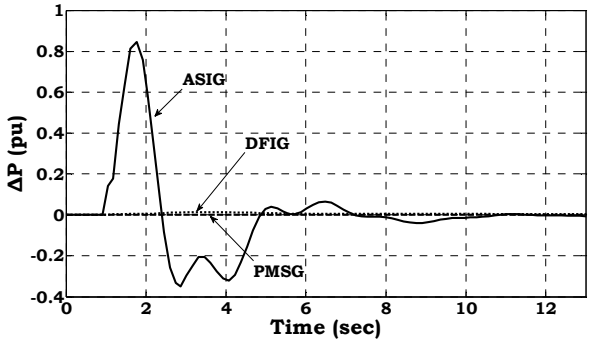

Fig. 99. Change in active power production during a frequency drop for the three main wind turbine configurations

6.2.2 Response of DFIG wind turbines in frequency events

The DFIG wind turbine configuration, which is the most common configuration for large wind turbines, is mainly based on an induction generator and a frequency converter connected to the rotor circuit via slip rings. Details on the model developed in this study, including control aspects, can be found in section 3.3.

As described in [52], the response of a DFIG wind turbine is slightly different than the one described above for synchronous and induction generators. The inertial response of the DFIG type is mostly based on the applied control scheme acting on the converter connecting the rotor to the grid [51]. The overall response can be explained as the result of two opposite torques acting on the rotor during a frequency change, i.e. a frequency drop: a decelerating torque, proportional to the rate of change of the rotor speed $\frac{d\omega}{dt}$ and therefore to the frequency $\frac{df}{dt}$, which makes the rotor speed follow the frequency drop – an accelerating torque, which is produced by the difference in the electromagnetic torque, controlled by the speed controller of the machine, and the aerodynamic torque acting on the rotor of the turbine. This last component tends to cancel the decreasing effect that would eventually make the DFIG have a similar response to a simple induction generator connected to the grid, [54].

6.2.3 Response of PMSG wind turbines in frequency events

A multi-pole PMSG wind turbine is connected via a full-scale frequency converter to the grid. The converter decouples the generator from the grid; the generator and the turbine system are not directly subjected to grid faults in contrast to the direct grid connected wind turbine generators. Therefore, the power output from the WTG does not change and no inertial response is obtained during a frequency event. The rotor speed of the multi-pole synchronous generator is not connected with system frequency at any means. Details for this wind turbine configuration can be found in section 3.2.

6.3 Frequency control in DFIG wind turbines

Large wind turbines nowadays substitute conventional generators in modern power systems under increasing wind power penetration conditions. The effect on the power

system inertia and the availability of inertia response from wind turbines have become key issues for the secure integration of wind energy into the electrical grids, especially in autonomous power systems like Rhodes. In power systems, like the one studied in this article, regular load shedding occurs due to large frequency deviations. Although sufficient spinning reserve is ensured to overcome any frequency problems, increasing wind power penetration is challenging the system security.

Supplementary control attributes have been proposed in the literature in order to achieve active frequency control by the wind turbines, [51], [52], [54]-[57]. In most of these publications, simple models for either the power system or the wind turbines are used based mainly on the assumption that the aerodynamic torque acting on the rotor during the frequency event does not vary significantly. In this section, the three different frequency control methods, which were applied in the DFIG wind turbine models used in the Rhodes power system model, are described:

- Inertia Control
- Droop Control
- Combined Control

Results from frequency events in the Rhodes power system when these control methods are used in the wind farms equipped with DFIG wind turbines are given in Section VI. The general control scheme is illustrated in Fig. 100.

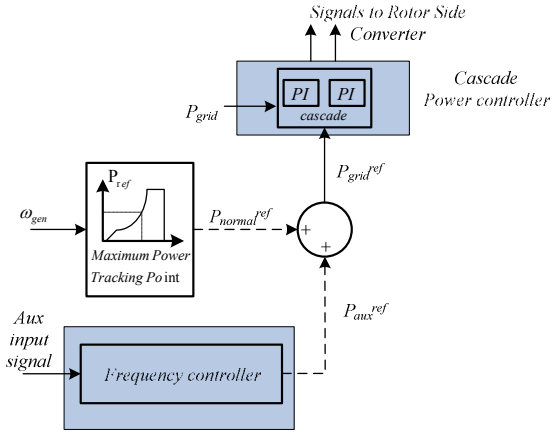

Fig. 100. General frequency control scheme for DFIG wind turbines.

6.3.1 Inertia Control

In this first method, the inertial response of the DFIG is restored through an additional loop in the power reference block providing the active power reference signal to the Rotor Side Converter. Details for the basic control structure of the DFIG model designed in this study for normal operation can be found in section 3.3. Fig. 101 shows the inertia control loop.

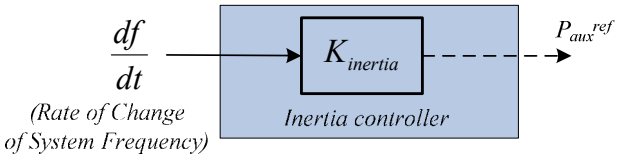

Fig. 101. Inertia controller for DFIG wind turbine.

This feature is often referred to as "virtual inertia" effect, thus the control aim is to control the DFIG wind turbine to adjust its power output when subjected to frequency deviations. The rate of change of frequency defines the additional power reference signal, which is added to the normal power reference provided by the Maximum Power Tracking Controller. This auxiliary signal introduces a term proportional to $2H\frac{df}{dt}$, where H is the total inertia constant of the wind turbine, [57]. This inertia constant is expressed in seconds and represents the time that the wind turbine is able to provide with rated active power when decelerating the rotor from the nominal speed down to zero using only the available kinetic energy in the rotor mass, [52]. Thus, in physical terms the values of the proportional parameter $K_{inertia}$ shown in Fig. 101 are restricted by this amount of energy. However, the wind turbine could be ordered to provide with even more active power, given that the stability of the system is ensured.

6.3.2 Droop Control

The second control method applied in the DFIG models is thee so called Droop control, illustrated in Fig. 102.

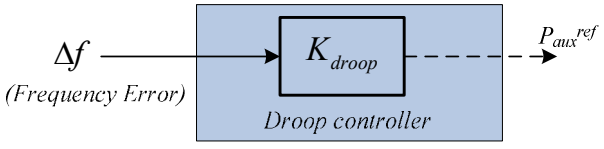

Fig. 102. Droop controller for DFIG wind turbine.

In this case, the additional reference signal is equal to:

$$P_{aux}^{ref} = K_{droop}\left(f - f_o\right) \qquad (6.1)$$

where f_o is the nominal system frequency, 50 Hz for the Rhodes power system. This control method is based on the primary frequency control applied to conventional generators. Typical values for the droop parameter of large conventional units are 3%-5%, depending on the type of unit.

This control loop aims to decrease the accelerating torque acting on the generator rotor during a frequency drop, as described above for DFIG wind turbines, [54]. The droop control can be assumed to be implemented in the wind farm controller level instead of individual wind turbine controller. This means that the overall wind farm controller provides the auxiliary signal P_{aux}^{ref} which is distributed to the individual wind turbine controllers. In that case, the communication delays should be taken into consideration, as the rate at which the wind farm changes its output during the first milliseconds following the frequency event is crucial for the overall system response. Results from both control levels, thus Droop controller on individual wind turbine controller and Droop controller on wind farm controller, are shown and compared.

6.3.3 Combined control

The last method tested in this study, is actually a combination of the two first control methods. Based on the analysis made in [54] and referred in section 6.2 for DFIG wind turbines, the sum of Droop and Inertia control should manage to counteract the opposite torques acting on the generator rotor during frequency phenomena. The Combined control scheme is given in Fig. 103.

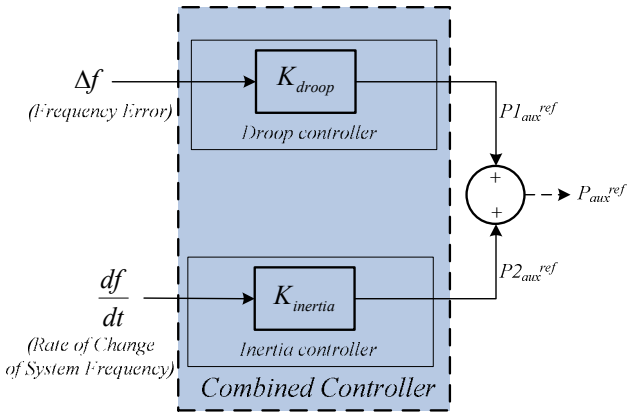

Fig. 103. Combined controller for DFIG wind turbine.

As a first approach, this last method of Combined Control seems to be optimum for the DFIG wind turbines. In most of the publications available, Droop Controller and Inertia controller have been treated independently. Discussion on the results from each control method proposed here is made in section 6.4.

6.4 Results

In this section, results from the Rhodes power system are presented. The frequency control capability of DFIG wind turbines is investigated for the load scenarios defined above. The standard event often used to check the dynamic security of power systems, thus the loss of the largest conventional generator, is simulated and the frequency response of the system under the different frequency control methods is illustrated. The emphasis on these results is given on the first seconds of the primary control operation of the system and the load shedding following the event is computed, based on the action of the under-frequency protection relay settings.

6.4.1 Results for SCENB

In SCENB, the wind farms online produce close or equal to their rated capacity. The total wind power production is 45.21 MW which stands for 27% of the total demand. The wind speeds in both wind farms equipped with auxiliary frequency control capability the wind is considered constant during the event studied, close to 11.5 m/s. The largest conventional unit produces 20.1 MW when ordered to trip, leading to loss of 11% of the total production. Fig. 104 shows the response of three wind farms during this fault, when

no auxiliary control is activated in the wind turbines. The wind farm with ASIG wind turbines increases its active power output during the first seconds following the frequency drop, contributing to the system inertia. On the other hand, the wind farm with DFIG wind turbines has almost negligible power contribution, while the PMSG wind farm does not change its active power output during the frequency drop. These results confirm the analysis made in Section III regarding the natural response of each wind turbine type. The change in active power output for each wind farm in Fig. 104 is given in p.u. of the rated capacity of each wind farm.

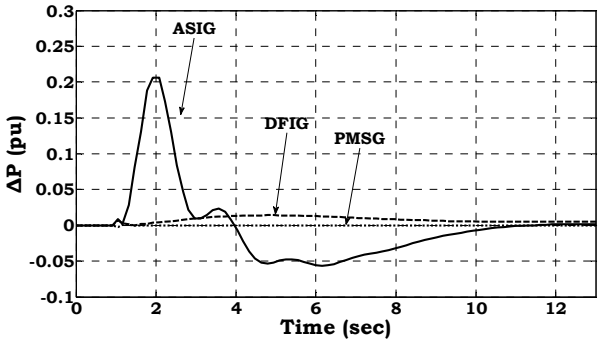

Fig. 104. Change in power in different wind turbine configurations during frequency drop (SCENB)

Fig. 105 shows the frequency response for all different control methods for frequency control in the wind farms with DFIG wind turbines described in Section IV. In SCENB, these two wind farms produce in total 15 MW – 9% of the total demand. In the same figure, the results for Droop control implemented in the wind farm level or the wind turbine level are included.

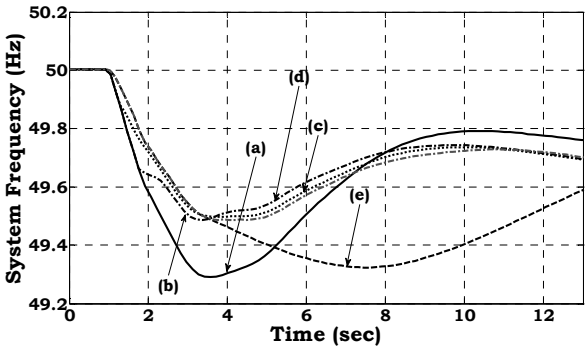

Fig. 105. System frequency for largest unit loss when frequency control is applied by DFIGs – (a) No auxiliary control, (b) Droop control on WF level, (c) Droop control on WT level, (d) Combined control, (e) Inertia control (SCENB)

When no aux control (case (a)) is used in the DFIG wind farms, the frequency reaches its minimum (see also Table II below) with the highest initial rate of change of frequency. In this scenario, even in the case with no auxiliary control provided from wind farms there is no load shedding as the system inertia is high enough to ensure moderate frequency drops. The Droop control implemented in the wind farm control level (case (b)) does not manage to improve the maximum rate of change of frequency, although the minimum frequency is higher compared to the case (a). The best case, in terms of minimum frequency, is as expected case (c), where Droop control is implemented in the wind turbine control level. On the other hand, the Inertia control (case (e)) achieves the slowest rate of change of frequency although the frequency minimum is the lowest among the different frequency control methods proposed here. The optimum performance seems to be achieved through the Combined control scheme (d) where both minimum frequency and maximum rate of change of frequency are improved. This last control method seems to combine the pos from the Droop and Inertia control schemes. The droop control implemented in the wind turbine control level (case (c)) has slightly higher minimum frequency but the difference is negligible (0.01 Hz).

Fig. 106 shows frequency drop during the first 2 seconds after the loss of the conventional unit to clarify the effect of each control method on the initial rate of change of frequency.

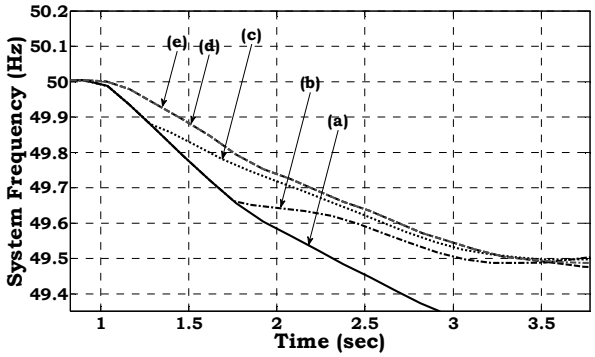

Fig. 106. System frequency for largest unit loss when frequency control is applied by DFIGs – Zoom in the first seconds after the event (a) No auxiliary control, (b) Droop control on WF level, (c) Droop control on WT level, (d) Combined control, (e) Inertia control (SCENB)

The results for this scenario are summarized in TABLE III, where the minimum frequency, the maximum rate of change of frequency and the load shedding are computed for all the cases demonstrated above.

TABLE III
RESULTS FOR SCENB – LOSS OF LARGEST INFEED

Frequency Control Scheme		Minimum Frequency (Hz)	Maximum Rate of change of frequency (Hz/sec)	Load Shedding (MW)
(a)	No auxiliary control	49.29	-0.4752	0
(b)	Droop control on WF level	49.48	-0.4752	0
(c)	Droop control on WT level	49.5	-0.4421	0
(d)	Combined control	49.49	-0.3552	0
(e)	Inertia control	49.32	-0.3552	0

The contribution of the wind farms during the frequency drop is obvious from the results presented above. From the wind turbine side now, the results for the rotor speed and the active power output of wind farm A1 (see TABLE II) equipped with DFIG wind turbines are illustrated here for all the cases of frequency control.

As already discussed in section 6.2, the rotor speed of the DFIG wind turbines is not affected if no auxiliary frequency control is applied. Therefore, the inertia response of the DFIG is negligible (see Fig. 107). In all the other cases, the rotor decelerates while the system frequency drops. Thus, the kinetic energy accumulated in the rotor mass is converted to electrical energy and delivered to the grid – giving the power surge during the primary frequency control period shown in Fig. 108.

When Inertia control is used (case (e)), the rotor speed goes back to its pre fault value, as the auxiliary power reference signal is calculated based on the derivative of the frequency $\frac{df}{dt}$. When the frequency stabilizes after the primary frequency control period,

although not nominal yet as the secondary control has not been activated in this time frame, the derivative goes to zero and the auxiliary power reference signal goes also to zero. However, in the rest of the frequency control schemes, when droop control is used, the rotor speed is decreasing reaching another steady state value, as the difference from the nominal value remains even after the stabilization of the frequency. This means, that the wind turbine is no longer operating in the maximum power tracking curve as the normal control demands, [55]. The tertiary response which re-establishes the rotor speed of the wind turbine may take place several seconds after the event, when the power system has overcome the imbalance and the stress to stabilize the frequency. This procedure could also be implemented as part of an Automatic Generation controller operating in the whole power system, including the wind farms as active components, [58].

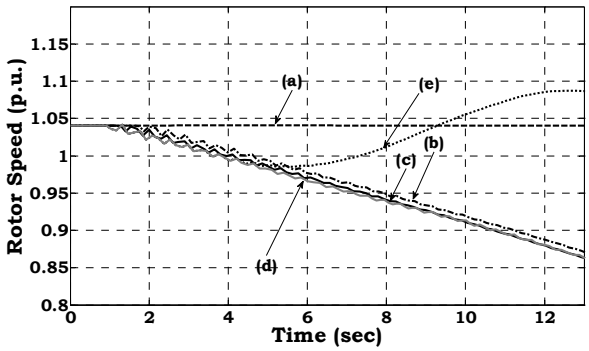

Fig. 107. Rotor speed deviations after largest unit loss for different frequency control methods applied in DFIGs - (a) No auxiliary control, (b) Droop control on WF level, (c) Droop control on WT level, (d) Combined control, (e) Inertia control (SCENB)

The active power output of the wind farm A1 is given in Fig. 108. In cases (d) and (e), where Inertia control and Combined control are used respectively, the wind farm increases its active power at a high rate, thus leading to lower rate of change of frequency as described in Table III above. In case (a) of course, when no auxiliary control is provided the active power change is negligible. In cased (b), where the Droop controller is assumed to work in the wind farm control level, the power surge is delayed compared to case (a).

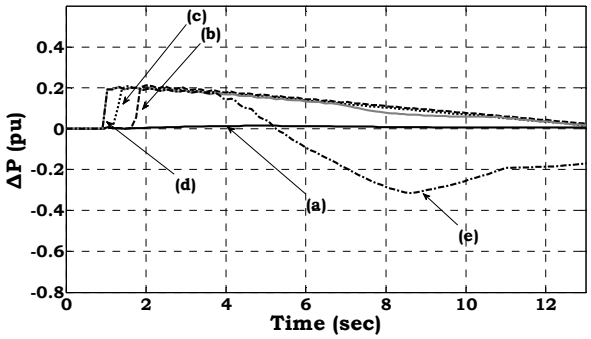

Fig. 108. Change in active power output after largest unit loss for different frequency control methods applied in DFIGs - (a) No auxiliary control, (b) Droop control on WF level, (c) Droop control on WT level, (d) Combined control, (e) Inertia control (SCENB)

6.4.2 Results for SCENC

In SCENC, the wind power penetration is maximum. The total wind power production is 28.2 MW in total 83 MW of demand (34 %). Although, the wind farms produce less than in the Maximum Wind Power Production scenario (SCENB) studied above, the impact of wind power in the power system operation is considered far more significant. The system inertia is decreased in this case, making the frequency control task in the system more complex. The wind speeds in this scenario is almost 9.3 m/s for the wind farms A1 and A2 (see TABLE II). The largest conventional unit in the system produces 21 MW before the protection system acts to take it out of operation – this means production loss equal to 25 % of the total demand. The fault is severe and the power system stability is checked for all the frequency control schemes designed in this study.

Fig. 109 illustrates the response of the three different wind turbine configurations available in the Rhodes power system, during the event, when no auxiliary control is activated in the DFIG wind farms. The comments made in section 6.2 are confirmed by the results (see also Fig. 104). Comparing to Fig. 104, which demonstrates the response for SCENB, the contribution of the ASIG in SCENC is higher. The change in the active power production of the wind farm with ASIG wind turbines is higher than 0.8 pu compared to almost 0.2 p.u. in SCENB. This can be explained comparing the frequency response in both cases. In SCENB (see Fig. 105 – case (a)), the frequency does not decrease as much as in SCENC (see Fig. 110 – case (b)), therefore, the rotor of the ASIG wind turbines decelerates more in the first scenario, leading to higher active power

contribution. In Fig. 109 the response of wind farms equipped with DFIG or PMSG wind turbines is almost negligible, as explained in section 6.2.

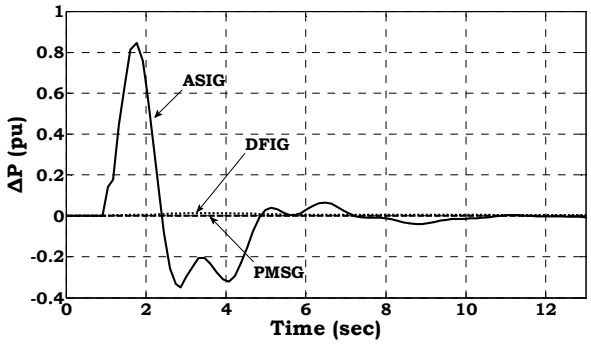

Fig. 109. Change in power in different wind turbine configurations during frequency drop (SCENC)

In Fig. 110 and Fig. 111 the system frequency for all the different frequency control schemes implemented in the wind farms A1 and A2 (see TABLE II) is shown. In this scenario, the minimum frequency following the event is very low compared to SCENB, whereas the maximum rate of change of frequency is significantly higher.

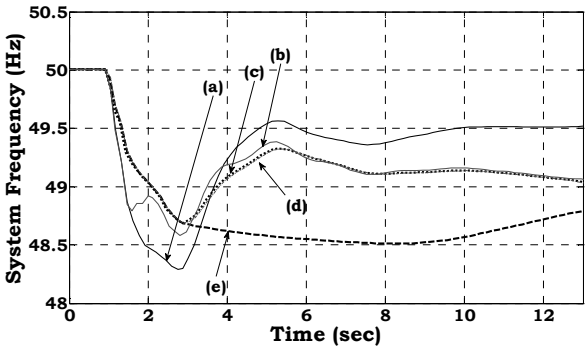

Fig. 110. System frequency for largest unit loss when frequency control is applied by DFIGs – (a) No auxiliary control, (b) Droop control on WF level, (c) Droop control on WT level, (d) Combined control, (e) Inertia control (SCENC)

In case (a), when the wind farms do not have auxiliary frequency control, the frequency drops below 48.5 Hz which is the upper zone of the under-frequency protection relay settings acting on the loads. This drop leads to disconnection of 15.1 MW of load – 18 % of the total demand. This load shedding is not considered accepted in terms of dynamic security terms, [5]. However, in all the other cases, where the frequency control is activated in the DFIG wind farms, the load shedding is avoided totally. The maximum frequency drop appears in case (e), where the inertia controller is used. The optimum frequency drop in terms of minimum frequency is achieved in cases

(c) and (d), thus when either Droop control is implemented on the wind turbine control level (case (c)) or when the Combined control is used (case (d)).

In this scenario, the effect of auxiliary frequency control on the maximum rate of change of frequency is very crucial. As illustrated in Fig. 111, where the initial drop of the frequency for all cases is zoomed in, and as summarized also in TABLE IV, this rate is very high compared to SCENB (see also TABLE III). The inertia of the system in this case is lower because the number of the conventional generators connected to the system in SCENC, and which are the ones determining the system inertia in large percentage, are reduced. The rate of change of frequency is close to 2.8 Hz/sec (in absolute value) in cases (a) and (b), although in the last case the minimum frequency does not drop below 48.5 Hz. Inertia control manages to reduce the rate to less than 1.8 Hz/sec, which is the highest rate among all the cases. Here also, as explained for SCENB above, the Combined control seems to be the best compromise in terms of minimum frequency and maximum rate of change.

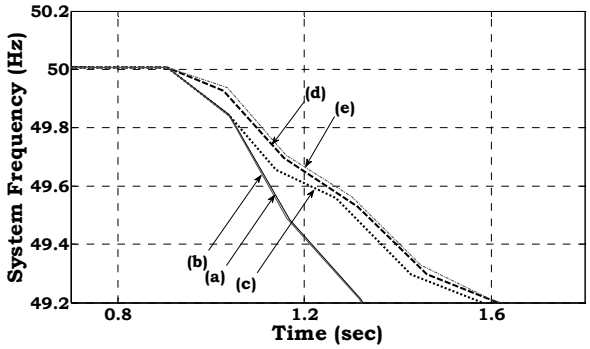

Fig. 111. System frequency for largest unit loss when frequency control is applied by DFIGs – Zoom in the first seconds after the event (a) No auxiliary control, (b) Droop control on WF level, (c) Droop control on WT level, (d) Combined control, (e) Inertia control (SCENC)

TABLE IV

RESULTS FOR SCENC – LOSS OF LARGEST INFEED

Frequency Control Scheme	Minimum Frequency (Hz)	Maximum Rate of change of frequency (Hz/sec)	Load Shedding (MW)

(a)	No auxiliary control	48.29	-2.8042	15.1
(b)	Droop control on WF level	48.58	-2.7926	0
(c)	Droop control on WT level	48.69	-1.8698	0
(d)	Combined control	48.68	-1.8474	0
(e)	Inertia control	48.515	-1.7857	0

Fig. 112 and Fig. 113 show respectively the rotor speed deviation and the change in active power output for wind farm A1, during the frequency drop. The comments made in SCENB are also valid here, regarding the differences among the various frequency control schemes. However, looking at the active power produced by the wind farm A1 in SCENC the contribution of the wind farms is more significant during the primary frequency response. The rotor deceleration is higher, thus more kinetic energy from the rotor mass is delivered to the grid as active power.

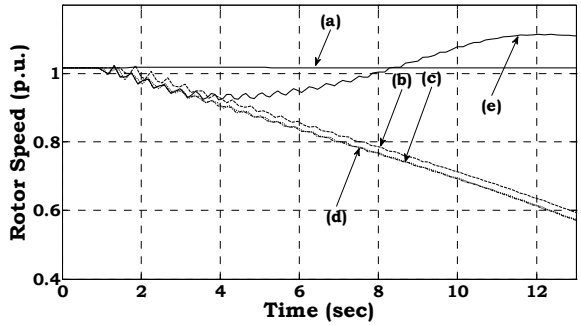

Fig. 112. Rotor speed deviations after largest unit loss for different frequency control methods applied in DFIGs - (a) No auxiliary control, (b) Droop control on WF level, (c) Droop control on WT level, (d) Combined control, (e) Inertia control (SCENC)

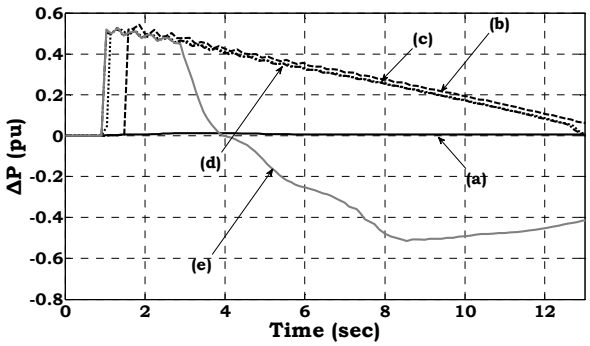

Fig. 113. Change in active power output after largest unit loss for different frequency control methods applied in DFIGs - (a) No auxiliary control, (b) Droop control on WF level, (c) Droop control on WT level, (d) Combined control, (e) Inertia control (SCENC)

6.4.3 Comparison between one or two wind farms providing auxiliary control in SCENB for combined control method

In the last part of the results section, comparative results will be shown for SCENB between the cases, where Combined frequency control is implemented only in one wind farm and the later, where the control is incorporated in both wind farms with DFIG wind turbines. All the results presented previously are extracted when both wind farms A1 and A2 have this frequency control capability.

As shown in Fig. 114 and also summarized in TABLE V below, in case (d1) only wind farm A1 provides auxiliary frequency control leading to bigger frequency drop and higher rate of change of frequency compared to case (d2) where also wind farm A2 is equipped with this control capability. Thus, the inertia of the system, including the "virtual" inertia provided by the DFIG wind turbines, is obviously reduced when the proportion of the wind turbines providing auxiliary control is smaller. It is noted here, that in this comparison the Combined control method was chosen, as it is concluded by the previous results that this scheme achieves the best performance among the other proposed ones.

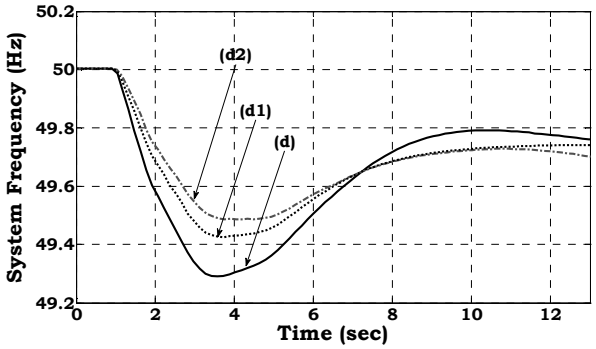

Fig. 114. System frequency for largest unit loss for different frequency control methods applied in DFIGs - (a) No auxiliary control, (b) Combined control provided by only one wind farm (c) Combined control provided by two wind farms

TABLE V

RESULTS FOR SCENB – LOSS OF LARGEST INFEED

Frequency Control Scheme		**Minimum Frequency (Hz)**	**Maximum Rate of change of frequency (Hz/sec)**	**Load Shedding (MW)**
(a)	No auxiliary control	49.29	-0.4752	0
(b)	Combined control through one wind farm	49.42	-0.3827	0
(c)	Combined control through two wind famrs	49.49	-0.3552	0

The conclusions from all the results presented in this section will be summarized in the next session, where also discussion on the expansion of the maximum allowed penetration in autonomous systems, like Rhodes, is made.

7. Conclusions

This report presented a detailed investigation of Rhodes power system dynamic security in the case of reference year 2012, when large wind farms are expected to be connected to the island. The conventional units, including Automatic Voltage Regulators and Speed Governors, were modeled in detail. The response of the governors during dynamic phenomena in the system is essential for the overall response. Especially the emergency rate of power undertake by the all different kinds of units i.e. steam, gas and diesel plants, is a major factor defining the overall system operation. The presented models includes also the models of the five wind farms which are connected in the system, comprising detailed models for three different wind turbine technologies – namely Doubly Fed Induction Generator (DFIG), Permanent Magnet Synchronous Generator (PMSG) and Active Stall Induction Generator (ASIG) based wind turbines.

Different load scenarios, relevant for the island operation, are analyzed, such as maximum wind power penetration scenario, maximum wind power production scenario and maximum load demand scenario.

In many non-interconnected systems the penetration of wind power has started to reach the boundaries of 30%. Serious concerns are expressed by the operators of these systems and wind fluctuations are one of the aspects that has to be evaluated before expanding the penetration levels, [59]. From the results, it is concluded that even in the worst case scenario, the Maximum Wind Power Penetration, the frequency fluctuations resulting from the wind speed fluctuations are not considered to pose security questions for the power system. However, the impact of wind variations is obvious in the system frequency and the correlation between wind speeds and system frequency has to be always investigated before reviewing the penetration levels. Increased wind power penetration does not only limit the ability of thermal plants to undertake power, but also limits inertia. Systems inertia in cases of increased wind penetration is crucial for system stability as it defines the rate of frequency drop. The designed models for the conventional units in Rhodes power system, were sufficient to undertake power despite the rapid wind changes and the resulting active power fluctuations delivered by the wind

farms. This study has proven that, when it comes to wind power fluctuations, the penetration levels of wind power can be expanded beyond 30% of the load.

However, the dynamic security during faults was also evaluated, [60]. Besides the protection system of such non interconnected power system as Rhodes, the FRT capability and the response of wind farms during and after severe disturbances in the system are crucial, in order to estimate the load shedding and the frequency deviations. Many times the collection of data needed for detailed modeling is not available; however, in any case, it has to be ensured that highest as possible accuracy of modeling is implemented.

A set of simulations is carried out in order to analyze the security of the system. It has been noticed that although the technology of the wind turbines connected in the non interconnected system is quite important, there are certain parameters (such as inertia, type of thermal plants, distribution of power production, under-frequency relays), that are crucial for system response. Especially the rate of power undertake of thermal units and the wind production, which in case without FRT capability, has to be tripped during grid faults, define to which extent load shedding is taking place.

The simulations have shown that in non-interconnected systems the load shedding following grid faults, can reach unaccepted levels. In some cases load shedding above 60-70% can be considered as partial black-out of the system and is of course not acceptable. Moreover, in other operating scenarios of the power system, like SCEN1 and SCEN2, the load being cut-off reaches levels of 35% and the frequency minimum falls beneath 49 Hz. The major reason for this transient behavior following a short circuit grid fault is the production loss which occurs due to the tripping of wind farms, which are not equipped with FRT capability. It has also been observed that, as also stated in [15], the rule of thumb of 30% penetration does not seem to be affirmed in all cases. For instance, in Rhodes, if the wind farms are not equipped with FRT and when wind power penetration levels reach more than 25% (i.e. SCEN2 and SCEN3), the load shedding is reaching not acceptable limits.

It is obviously that the implementation of FRT capability in wind turbines improves system response to faults within acceptable limits of load shedding and frequency dips.

Another issue, which should be remarked, is that the increased wind power penetration does not only limit the ability of thermal plants to undertake power, but also the inertia of the system. Systems inertia in cases with increased wind penetration is crucial for system stability, as it defines the rate of frequency drop.

There are some measures that can further enhance the dynamic security of systems like Rhodes:

The review of the frequency protection system settings can be done, if the dynamic security is ensured through FRT capability of wind farms online. The protection settings are quite sensitive and large amounts of load can be cut off just after the fault incident.

Systems like SVC or STATCOM for fast voltage control systems can guaranty the uninterrupted operation of wind parks, especially those consisting of fixed speed wind turbines. For instance, the substation, where most of these wind parks are connected, could be considered as the most appropriate for this installation. Under these conditions, wind power penetration could increase beyond 30% of the load, keeping the dynamic security of the system in the acceptable levels.

The third part of the investigations provided a survey on frequency control issues of the autonomous power system with high wind power penetration, [61]. Frequency response during severe faults, i.e. the sudden loss of the biggest conventional generator, was simulated for two different load scenarios. These scenarios correspond to different system inertia but also to different operating points of the wind turbines. The wind turbines have different response when the system frequency varies, depending on the specific electrical configuration characteristics. Although the fixed speed ones contribute to the system inertia during frequency phenomena, this is not the case for DFIG and PMSG wind turbines, where the rotor is partially or totally detached form the system frequency respectively. The under-frequency protection system acting on the loads connected to MV substations can measure either the rate of change of frequency or the actual frequency to act on the relays. Modeling the protection system in the power system provides more accurate results regarding the load shedding, a variable that defines the dynamic security level of a system. As wind power penetration is increasing in modern power systems, the wind turbines have to contribute to the frequency stability of the system, acting similar to conventional power plants. In this article, three different

frequency control schemes were investigated to enhance the primary frequency support of DFIG wind turbines. Simulation ended up to the following conclusions:

1. Non interconnected systems face the problem of decreased system inertia, especially when wind farms tend to substitute conventional units under increasing wind power penetration conditions. The DFIG wind turbines can be equipped with auxiliary Inertia control, providing with valuable inertia response during the first seconds following the frequency event. This control, reestablishes in the DFIG wind turbines the intrinsic characteristic of the fixed speed ASIG wind turbines, thus, using the kinetic energy accumulated in the rotor mass to support the grid during frequency variations.
2. Additional control methods can also be used in DFIG wind turbines, like Droop control used is conventional generators providing primary frequency support. The case, where the Droop control is implemented in the wind farm control level, instead of the turbine level, was also investigated to check the effect of communication delay in the response of the wind farm. Although when the Inertia control is used, the rate of change of frequency is significantly reduced, the Droop control seems to benefit more power system when looking at the minimum frequency after the event.
3. A Combined control, where both Inertia and Droop control schemes are used, was incorporated in the model. This last method manages to combine the positive effects of both methods, improving not only the initial rate of change of frequency after the fault but also ensuring lower frequency drop.
4. In some cases, when wind power production is higher than 30 % of the total demand, the auxiliary frequency control implemented in two wind farms in the Rhodes power system, manages to avoid load shedding totally. Therefore, the rule of thumb of 30 % penetration, which is often used in autonomous power systems, can be further expanded as long as auxiliary frequency control is provided by wind farms.
5. The benefits of the primary frequency support from modern wind turbines increase as the number of the turbines with this capability rises. This means that, if all new wind farms installed in autonomous power systems are equipped with

primary frequency control capability, the frequency stability can be ensured even for penetration levels that today are hard to consider.

6. From the wind turbine side, in some cases the turbine may be forced to operate away from the maximum power-tracking curve, which means economic cost for the wind farm. So, before the system operators set any requirements for frequency control, the economic costs of frequency control for the wind turbine owner should be addressed.
7. The review of the frequency protection system settings can be done, as long as the frequency stability of the system is ensured. In many cases, the protection settings are quite sensitive and large amounts of load are cut off. The review of the protection system in modern power systems has to follow the progress made in the wind farms' capability to support the grid during disturbances.
8. Although, technology such as flywheels can support system inertia in autonomous power systems, advanced frequency control implemented in wind turbines will make it possible to achieve the penetration levels for wind power that today seem hard to reach.

References

[1] P. Kundur, Power System Stability and Control, Ed. McGraw-Hill, 1994.

[2] DIgSILENT GmbH. DIgSILENT technical documentation—PowerFactory, 2006.

[3] J. Mantzaris, M. Karystianos, C. Vournas, "Comparison of Gas Turbine and Combined Cycle Models for System Stability Studies", presented at the 6th Mediterranean. Conf. MedPower, Thessaloniki, Greece, 2008

[4] T. V. Cutsem, C. Vournas, Voltage Stability of Electric Power Systems, Ed. Springer, 1998

[5] I. D. Margaris, J. C. Mantzaris, M. E. Karystianos, A. I. Tsouchnikas, C. D. Vournas, N. D. Hatziargyriou, I. C. Vitellas, "Methods for evaluating penetration levels of wind generation in autonomous systems", accepted for presentation in IEEE PowerTech Conf., Bucharest, June 2009.

[6] Sørensen P., Hansen A.D., & Rosas P.A.C., " Wind models for prediction of power fluctuations from wind farms", Proc 'The Fifth Asia-Pacific Conference on Wind Engineering (APCWEV)', 2001, Kyoto, Japan. Journal of Wind Engineering no.89, pp. 9-18.

[7] Sørensen P., Hansen A.D., Janosi L., Bech J., & Bak-Jensen B. "Simulation of interaction between wind farm and power system". Risø National Laboratory. Risø-R-1281, 2001.

[8] Øye,& S. (1991). "Dynamic stall - simulated as time lag of separation". In Vol. Proceedings of the 4th IEA Symposium on the Aerodynamics of Wind Turbines, McAnulty, K.F- (Ed.), Rome, Italy.

[9] Akhmatov V., An aggregated model of a large wind farm with variable-speed wind turbines equipped with doubly-fed induction generators, Wind Engineering, Vol 28, No 4, 2004, pp 479-488.

[10] Poeller M., Achilles S., "Aggregated Wind Park Models for Analyzing Power System Dynamics", Fourth International Workshop on Large-Scale Integration of Wind Power and Transmission Networks, October 20.21, Billund, Denmark, DIgSILENT, 10p.

[11] Jauch C, Hansen AD, Sørensen P, Blaabjerg F. Simulation model of an active-stall fixed-speed wind turbine controller. Wind Engineering, 2004, Vol.28, No.2, pp. 177- 195.

[12] Hansen, A.D.; Sørensen, P.; Iov,F.; Blaabjerg, F., Grid support of a wind farm with active stall wind turbines and AC grid connection. Wind Energy 2006, vol. 6, pp 341-359.

[13] Akhmatov V., Knudsen H., Nielsen A.H., Pedersen J.K., Poulsen N.K., Modelling and transient stability of large wind farms, Electrical Power and Energy Systems 25 (2003), 123-144

[14] Sørensen P, Iov F, Blaabjerg F, Skaarup J, Test and simulation of dynamic phase compensation from Mita-Teknik A/S, Risø-R-1438 (EN), 2004.

[15] Hansen A.D., Jauch C., Sørensen P., Iov F., Blaabjerg F. Dynamic wind turbine models in power system simulation tool DIgSILENT, Risø-R-1400(EN), 2003.

[16] Heier S. Grid Integration of Wind Energy Conversion Systems,1998, ISBN 0 471 97143.

[17] DIgSILENT GmbH, DIgSILENT Technical Documentation – PowerFactory DSL Models, August 2006.

[18] Kundur P. (1994), Power System Stability and Control, McGraw Hill.

[19] Hansen A.D., Michalke G., Modelling and fault ride-through capability of a full converter wind turbine with multi-pole PMSG, Brusells, EWEC 2008.

[20] Hansen A.D., Michalke G., Multi-pole PMSG wind turbines' grid support capability in uninterrupted operation during grid faults, submitted to IET Renewable Power Generation, In press 2009.

[21] Hansen, A.D.; Sørensen, P.; Iov, F.; Blaabjerg, F., Control of variable pitch/variable speed wind turbine with doubly-fed induction generator, J. Wind Eng. (2004), vol. 28, No. 4, p 411-432

[22] Akhmatov V., Analysis of dynamic behavior of electric power systems with large amount of wind power, PhD thesis, 2003, Ørsted DTU.

[23] Hansen A.D., Michalke G., Sørensen P., Lund T., Iov F. Co-ordinated voltage control of DFIG wind turbines in uninterrupted operation during grid faults, Wind Energy, Vol. 10, No. 1, 2007, pp.51-68.

[24] Hansen A.D., Michalke G., Fault ride-through capability of DFIG wind turbines, Renewable Energy, vol 32 (2007), pp 1594-1610

[25] Akhmatov V., Variable-speed wind turbines with doubly-fed induction generators. Part II: Power System Stability. Wind Engineering, Vol. 26, No. 3, 2002, pp 171-188.

[26] Akhmatov V., Variable-speed wind turbines with doubly-fed induction generators. Part IV: Uninterrupted operation features at grid faults with converter control coordination. Wind Engineering, Vol. 27, No. 6, 2003, pp 519-529.

[27] Eping C., Stenzel J., Poeller M., Mueller H., Impact of Large Scale Wind Power on Power System Stability, Fifth INternational Workshop on Large-Scale Integration of Wind Power and Transmission Networks, April 7-8, 2005, Glasgow, Scotland, 9p.

[28] Kayikci M., Anaya-Lara O., Milanovic J.V., Jenkins N., Strategies for DFIG voltage control during transient operation, CIRED, 18th Int. Conference on Electricity Distribution, 2005, Turin, 5p.

[29] C. Luo, and Boon-Teck Ooi, "Frequency Deviation of Thermal Power Plants Due to Wind Farms", IEEE Trans. On energy Conversion, vol. 21, no. 3, September 2006.

[30] M. P. Pblsson, T. Toftevaag, K. Uhlen, and J. O. G. Tande, "Control Concepts to Enable Increased Wind Power Penetration", presented at IEEE Power Engineering Society General Meeting, vol. 3, pp. 1984 – 1990, July 2003.

[31] A. H. Kasem, E. F. El-Saadany,H. H. El-Tamaly, and M. A. A. Wahab, "A New Fault Ride-through Strategy for Doubly Fed Wind-Power Induction Generator", presented at Electrical Power Conference, pp. 1-7, Canada, Oct. 2007.

[32] B. M. Buchholz1, Z. A. Styczynski, and W. Winter, "Dynamic Simulation of Renewable Energy Sources and Requirements on Fault Ride Through Behavior", presented at IEEE Power Engineering Society General Meeting, pp. 7, 2006.

[33] A.D. Hansen, P. Sørensen, F. Iov, F. Blaabjerg,, "Centralised power control of wind farm with doubly-fed induction generators". Renewable Energy, vol 31 (2006), 935-951.

[34] Hansen A.D., Michalke G., Fault ride-through capability of DFIG wind turbines, Renewable Energy, vol 32 (2007), pp 1594-1610

[35] Hansen A.D., Michalke G., Sørensen P., Lund T., Iov F. Co-ordinated voltage control of DFIG wind turbines in uninterrupted operation during grid faults, Wind Energy, Vol. 10, No. 1, 2007, pp.51-68.

[36] Hansen A.D., Michalke G., Modelling and control of variable speed multi-pole PMSG wind turbine, Wind Energy , 2008, Vol.11(5), pp 537-554.

[37] Hansen A.D., Michalke G., Multi-pole PMSG wind turbines' grid support capability in uninterrupted operation during grid faults, submitted to IET Renewable Power Generation, June 2008, accepteret i nov 2008.

[38] Akhmatov V., Knudsen H., Nielsen A.H., Pedersen J.K., Poulsen N.K., Modelling and transient stability of large wind farms, Electrical Power and Energy Systems 25 (2003), 123-144.

[39] N. Kakimoto, K. Baba, "Performance of Gas Turbine-Based Plants During Frequency Drops", IEEE Transactions on Power Systems, vol. 18, No 3, August 2003.

[40] J. Mantzaris, M. Karystianos, C. Vournas, "Comparison of Gas Turbine and Combined Cycle Models for System Stability Studies", presented at the 6th Mediterranean. Conf. MedPower, Thessaloniki, Greece, 2008.

[41] P. Sørensen, N. A. Cutululis, A. Vigueras-Rodríguez, H. Madsen, P. Pinson, L. E. Jensen, J. Hjerrild and M. Donovan, "Modelling of power fluctuations from large offshore wind farms", Wind Energy, vol. 11, pp. 29–43, 2007.

[42] V. Akhmatov, Analysis of dynamic behavior of electric power systems with large amount of wind power, PhD thesis, 2003, ørsted DTU.

[43] M. Poeller, S. Achilles, "Aggregated wind park models for analyzing power system dynamics", presented in Fourth international workshop on large-scale integration of wind power and transmission networks, October 2003, Billund, Denmark, DIgSILENT, 10pp.

[44] A.D.Hansen, L.H.Hansen, "Market penetration of different wind turbine concepts over the years", EWEC 2007, Milano, 6pp.

[45] A.D. Hansen, G. Michalke, "Fault ride-through capability of DFIG wind turbines", Renewable Energy, vol 32 (2007), pp 1594-1610.

[46] G. Gail, A.D. Hansen, T. Hartkopf, “Controller design and analysis of a variable speed wind turbine with doubly-fed induction generator”, EWEC, Athens, 2006.

[47] M.H. Hansen, A.D. Hansen, T.J. Larsen, S. øye, P. Sørensen, “Control design for a pitch-regulated variable speed wind turbine“, Risø-R-1500 (EN), 2005, 84 pp.

[48] C. Jauch, A. D. Hansen, P. Sørensen and F. Blaabjerg, “Simulation Model of an Active-stall Fixed-speed Wind Turbine Controller”, Wind Engineering, Vol. 28, no.2, pp. 177-195, 2004.

[49] A. D. Hansen, C. Jauch, P. Sørensen, F. Iov, F. Blaabjerg, “Dynamic wind turbine models in power system simulation tool DIgSILENT”, report Risø-R-1400(EN), 2003.

[50] T. Ackermann, Wind Power in Power Systems, Ed. Wiley, 2005.

[51] G. Lalor, A. Mullane and M. J. O’Malley, “Frequency Control and Wind Turbine Technologies”, IEEE Transactions on Power Systems, vol. 20, no. 4, November 2005.

[52] J. Morren, J. Pierik and S. W.H. de Haan, “Inertial response of variable wind turbines”, Electric Power Systems Research, Elsevier, pp. 980-987, Wind Energy, vol. 76, 2006.

[53] N. R. Ullah, T. Thiringer and D. Karlsson, “Temporary Primary Frequency Control Support by Variable Speed Wind Turbines — Potential and Applications”, IEEE Transactions on Power Systems, vol. 23, no. 2, May 2008.

[54] G. Ramtharan, J.B. Ekanayake and N. Jenkins, “Frequency support from doubly fed induction generator wind turbines”, IET Renew. Power Gener., 2007, 1, (1), pp. 3–9.

[55] J. Ekanayake,L. Holdsworth and N. Jenkins. “Control of DFIG wind turbines”, Power Engineer [see also Power Eng. J.], 2003, 17, (1), pp. 28–32.

[56] J. Ekanayake, and N. Jenkins, “Comparison of the response of doubly fed and fixed-speed induction generator wind turbines to changes in network frequency”, IEEE Trans. Energy Conversion, 2004, 19, (4), pp. 800–802.

[57] L. Holdsworth , J.B. Ekanayake and N. Jenkins, “Power system frequency response from fixed speed and doubly fed induction generator-based wind turbines”, Wind Energy 2004; 7 : 21-35. DOI:10.1002/we.105.

[58] A. Suwannarat, B. Bak-Jensen, Z. Chen, H. Nielsen, J. Hjerrild, P. Sørensen, and A. D. Hansen, "Power system operation with large scale wind power integration", PowerTech 2007.

[59] I. D. Margaris, A. D. Hansen, N. A. Cutululis, P. Sørensen and N. Hatziargyriou, "Impact of wind power in autonomous power systems – Power fluctuations – Modeling and Control issues", accepted for publication in Wind Energy journal, 2010.

[60] I. D. Margaris, A. D. Hansen, P. Sørensen and N. Hatziargyriou, "Dynamic Security Issues in Autonomous Power Systems with increasing Wind Power Penetration", under review in EPSR journal.

[61] I. D. Margaris, A. D. Hansen, P. Sørensen and N. Hatziargyriou, "The challenge of frequency control in autonomous power systems with increasing wind power penetration", to be submitted in IEEE Transactions.